THEORETICAL MODELLING OF ELECTROSTATIC WAVES IN A MAGNETIZED DUSTY PLASMA

THESIS

Submitted to

DELHI TECHNOLOGICAL UNIVERSITY

in fulfilment of the requirements for the degree of

DOCTOR OF PHILOSOPHY

in

PHYSICS

by

Ms. ANSHU
(2K18/PhD/AP/25)

Under the supervision of

Prof. Suresh C. Sharma
Supervisor
Department of Applied Physics
Delhi Technological University, Delhi

Prof. Jyotsna Sharma
Co-Supervisor
Department of Applied Physics
Amity University, Manesar

Department of Applied Physics
Delhi Technological University, Delhi-110042, India

OCTOBER 2023


Dedicated to
Maa
&
Papa

DELHI TECHNOLOGICAL UNIVERSITY

(Govt. of National Capital Territory of Delhi)
Shahbad Daulatpur, Bawana Road, Delhi-110042

CERTIFICATE

This is to certify that the thesis entitled "***Theoretical Modelling of Electrostatic Waves in a Magnetized Dusty Plasma***" submitted by **Ms. Anshu (2K18/PhD/AP/25)** to Delhi Technological University (DTU), Delhi, India for the degree of Doctor of Philosophy, is a bonafide record of the research work carried out by her under our supervision and guidance. The work embodied in this thesis has been carried out in the Plasma & Nano Simulation Lab, Department of Applied Physics, Delhi Technological University (DTU), Delhi, India. The work of this thesis is original and has not been submitted in parts or fully to any other Institute or University for the award of any other degree or diploma.

Prof. Suresh C. Sharma
Supervisor
Delhi Technological University
Delhi-110042, India

Prof. Jyotsna Sharma
Co-Supervisor
Amity University, Manesar
Gurugram-122412, India

Prof. A.S. Rao
Head of the Department
Department of Applied Physics
Delhi Technological University
Delhi-110042, India

DELHI TECHNOLOGICAL UNIVERSITY
(Govt. of National Capital Territory of Delhi)
Shahbad Daulatpur, Bawana Road, Delhi-110042

CANDIDATE'S DECLARATION

I, **Ms. Anshu**, hereby certify that the thesis titled "***Theoretical Modelling of Electrostatic Waves in a Magnetized Dusty Plasma***" submitted in the fulfilment of the requirements for the award of the degree of Doctor of Philosophy is an authentic record of my research work carried out under the supervision of **Prof. Suresh C. Sharma** and **Prof. Jyotsna Sharma**. This work in the same form or any other form has not been submitted by me or anyone else earlier for any purpose. Any material borrowed or referred to is duly acknowledged.

Anshu
(2K18/PhD/AP/25)
Department of Applied Physics
Delhi Technological University
Delhi – 110042, India

ACKNOWLEDGEMENT

Above all, I extend my heartfelt gratitude to the almighty for providing me with the strength and patience needed to persevere throughout these years of hard work.

I hope this acknowledgement serves as a little token of my sincere appreciation to everyone who helped me in this journey.

I wholeheartedly want to thank my supervisor, **Prof. Suresh C. Sharma**, for his excellent mentorship, patience, motivation, enthusiasm, immense knowledge, and continuous support all these years. His persistent commitment and rich reservoir of knowledge have not only made the journey easier but have also been instrumental in shaping the core of my thesis. I would also look to him for consolation during my PhD journey at times of uncertainty and tiredness, and his insightful advice and consoling words never ceased to lift my mood. His mentorship is a rare gem and I consider myself extraordinarily fortunate to have had the privilege of being nurtured under his unparalleled guidance. He is not just an advisor; he is a beacon of inspiration and mentorship that is truly one of a kind, a rare gem in the realm of academia.

Special thanks to my Co-Supervisor, **Prof. Jyotsna Sharma**, for having immense faith in me and standing by me through these years. I am grateful for the insightful discussion, valuable advice and trust she showed during the research work. She is a person with foresight, benevolence, enthusiasm, patience, and endurance. She never turns me to wait for any research-related discussion and work. I consider myself incredibly fortunate to have had the privilege of completing this arduous journey under her expert guidance.

My sincere thanks also go to **Prof. Prateek Sharma**, Hon'ble Vice-Chancellor, DTU, **Prof. Yogesh Singh and Prof. J. P. Saini,** Ex-Hon'ble Vice-Chancellors, DTU, and other officials for their valuable support and for providing ample facilities to conduct this research. I would also like to acknowledge the DTU's financial support to attend the 46th European Physical Society Conference on Plasma Physics in 2019.

I would also thank **Prof. Rinku Sharma**, Dean (Academic-PG), DTU, and **Prof. A.S. Rao**, Head of the Department of Applied Physics, DTU and all other faculty and staff members for their help and cooperation throughout my research. Thanks to the Department of Applied Physics, Delhi Technological University (DTU), for providing the required facilities so that I can work voraciously, barring the time limit.

I express my heartfelt gratitude to my fellow lab mates in the Plasma & Nano-Simulation Research Laboratory for the stimulating discussions, selfless support, and all the fun we had, that kept me going in this challenging yet beautiful journey. I would also like to express my gratitude to my senior, **Dr. Kavita Rani**, for generously giving her time to discuss my work.

A special thanks to all my friends within and outside DTU for keeping me sane. To my first friend cum senior at DTU, **Dr. Jyotsana Panwar**, I wish I could tell you how grateful I am for all you have done for me during my initial days of research. To my college companions: **Dr. Vishal Singh**, **Jyoti, Jasveer**, **Sunil** and **Sandeep,** you know how much you all mean to me and I can't imagine my life at DTU without you guys! I extend a special appreciation to Vishal for consistently being there and assisting me at every possible step throughout these years. To **Falta**, **Dr. Parveen, Ankit, Rajat Bajaj** and **Dr. Aman** you guys are always there to support me! To **Priya**, **Shivani**, **Vinay** and **Sharad,** I extend my heartfelt gratitude for your constant warmth and endearing presence as juniors. The moments shared with them will forever be cherished as golden memories in my life.

I want to pay high regard to my father, **Mr. Satpal Dahiya** and my mother, **Mrs. Rajesh Dahiya** for their love, constant care, and emotional support throughout my life. My father has been the most significant pillar of support during these years. My mother has invested all her time in trying to make me a successful person. She has always taught me to work beyond my limits. My parents have always supported me in everything and provided me with the best facilities for me to reach here. The encouragement and blessings from my elder brother **Mr. Sumit,** my sister-in-law **Mrs. Monika,** my younger brother **Mr. Puneet** and my sister-in-law **Mrs. Shelly** always motivated me to accomplish this thesis work. Their faith, trust and confidence in me always pushed me towards my goal. And finally, I would like to thank my lovely nieces, **Gaurvi** and **Ravya**, for their contagious laughter and light hearted presence, which lightened my challenging PhD journey and offered a welcome feeling of joy and innocence. Their beaming smiles served as an endless source of motivation and a timely reminder of the value of maintaining balance in one's life. The support, compassion, tolerance, and encouragement from my family got me through this challenging journey. I sincerely appreciate all that you have done for me over the years.

Anshu

ABSTRACT

The main aim of the thesis is to understand the intrinsic behaviour of electrostatic waves in a magnetized dusty plasma. It is crucial to learn about the behaviour of dusty plasmas in order to better understand both laboratory and space plasmas. Dusty plasmas are distinguished from other forms of plasmas in various astronomical and laboratory contexts by the presence of solid particles inside the plasma medium. The incorporation of these dust grains increases complexities in the system and sheds new light on the behaviour of waves and instabilities. The first step in our investigation is to identify the fundamental ideas that govern dusty plasmas, including the complex interactions that occur between charged dust particles, electrons, and ions in a magnetized plasma. We examine the propagation of electrostatic waves and instabilities within a plasma as well as the mechanisms that generate these waves, delving into the complex nature of electrostatic waves and instabilities. The results of these studies have numerous applications in a variety of domains, including materials processing, geophysical phenomena, astrophysics, microelectronics, fusion science, and the solar wind. The main goal of our research is to understand the intricate interactions that take place between charged dust particles, the plasma environment, and the magnetic field to collectively influence the characteristics of electrostatic waves.

In this thesis, different theoretical models have been developed with the help of the basic equations i.e., the Vlasov Equation, the Equation of Continuity and Motion and Poisson's Equation to govern the behaviour of waves and instabilities. With the help of these equations, the expressions of frequency and the growth rate have been discovered and the effect of these have been analyzed on different plasma parameters like the gyroradius parameter, temperature, and relative density ratio etc.

These studies advance our knowledge of electrostatic waves and instabilities in a magnetized dusty plasma by providing important information regarding the way these waves include charged particle movement, wave-particle interactions, and the overall equilibrium of these systems. The waves and instabilities used in our work are Lower Hybrid Waves (LHWs), Electrostatic Ion Cyclotron Waves (EICWs) and Inhomogeneous Energy Density Driven Instability (IEDDI). LHWs are electrostatic low-frequency plasma waves due to the longitudinal oscillation of ions in a magnetized plasma and these waves can be studied in tokamak plasmas, and lunar dusty plasma and have recently received significant attention for

affecting the current drive at a very high density. The EICWs are one of the fundamental modes when the plasma is magnetized, and the electrons drift along magnetic field lines. The EIC is a field-aligned current-driven instability with one of the lowest threshold drift velocities among current-driven instabilities and these waves have applications in space plasma. A flow of energy from one region to another region can enable the mode to grow, giving rise to instability. This is the physical mechanism underlying the IEDDI and this instability can be used to explain a wide range of experiments in Earth's Ionosphere and other space applications.

Further studies on these waves and instabilities have been done in collisionless and collisional plasma. Collisions increase the interactions between charged particles and dust particles, changing the dispersion relation of the waves and exhibiting distinct characteristics. Moreover, these waves can be studied in the presence of the transverse direct current electric field. This electric field changes the dispersion characteristics of waves and the wave behaviour can be studied with different plasma parameters. Numerous analytical methods, including fluid theory and kinetic theory, have been used to study these waves. The two approaches possess unique mathematical equations guiding the behaviour of the waves. Additionally, using electron or ion beams can be used to induce the excitation of waves and instabilities. From fusion science to space plasma, it is essential to comprehend the physics of beam-plasma interactions. These systems have numerous uses, such as particle acceleration, diagnostics and plasma heating.

The investigation of electrostatic waves in magnetized dusty plasmas and the analysis of the impacts of various plasma parameters on wave dispersion characteristics are the main objectives of the present work. Our analytical model and the results from numerical calculations would help in understanding the experimental results from several leading groups worldwide.

LIST OF PUBLICATIONS

Publications in Peer Reviewed Journals

1. **Anshu**, Jyotsna Sharma, and Suresh C. Sharma, "In the existence of a transverse dc electric field, the kinetic theory of current-driven electrostatic ion cyclotron waves excitation in a magnetized dusty plasma", *Contributions to Plasma Physics* 62.9, e202200073 (2022).
2. **Anshu**, Jyotsna Sharma, and Suresh C. Sharma, "Kinetic treatment of lower hybrid waves excitation in a magnetized dusty plasma by electron beam", *Indian Journal of Physics* published on 29th August 2023.
3. **Anshu**, Jyotsna Sharma, and Suresh C. Sharma, "Analytical Modelling of Inhomogeneous Energy Density Driven (IEDD) Instability in a Magnetized Dusty Plasma Cylinder", *Brazilian Journal of Physics* on 54 (8), 2024.

Communicated Papers

1. **Anshu**, Jyotsna Sharma, and Suresh C. Sharma, "Investigating EIC Waves in Magnetized Dusty Plasmas: Unveiling the Impact of Collisions in the Presence of DC Electric Field".
2. **Anshu**, Jyotsna Sharma, and Suresh C. Sharma, "Kinetic Theory of Resonant Ion-Cyclotron Instability Induced by Ion Beams in Collisional Magnetized Dusty Plasmas Under the Influence of DC Electric Field".

Publications in Conferences

1. **Anshu**, Jyotsna Sharma and Suresh C. Sharma presented a poster entitled," Lower hybrid waves excitation by a relativistic electron beam in a magnetized dusty plasma: kinetic theory", *46th EPS Conference on Plasma Physics* held from 8th - 12th July 2019 at the University of Milan, Bicocca, Italy and published the same in ECA Vol. 43C, P2.3016, **ISBN:979-10-96389-11-7**.

International / National Conference Presentations

1. **Anshu**, Suresh C. Sharma and J. Sharma presented an oral talk entitled, "A study of EIC wave in the presence of magnetized dusty plasma using kinetic treatment", *2nd International Conference on Plasma Theory and Simulations (PTS -2022)*, Virtual mode by the Department of Physics, University of Lucknow, India, 20th – 22nd June, 2022. **(Best Oral Award)**
2. **Anshu**, Suresh C. Sharma and J. Sharma presented a poster entitled, "Theoretical Study of Dust Grain Parameters on Electrostatic Ion Cyclotron Waves in a Magnetized Plasma", *23rd International Conference on Cyclotrons and Their Applications (CYC2022)*, Virtual mode by the China Institute of Atomic Energy (CIAE) and Huazhong University of Science and Technology (HUST), China, 5th – 9th December 2022.
3. **Anshu**, Suresh C. Sharma and J. Sharma presented a poster entitled, **"**The collisional study of EIC waves in a magnetized dusty plasma with the inclusion of a dc electric field", *3rd International Conference on Plasma Theory and Simulations (PTS -2023)*, School of Physical Sciences, JNU 2023, India, 21st - 23rd September, 2023.
4. **Anshu**, Suresh C. Sharma and J. Sharma presented a poster entitled, **"**The Impact of Collisions on an Electrostatic Ion Cyclotron Wave in a Magnetized Dusty Plasma", *2nd International Conference on International Conference on Atomic, Molecular, Material, Nano and Optical Physics with Applications (ICAMNOP–2023),* Department of Applied Physics, DTU 2023, India, 20th - 22nd December, 2023. **(Best Poster Award)**

CONTENTS

Page No.

Chapter 7

LIST OF FIGURES

Chapter 3

Chapter 4

Chapter 5

LIST OF TABLES

1

INTRODUCTION

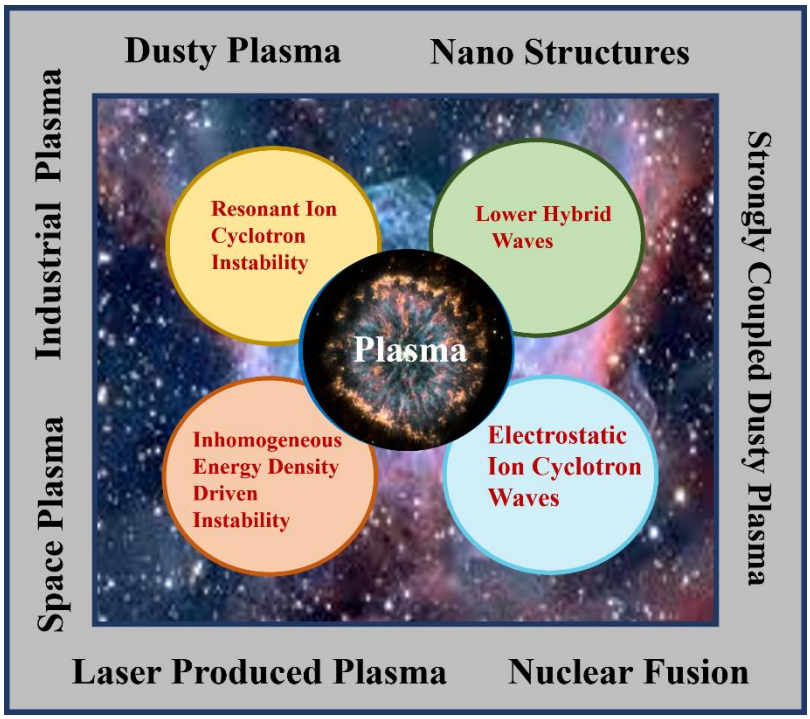

The goal of this chapter is to give a fundamental grasp of plasma and dusty plasma. It provides a thorough introduction to these plasmas, emphasizing key traits including the characteristics, formation and charging of dust grains and illuminating their pervasiveness in numerous situations. This chapter also explores the fascinating phenomenon of waves and instabilities that appear in dusty plasma, elucidating their relevance and implications. It investigates the various methodologies used to study these waves and instabilities in the context of dusty plasma. The prospective applications of these waves are also briefly discussed in this chapter, highlighting the broad influence and continued significance of waves and instabilities in modern science and technology. In this chapter, there is also a brief discussion of the objectives.

1.1 BACKGROUND

The human desire to explore the universe and comprehend natural principles has made plasma an interesting field of research. The fundamental and fascinating phase of matter known as plasma, sometimes known as the "fourth state of matter," has long captured the interest of researchers and scientists. Due to its special features, caused by the existence of highly charged ions and free electrons, it differs from the more typical states of matter, such as solids, liquids, and gases. From the intense heat of stars to the Earth's ionosphere, where the Northern Lights dance in the night sky, plasmas can be found throughout the universe. Contrarily, a large proportion of the universe's solid matter is found as dust, according to multiple observations [1, 2]. As a result, dust and plasma are the two basic elements that make up most of the universe. The intriguing interaction between these two fundamental components has led to the development of the dusty plasmas field, a whole new area of scientific study. Comprehending and utilizing the characteristics of plasmas and dusty plasmas is not only an area of exploration but also a practical requirement, across various domains. Plasma physics can reorganize our understanding of the universe because it has been a major milestone in the study of waves and instabilities. Additionally, it has a wide range of uses in plasma heating, tokamak, fusion, cosmology, astrophysics, food industry, radiation processing, proton therapy for cancer treatment and many more [3-6].

1.2 PLASMA

The phrase "plasma" has its origin in Greek, where it denotes “configuration” or “formation”. The term "fourth state of matter" was first introduced by W. Crookes to label the ionised medium within a gas discharge tube in 1879 [7]. The name "plasma" was first used to describe this distinct “fourth state of matter” in 1929 by Tonk and Langmuir while they were studying oscillations in an electric discharge tube [8].

In the expanse of the universe there exist four states of matter that occur naturally*: solid, liquid, gas and* ***plasma***. The basis for this classification is the thermal energy that the individual atoms or molecules contain, along with the strength of the interparticle binding interactions. The strongest interparticle bonds can be found in solids, whereas they are relatively weaker in liquids and almost non-existent in gases. As heat is given to solids, the thermal energy within the particles gradually outweighs the potential energy holding them together, leading to the breakdown of these interparticle interactions. This process causes a change in phase, turning the substance into a liquid. When a liquid is heated past a certain point, a change from a liquid

to a gas occurs. As heat is given to solids, the thermal energy within the particles gradually outweighs the potential energy holding them together, leading to the breakdown of these interparticle interactions. This process causes a change in phase, turning the substance into a liquid. When a liquid is heated past a certain point, a change from a liquid to a gas occurs. However, when a gas is exposed to extremely high temperatures, often at or above 10,000 K, the gas particles collide so intensely that they steal electrons from one another. This particular state, which consists of an amalgam of ions and electrons, is known as an ionised gas or simply a plasma as shown in Figure 1.1.

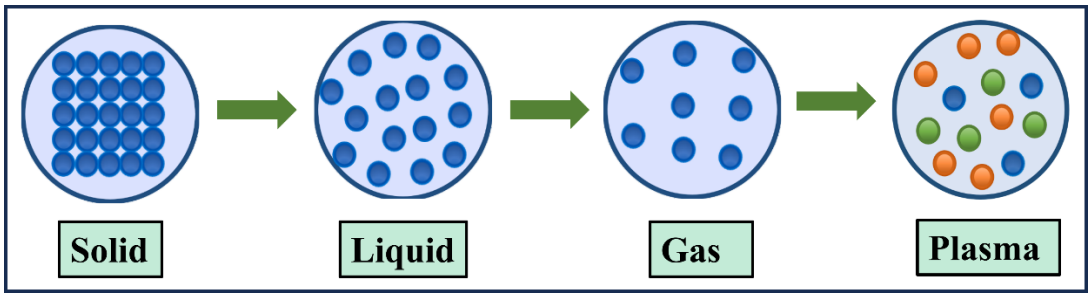

Figure 1.1: Diagram representing different states of matter

At a specific temperature, Saha's Equation can be used to determine the level of ionisation in a gas [9]

$$\frac{n_i}{n_n} \approx 2.4\times10^{21}\frac{T^{3/2}}{n_i}\exp(-U_i / k_B T)\,, \tag{1.1}$$

where n_i and n_n refers to the ionized gas density and neutral atoms density; U_i depicts the ionization energy; T is the temperature of gas (K) and k_B refers to the Boltzmann constant.

The gas is completely ionised when the number of ions exceeds the number of neutral particles at extremely high temperatures. This is the cause of the naturally occurring plasma in celestial bodies (with temperatures in the millions of degrees). Plasma accounts up nearly 99% of the visible universe.

Definition: Plasma comprises of three species i.e., neutral particles, electrons and ions which exhibits collective behaviour.

Any ionised gas cannot be classified as plasma. The ionised gas must satisfy some requirements such as **quasineutrality** and **collective behaviour** in order to be referred to as plasma [10]. The term "quasineutrality" refers to the property of plasmas where the number density of electrons is almost equal to the number density of ions for plasmas with lengths much longer

than the Debye length ($l >> \lambda_D$). Individual charges are shielded within plasmas by the existence of other charges, and this shielding effect extends across a specific length known as the "Debye length" i.e., λ_D. As a result, the plasma attains quasi-neutrality condition and number densities becomes equal. The expression for the screening length along with temperature T in a plasma with density n_e is given by

$$\lambda_D = \left(\frac{\varepsilon_0 k_B T}{n_e e^2} \right)^{1/2} . \tag{1.2}$$

Charged particles that constitute plasma move in such a way that they produce magnetic and electric fields. Due to these long-range electromagnetic forces, even distant particles can be affected. Essentially, the idea of collective behaviour suggests that the movement of these charged particles depends not just on the immediate surroundings but also on the state of the plasma farther away. The Debye sphere must contain a considerable number of particles N_D generally much larger than 1 i.e., $N_D >> 1$. This requirement is crucial since Debye shielding is only viable when the charge cloud contains enough particles.

Two fundamental scales are required for the description of a plasma: the length scale, denoted by the Debye length (λ_D), and the time scale (ω^{-1}). We have already discussed the idea of the Debye length, but in order to understand the time scale, it is necessary to appreciate the dynamic properties and behaviour of plasma oscillations. When electrons in a plasma are disturbed from their equilibrium positions, it results in a space-charge separation with the ions in background. In order to return the plasma to its neutral state, an electric field is created. This field pulls the electrons back to their initial places. The electrons, however, exceed their equilibrium positions as a result of inertia and begin oscillatory motion around the mean position, as seen in Figure 1.2. This oscillation is distinguished by a particular frequency known as the "plasma frequency." Due to ions higher mass, they are often thought of as being immobile in the background since they are unable to react to the high-frequency electric field's fluctuations. Plasma frequency (*rad/sec*) is mathematically defined as

$$\omega = \sqrt{\frac{ne^2}{\varepsilon_0 m'}} , \tag{1.3}$$

where e and m' defines the electronic charge and mass of plasma, n refers to the density, ε_0 is the vacuum permittivity. A fundamental criterion for any given plasma is that $\omega\tau > 1$, where τ

is the mean duration between particle collisions within the plasma. This criterion ensures that the motion of charged particles is still primarily driven by Coulombic forces by requiring that the plasma frequency be greater than the collision frequency.

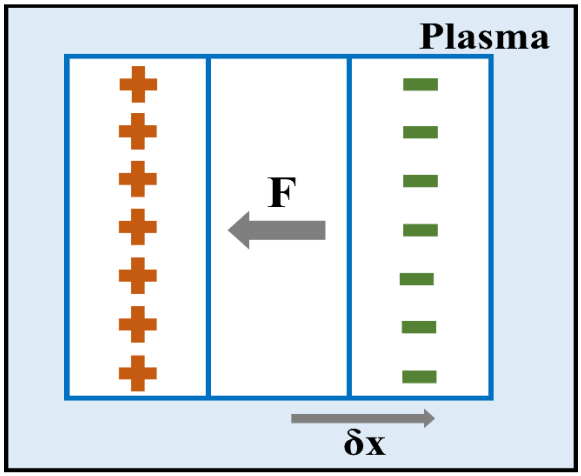

Figure 1.2: Schematic illustration of a plasma slab with displaced electrons (-) relocated by a distance of δx away from the stationary ions (+). A restoring force (F) pulls the electrons back and plasma oscillations set up about the equilibrium position.

1.3 DUSTY PLASMA

In 1924, Langmuir observed dusty plasma in a tungsten arc discharge, which was the beginning of the history of dusty plasmas. He explained the peculiar phenomena of charging tungsten vapours by attaching electrons to their surface and causing them to move while being affected by electric fields. In 1941, Spitzer [11] introduced the first statement of the theory that dust grains charge through photoelectric emission brought on by Ultraviolet (UV) light in the interstellar medium. Due to two different discoveries, the study of dusty plasma has experienced substantial growth. The first entailed the observation of dynamic radial spokes within Saturn's B Rings [12], which was done by the Voyager 2 spacecraft [13] (see Figure 1.3) and the second observation was that in the field of semiconductors, where the dust contamination comes from [14]. The study of dusty plasma has long been a subject of interest to astronomers, but at the same time, semiconductor producers were battling the lingering problem of dust contamination. The astronomy community and the semiconductor sector came together as a result of these issues and together they discovered a common framework for examining the fascinating phenomena related to the charge and movement of dust grains [15-17]. After extensive research, scientists have discovered an important characteristic of dusty

plasmas: the change from a fluid to a crystalline state, generally known as a "plasma crystal"[18-21].

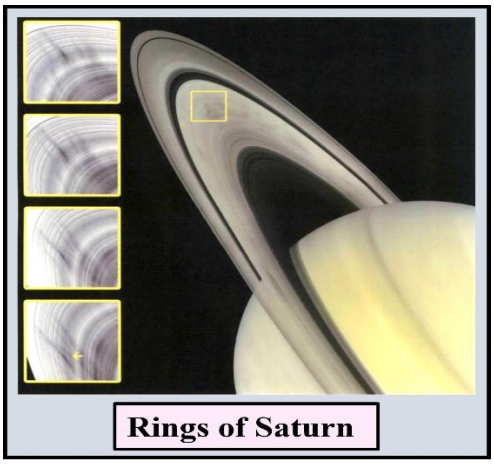

Figure 1.3: Picture illustrating the rings of Saturn with the radial spokes shown by the arrow mark [22].

Four-component plasma operating at low temperatures is known as dusty plasma. Along with the background of neutral particles, ions and electrons it also includes a further component made up of dust particles. The plasma system becomes even more complex as a result of the additional macroparticle, that's why it is also referred to as a "complex plasma" [23].

Definition: Dusty plasma comprises of four species i.e., electrons, ions, neutral particles and charged dust particles. They are electrically conducting gases that exist at low temperatures and are partially or fully ionized.

The size of dust grains ranges from nanometres to millimetres, and they are massive i.e., 10^{12} times the mass of proton. The dust grain charge for 1μm sized particles is of the order of 10^3e-10^4e, where "e" is the electronic charge. Typically, electrons, which are more agile than the heavier ions, interact with dust grains frequently, causing them to become negatively charged. This aspect not only heightens interest but is also extremely significant technologically. When a dust grain's radius "r" is considerably lower than its Debye length "λ_D" the particle is said to be "isolated" i.e., $r << \lambda_D < r_{D.}$. However, when $r << r_D < \lambda_D$, they are referred to as "non-isolated" and "r_D" denotes the average intergrain distance. Isolated charged dust grains have little effect on the plasma's characteristics, however non-isolated charged dust grains cause the plasma to experience collective phenomena. Due to the existence of this, not only the wave modes will be affected, but also the different dust wave modes will introduce. To fully

comprehend the collective wave phenomena coming from the dynamics of dust particles within the plasma, it is essential to comprehend the characteristics of dust grains.

1.3.1 CHARACTERISTICS

Dust grains can have an impact on the plasma surroundings in the same way that the plasma has an impact on the dust grains and they can also display novel and peculiar behaviour. Reassessing important characteristics, such as macroscopic neutrality, Debye length is beneficial for gaining a thorough understanding of the fundamental principles driving dusty plasmas. We will give thorough descriptions of these characteristics in the sections that follow.

1.3.1.1 QUASI-NEUTRALITY

Dust particles are principally charged in a dusty plasma system by absorbing electrons and ions from the background plasma. As a result, dusty plasma maintains its macroscopically neutral state in the absence of any external forces, much like an electron-ion plasma. This implies that the overall electric charge within the dusty plasma maintains at a net balance of zero in an equilibrium condition, in the absence of any external forces. The neutrality condition determines the densities in an equilibrium state is denoted by the formula

$$en_{0i} - en_{0e} + Q_d n_{0d} \approx 0, \tag{1.4}$$

where $n_{0i,0e,0d}$ represents the concentrations of ions, electrons and dust grains, respectively; $Q_d (= \pm Z_d e)$ denotes the positively (negatively) charged dust grains; Z_d is the dust charge state and e refers to the electronic charge. Note that depending on plasma parameters, the dust grains charge can change significantly.

1.3.1.2 DEBYE LENGTH

The Debye length is a crucial physical characteristic of dusty plasma: it specifies the length of the scale over which other charged particles (like ions) in the plasma are affected by the electric field of a single charged particle [24]. Charged particles are rearranged as a result, effectively concealing all electrostatic fields within the Debye distance which is known as "Debye Shielding" (see Figure 1.4). A dusty plasma is surrounded by negatively charged dust grains and an electron cloud when a positive potential is applied to it. On the other hand, a plasma is surrounded by positively charged dust grains and an ion cloud when a negative potential is applied to it. The charge distribution within the cloud is unaltered in the case of

perfect shielding, imitating a "cold" plasma. At finite temperatures, however, charged particles have a propensity to break off from the margins of these clouds, resulting in a potential of about $k_B T / e$ penetrating into the plasma which further results in insufficient shielding. The Debye length is a term used to describe the approximate thickness of a sheath or charged cloud. According to Shukla and Mamun [25], the Debye length has the following mathematical formula:

$$\lambda_D = \frac{\lambda_{De}\lambda_{Di}}{\sqrt{\lambda_{De}^2 + \lambda_{Di}^2}}, \tag{1.5}$$

where $\lambda_{De} = \sqrt{T_e / 4\pi n_{0e} e^2}$ and $\lambda_{Di} = \sqrt{T_e / 4\pi n_{0i} e^2}$ refers to the electron and ion Debye lengths, respectively.

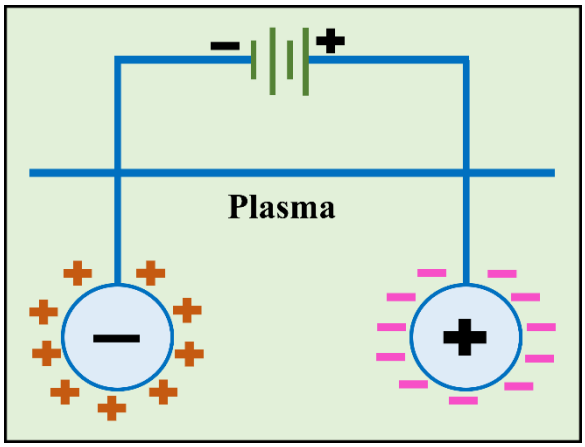

Figure 1.4: Diagram illustrating Debye Shielding

1.3.2 METHODS OF PRODUCTION

The production of dust grains is necessary for laboratory research since they are essential to the study of dusty plasmas. As dust grains are heavy so gravity naturally causes micron-sized grains in a plasma to fall to the bottom of the plasma. However, in order to prevent this gravitational settling due to their levitation and confinement within the plasma, an external field must be applied [26]. Due to the fact that the relaxation period for microparticles is typically far longer than the time it takes for them to get charged, this difficulty does not pose a serious problem in most laboratory plasma conditions. This has made it possible to create a dusty plasma by simply adding dust particles using techniques like sprinkling. Over time, numerous methods for producing dusty plasmas have been devised, each of which serves a particular purpose in terms of study and applications. Some of the methods are following:

- Using a Q-Machine, dust grains can be introduced into a plasma to create dusty plasmas [27, 28].
- They can also be created by growing dust inside plasmas made of chemically reactive gases like silane (SiH_4) and oxygen (O_2) [29].
- By suspending negatively charged 40 μm Silica (SiO_2) particles in an argon glow discharge [30].

To further understand the behaviour of completely magnetized dusty plasmas, the MDPX experiment for magnetised dusty plasmas was developed with regard to fusion plasmas and astrophysical plasmas [31]. In the following section, we'll give an overview of an important method to examine dusty plasmas in the laboratory.

1.3.2.1 Q-MACHINE (DUSTY PLASMA DEVICE)

A single ended Q-machine modified to spread dust throughout the plasma column is known as a dusty plasma device (DPD). Figure 1.5 provides a schematic illustration of a Q-machine to help explain the procedure. A fully ionised potassium plasma column with a length of roughly 80 cm and diameter of roughly 4 cm and is produced within this system. A heated Tantalum Plate, which reaches temperatures of about 2500K, is used to create this plasma through surface ionisation, which uses potassium atoms from an atomic beam oven. An approximately 4000 Gauss longitudinal magnetic field is used to confine the plasma column radially. In this configuration, the plasma has similar electron and K^+ ion concentrations of around 0.2 eV. A low pressure of roughly 10^{-6} Torr is maintained for the neutral gas. By making this choice, the mean free paths for electron-neutral and ion-neutral collisions are made to be substantially longer than the machine's physical dimensions. The dust dispenser system, which consists of a spinning metal cylinder and a fixed screen, encloses a portion of the plasma column. This configuration makes it easier to introduce dust particles into the plasma. The dust is initially loaded at the bottom of the rotating cylinder and then is moved to the top, where it is released and falls onto the stationary screen. A series of strong metal bristles attached within the cylinder sweeps across the screen's outside surface as it rotates. This technique makes sure that dust particles are distributed evenly throughout the plasma column. The bottom-collecting dust grains are then recycled to keep the dust density within the plasma column constant and this ongoing process of dust recycling is essential.

Typically, the materials used in these investigations as dust grains include hydrated aluminium silicate, or kaolin ($Al_2Si_2O_7nH_2O$), and alumina (Al_2O_3). The shape and size of these dust

particles varies. A comprehensive investigation of the samples is performed using an electron microscope. A portable Langmuir probe that travels the axis of the plasma column perpendicular to the magnetic field serves as the main testing tool. This probe measures the charge as well as an electron current by the suspended dust grains. The Q-machines are useful tools for studying instabilities and waves in dusty plasmas.

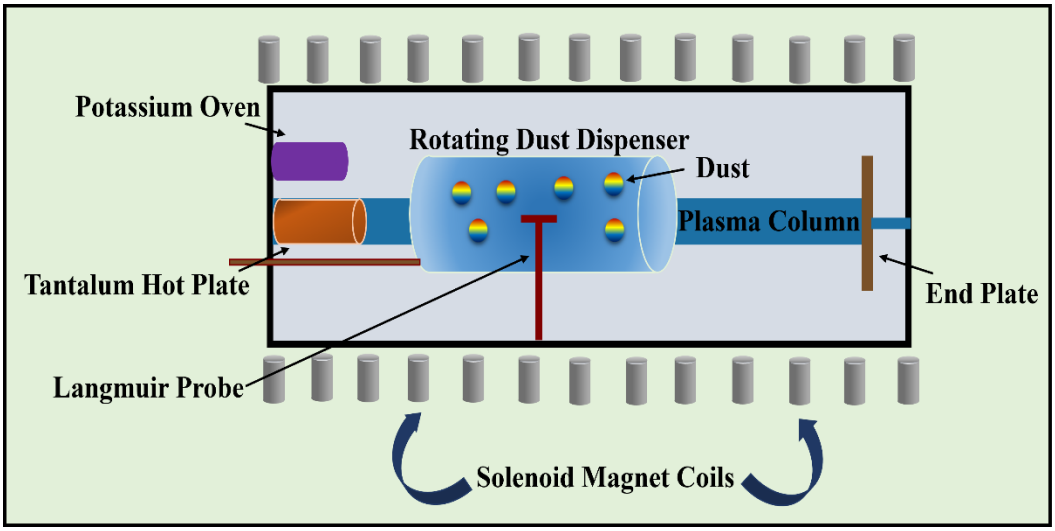

Figure 1.5: Illustration of a Q-machine configuration featuring a rotating dust dispenser and a movable Langmuir probe

1.3.3 CHARGING OF DUST GRAINS

Spitzer gave the first explanation of the procedures for governing dust grain charge in the interstellar medium in 1941 [11]. There are fundamentally three main mechanisms involved in charging dust grains [25]:

- Interactions between dust particles and photons.
- Interaction of dust grains with energetic particles such as electrons and ions.
- Interactions between plasma components and dust particles.

The charge on dust grains embedded in a plasma is created by a variety of methods such as [32]

- Ion Sputtering
- Thermionic Emission
- Photoelectron Emission by UV light
- Secondary Electron Emission
- Collection of electrons and ions from the plasma and many others.

As probes, dust grains alter their potential until an equilibrium is achieved when the overall current, encompassing contributions from ions (I_i), electrons (I_e), photoemission (I_{pe}) and secondary emission (I_{se}) on the surface of the dust grains, reaches zero.

$$\sum I = I_i + I_e + I_{pe} + I_{se} \approx 0 . \tag{1.6}$$

Dust grains adopt a negative potential, indicated as $\phi_S = V_S - V_p$, relative to the plasma in a conventional laboratory plasma environment where contributions from secondary electron emission and photoemission are negligible, this potential develops because of the high electron mobility until $I_i \approx I_e$. Here, V_S and V_p stands for the potential at the grain surface and at the plasma.

The charge on the dust grain is the culmination of different processes. The finding of an equilibrium charge on a dust grain can be quite challenging when all these processes are taken into consideration. In a plasma, electrons having mass m_e (temp T_e) and an ions having mass m_i (temp T_i), the electron thermal velocity is significantly greater than the ion thermal velocity and due to this the dust charge Q and its surface potential ϕ_S will become negative. On the surface of the dust grain, the plasma particles can also generate ion and electron currents. This overall current implies the charging rate dQ/dt of the dust grain by the various charging procedures. A particle engulfed in a plasma that is initially neutral will eventually become charged by bringing both ion and electron currents, following the relation [33, 34]

$$\frac{dQ}{dt} = I_i + I_e . \tag{1.7}$$

and $I_i + I_e = 0$ is the condition for charge equilibrium.

The method of charging a dust grain is simply shown in the Figure 1.6. The dust grain charge has the connection with the surface potential i.e., $Q = \phi_S C$, where C denotes the capacitance of dust grain. The surface potential of the dust grain augments as a result of the dust grain absorbing plasma ions and gaining a positive charge. In general, there is a negative potential at the surface, which attracts ions and repels electrons. To accomplish zero current at equilibrium, the ion current rises and the electron current falls. The electric charge of dust particles fluctuates over time because grain charging relies on the plasma potential and is unstable, making it necessary to examine it as a dynamic variable [35, 36].

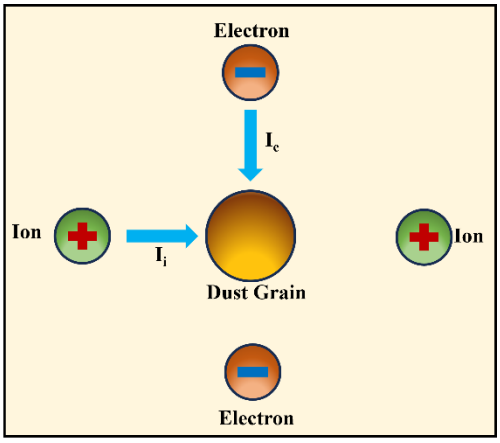

Figure 1.6: Schematic showing charging of dust grains

1.3.3.1 DUST CHARGE FLUCTUATIONS

It is evident that any fluctuations in dust charge can be caused by disturbances in plasma currents and ultimately leads to collective effects [32]. Following is the expression for dust charge fluctuations:

$$\frac{dQ_{1d}}{dt} = \frac{I_{1e}}{I_{0e}} + \frac{I_{1i}}{I_{0i}}, \tag{1.8}$$

where I_{1e} and I_{1i} refers to the perturbed plasma currents; $Q_{1d} = Q_d - Q_{0d}$ denotes the perturbed charge on dust. In order to facilitate their collective participation, dust particle sizes are kept substantially smaller than the plasma's Debye length and perturbation's wavelength.

The dynamics of dust charge fluctuations are given by:

$$\frac{dQ_{1d}}{dt} + \eta Q_{1d} = -|I_{0e}|\left(\frac{n_{1i}}{n_{0i}} - \frac{n_{1e}}{n_{0e}}\right), \tag{1.9}$$

where $\eta = \frac{|I_{0e}|e}{C_d}\left(\frac{1}{T_e} + \frac{1}{T_i - e\phi_{0S}}\right)$ represents the charging rate of dust and ϕ_{0S} refers to the equilibrium floating potential of dust grains; $C_d = \left(a\left(1 + \frac{a}{\lambda_{eD}}\right)\right)$ denotes the capacitance of dust grains and λ_{ed} represents the electron Debye length.

The variations in dust charge are controlled by changes in the perturbations in ion and electron densities within a plasma as well as a natural decay rate denoted as η, as shown clearly by Eq.

(1.9). The grain potential deviates from its equilibrium floating potential, these charge fluctuations physically diminish over time as a result of the opposing action of plasma currents [33].

1.3.3.2 MAGNETIZED AND UNMAGNETIZED DUSTY PLASMA

The behaviour of waves and instabilities within these complex systems are significantly influenced by the behaviour of magnetized and unmagnetized dusty plasmas, which are two crucial domains within the larger field of plasma physics.

Unmagnetized Dusty Plasma

Charged dust grains interact with the nearby charged plasma particles in unmagnetized dusty plasmas, which are characterised by the predominance of electrostatic forces. This complicated interaction greatly affects the electrostatic waves and instabilities that are observed. With the help of the electric fields present in these plasmas, dust charge fluctuations are processed, leading to the emergence of different modes of oscillation such as dust ion acoustic waves, dust acoustic solitons, and other coherent nonlinear structures [37, 38].

Magnetized Dusty Plasma

On the other hand, magnetized dusty plasmas add a fresh perspective to the research by taking the impact of magnetic fields into account. These fields have a major effect on the behaviour of the dust particles in addition to the charged plasma particles. Magnetic fields allow for the confinement and arrangement of dust grains and charged particles into special structures including dust crystals and dust chains, which are essential in controlling the behaviour of electrostatic waves. Different wave modes and instabilities, such as magnetohydrodynamic-like waves, manifest in magnetized dusty plasmas. The dynamics of the dust charge are significantly altered by magnetic fields, which also result in a variety of unique electrostatic wave behaviours and instabilities [39, 40]. These distinguishing characteristics are crucial for comprehending fusion plasmas, space plasmas, and astrophysical events where magnetic fields prevail in producing electrostatic waves and instabilities [41].

In addition to advancing our knowledge of dusty plasmas, the investigation of the aforementioned phenomena in both unmagnetized and magnetized dusty plasmas has important implications for the advancement of technology.

1.3.3.3 IMPORTANCE OF STUDY OF DUSTY PLASMA

Dusty plasmas have distinctive qualities that render them incredibly interesting research. In this section, we discuss the main factors that make the study of dusty plasmas so crucial.

- The introduction of dust particles into the typical electron-ion plasma alters the pre-existing wave modes such as dust acoustic waves [42]. Additionally, it adds a completely new domain of waves, instabilities and collective mode of oscillations that are conspicuously lacking in conventional plasmas.
- The timeframes governing their motions differ significantly due to the significant mass variations between the dust grains and the background plasma. Many of these intriguing occurrences can be seen with the unaided eye because the typical dust phenomena frequency can be as slow as a few Hertz. CCD cameras can record and capture each dust particle's unique motion with the help of laser illumination on the particles. The approach makes it possible to create a detailed phase space map that includes the positions and velocities of dust particles as they move across the plasma backdrop over time. This enhances our ability to explore the molecular details of plasma physics.
- The plasma parameters can be adjusted by altering the plasma conditions. Thus, the dusty plasma can realise several states of matter. The dusty plasma medium displays behaviour like a liquid state under the effect of moderate correlations and dust grains condense into an ordered crystal form under the effect of strong correlations. Many theoretical and experimental studies within dusty plasmas have examined a number of transport properties [43] of the fluid phase, including thermal conductivity [44], viscoelasticity [45], diffusion [46] and more. This provides a clear connection between the behaviour of the dusty plasma medium and a number of other physics fields, including complex fluid systems and soft condensed matter physics.

Dusty plasmas are also used for industrial purposes in addition to the above qualities. The following are some industrial and technological uses for the dusty plasmas [47]:

- The incorporation of nano-crystalline silicon in the layer of amorphous hydrogenated silicon particles created in silane plasmas has been proven to boost the efficiency and lifetime of silicon solar cells [48].
- Because of the lattice plane's micrometre-scale spacing, dusty plasma crystals are thought to be suitable for electromagnetic radiation at terahertz (THz) frequencies as

tunable filters [49]. This concept calls for employing dust crystals as Bragg diffraction gratings. The dust crystal interplanar distance depends on dust and plasma parameters, making the dust crystal filters tunable.

As a result, the field of dusty plasmas emerges as an intriguing and quickly developing multidisciplinary field that attracts a collaborative effort of physicists, chemists, and engineers across the world.

1.4 OCCURRENCE OF DUSTY PLASMAS

Across a wide range of spatial scales, dusty plasmas are extremely important in both technology applications and astrophysical phenomenon. Dusty plasmas can be created in laboratory environments including fusion experiment and plasma processing reactors and can also occur naturally in large-scale astronomical environments including comet tails, planetary rings etc. The occurrence as well as importance of dusty plasmas in both space and laboratory contexts will be briefly discussed in the sections that follow.

1.4.1 DUSTY PLASMA IN SPACE

Numerous astronomical phenomena and objects, such as noctilucent clouds, cometary tails, the nebula, planetary rings, interstellar clouds and others as shown in Figure 1.7, contain dust [50, 51]. Due to the frequent presence of charged dust particles in the vicinity of Earth and the interstellar medium, spacecraft may face both physical damage and electrical issues which will help us to comprehend phenomena like planetary rings and comet tails etc. Scientists are intrigued by presence of dust across space such as stream of particles moving around our solar system, in order to improve our understanding of planet and earth formation and if there is the possibility of life on other worlds [52, 53]. Due to the wide range of usage of dusty plasmas in diverse fields, it is crucial to understand the basic properties of space plasma. The space is composed by elements like hydrogen and helium, cosmic dust which is applicable for interstellar space also and particles in this space is defined by interstellar medium [51]. This medium primarily composed of hydrogen atoms and cosmic dust where the hydrogen atoms are much smaller than cosmic dust. There are a lot of dust grains throughout our solar system, including the sun and the planets that revolve around it. Lunar ejecta, anthropogenic pollution, micrometeoroids and space debris are a few of the sources of these dust grains throughout the solar system [54].

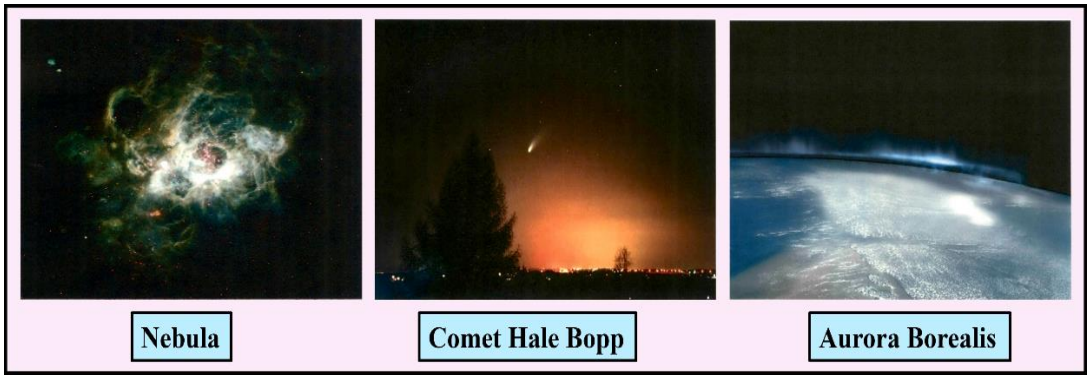

Figure 1.7: Picture illustrating Nebula NGC 604 in the Triangulum Galaxy M3 3 [*http://upload. wikimedia. org*]; Comet Hale Bopp[*http://www.eurastro.de*]; Northern lights above Earth's surface: the Aurora Borealis [*http://orbitingfrog. com*]

1.4.2 DUSTY PLASMA IN LABORATORY

The major differences between astrophysical and space dusty plasmas make laboratory dusty plasmas unique from them. They are kept in enclosed, regulated environments that have different structural, conductivity and thermal parameters that affect the behaviour of the dusty plasma. Furthermore, the presence of external circuits in dusty plasmas creates diverse boundary effects. The main goal of early studies was to reduce or stop dust particles from coming into touch with surfaces in order to control contamination in plasma processing reactors. This breakthrough opened up a broad spectrum of particle processing opportunities, encompassing bulk alterations like melting and crystallisation and surface changes like coating and etching and many others.

1.5 WAVES AND INSTABILITIES IN DUSTY PLASMAS

In both magnetized and unmagnetized dusty plasmas, different plasma oscillation modes have been seen. To study these different modes, waves in plasma are categorized in two types i.e., Electrostatic and Electromagnetic waves. These waves behave differently depending on their own characteristics and parameters. Electrostatic waves (ESWs) are particularly important in the context of dusty plasmas unlike electromagnetic waves because they are primarily controlled by the charged dust grains, producing peculiar behaviours and events. The dynamics and instability of dusty plasmas are strongly influenced by these waves, making them an important aspect for study into these intricate systems. ESWs are often low frequency waves having frequencies in the range from Hz to kHz because dust grains are massive which creates a significant gap in the time scales between the dust particles and the background plasma. ESWs are purely longitudinal in nature and the direction of propagation is parallel to the

electric field i.e., $\vec{k} \times \vec{E} = 0$. Additionally, based on the oscillating species i.e., ions and electrons, waves in plasmas can be further categorised. Electrons move more quickly in plasmas than ions do, mainly because they have a much smaller mass and due to this the electron thermal velocity is much larger than the ion thermal velocity resulting in larger electron temperature as compared to ion temperature. With the supposition of stationary and heavy ions, the electron mass affects modes associated to electrons. In contrast, ion mass affects modes connected to ions with the supposition of massless electrons and the Boltzmann relation characterises the redistribution of electrons. It's interesting to note that the Lower Hybrid mode and the Gould-Trivelpiece mode both depend on ion and electron masses. Another way to group several modes is according to the way they propagate which can be oblique, perpendicular and parallel to the stationary magnetic field in a magnetized dusty plasma. Moreover, these waves can be classified depending upon the collisionality of the dusty plasma i.e., collisionless and collisional dusty plasmas. The following are the key differences in both the plasmas:

- The interaction between dust grains and the charged particles increases due to the collisions which exhibit less collective behaviour of the wave than the collisionless plasma.
- Particle collisions enhance damping and energy loss during propagation of the waves in magnetized dusty plasma as compared to collisionless dusty plasma.
- Collisional plasmas have stronger dampening effects due to which waves travel shorter distances in plasma in comparison to collisionless plasma.
- Dust grains can participate in wave motion to a greater extent in collisionless plasmas than in collisional plasma.

These variations demonstrate the significant influence of collisionality on wave behaviour in dusty plasmas, emphasizing the necessity of studying both collisionless and collisional dusty plasma.

The wave propagation and the behaviour of dusty plasma are strongly influenced by the above aforementioned parameters. The different waves have diverse characteristics in magnetized dusty plasma depending on their plasma parameters and dispersion relation. Some of the waves and instabilities are briefly addressed in the section that follows.

1.5.1. LOWER HYBRID WAVES (LHWs)

The Lower Hybrid Waves are longitudinal oscillations of ions and electrons in a magnetized plasma. The dominant properties of these oscillations (involving both electrons and ions) are strongly electrostatic. The propagation direction of the wave should be exactly perpendicular to the magnetic field. The oscillation frequency is expressed as follows

$$\omega = \left[\left(\omega_{ci} \omega_{ce} \right)^{-1} + \omega_{pi}^{-2} \right]^{-1/2}, \tag{1.10}$$

where ω_{ci} and ω_{ce} refers to the cyclotron frequency of ions and electron respectively; ω_{pi} denotes the ion plasma frequency. This frequency is referred to as the lower hybrid frequency due to the fact that it is a "hybrid" or blend of two separate frequencies.

In the field of plasma physics, LHWs are undoubtedly useful, especially in the context of current driving in fusion studies [55]. These waves are capable of effectively transferring energy to the ions and electrons that constitute a plasma. Due to this feature, the researchers can control the energy deposited into the plasma, which can support and improve the plasma current, by carefully regulating the parameters of LHWs. These conditions are essential for maintaining the high temperatures and high pressures for nuclear fusion processes to take place. A promising method for reaching and sustaining the plasma characteristics required for realistic fusion energy production is lower hybrid current driving. LHWs can be driven by many methods like ion and electron beam and these waves are responsible for many linear and non-linear phenomenon. The excitation and dispersion properties of LHWs have been the subject of many experimentalists and theorists [56, 57].

1.5.2. ELECTROSTATIC ION CYCLOTRON WAVES (EICWs)

The Electrostatic Ion Cyclotron Waves are longitudinal oscillations of ions and electrons in a magnetized plasma. The propagation direction of the wave should be nearly perpendicular to the magnetic field. The dispersion relation is expressed as follows

$$\omega^2 = \omega_{ci}^2 + k^2 v_s^2, \tag{1.11}$$

where ω_{ci} refers to the cyclotron frequency of ions and v_S refers to the ion sound speed.

EICWs are one of the fundamental modes when the plasma is magnetized. The EICWs has a small but limited wave number along the field, allowing electrons travelling along the magnetic

field to destabilize it. The EICWs is a field-aligned current-driven instability with one of the lowest threshold drift velocities among current-driven instabilities [58]. In the field of dusty plasma, EICWs play a key role in the investigation and management of dust particle dynamics, which is essential for plasma processing and dust reduction in space environments. Additionally, comprehending these waves can aid in constructing and enhancing experiments and technologies dependent on plasma. EICWs have significance in comprehending cometary tail dynamics and planetary ring formation in astronomical scenarios [59]. These waves are excited by various methods and the dispersive properties of these waves has been a subject of interest by many experimentalists and theorists [60, 61].

1.5.3. INSTABILITIES IN DUSTY PLASMA

The introduction of diverse free energy sources can cause dusty plasma to become unstable that may be brought on by outside influences, pressure gradients, localization of electric field, changes in dust charge, or the movement of electron or ion beams within the plasma. In addition to these aspects, dusty plasma can also exhibit conventional hydrodynamic instabilities including Inhomogeneous Energy Density Driven, Rayleigh Taylor, Kelvin Helmholtz, and other parametric instabilities. Due to their importance in understanding phenomenon including the solar wind, the magnetopause, the Earth's ionosphere, and fluid dynamics, these instabilities have attracted a lot of interest. Understanding the mechanisms governing the emergence of voids and increase or dampening of wave amplitudes detected in laboratory and space plasmas, demands investigation into these instabilities and the dispersion relationship with various plasma properties has been established by many researchers [2, 62, 63]. The next section provides an explanation of one of the instabilities.

1.5.3.1 INHOMOGENEOUS ENERGY DENSITY DRIVEN INSTABILITY (IEDDI)

The Inhomogeneous Energy Density Driven Instability was primarily suggested by Ganguli et al. and relies on the nonlocal approximation [64, 65]. A flow of energy from one region to another region can enable the mode to grow, giving rise to instability, which is referred to as the IEDDI [66]. This is the physical mechanism underlying the IEDDI. IEDD waves have a wide frequency range that is close to the ion cyclotron frequency and typically propagate in the $\vec{E}\times\vec{\mathrm{B}}$ direction [67]. The parameter $R = k_\theta v_E(r)/k_z v_{ed}$, the ratio of the azimuthal and axial doppler shifts in cylindrical coordinates is the key parameter to determine which type of waves exist in the system [67]. For R << 0.1, the electrostatic ion cyclotron waves are current-driven (EIC Instability) [68]. For R >> 0.1, the EIC waves are driven by the transverse, localized, dc

electric field (IEDDI) [66]. An IEDDI can explain a wide range of experiments in Earth's ionosphere and might be beneficial for other space applications [69, 70]

The aforementioned waves and instabilities can also be studied in the presence of transverse direct current electric field. This electric field changes the dispersion characteristics of waves and the wave behaviour can be studied with different plasma parameters. This expanded understanding has applications in the domains of materials science, fusion research, and space physics. Additionally, these waves and instabilities can be excited by employing electron or ion beams. From fusion science to space plasma, it is essential to comprehend the physics of beam plasma interactions. These systems have numerous uses, such as particle acceleration, diagnostics and plasma heating.

1.6 BEAM PLASMA INTERACTION

The interaction of intense particle beams with dusty plasmas is a complex and fascinating event from a scientific perspective. The kinetics of these interactions shed light on basic plasma phenomenon and offer priceless information for a variety of uses, such as controlled fusion and space exploration [71, 72].

A large number of oscillation modes can be produced within the plasma, and some of these modes cause the amplitudes of these oscillations to be amplified at the expense of the energy of the beam. The fundamental principle governing how beams and plasma interact is that as a beam travel through plasma, if its frequency coincides with that of a wave, it converts its energy into wave energy resulting in the growing wave. The core of this fascinating field of study is underpinned by these beam-energy interactions, which demand that waves and particles maintain phase matching for as long as possible. These interactions can occur via Cerenkov and cyclotron interaction. The notion of employing electron or ion beam for the excitation of the wave in the magnetospheric and ionospheric plasma was firstly discovered in 1970 and this innovative concept took shape as the French-Soviet ARAKS project [73]. The beam is used as a plasma mode radiating antenna in a number of experiments to examine ESWs produced by electron or ion beams [74, 75]. A beam-plasma system is capable of supporting several plasma modes due to momentum and energy conservation.

1.7 DIFFERENT APPROACHES TO STUDY WAVES AND INSTABILITIES

Numerous unique methods have been devised and used in the quest to understand the complex nature of waves and instabilities in dusty plasma. These methods provide a different

perspective on the behaviour of waves and have different dynamics respectively. This section will examine a variety of methodologies, including Fluid Theory, Kinetic Theory, and Kappa Distribution Theory, shedding light on the intricacy of wave investigations and instabilities in the area of dusty plasma. Some of the approaches will also be briefly explored.

1.7.1 FLUID THEORY

The dynamics of waves in diverse plasma environments is examined using the basic structure of fluid theory. It offers an insightful viewpoint on instabilities, wave propagation, and the intricate interaction of particles and fields within plasma. Plasma is understood in fluid theory as a continuous, macroscopic fluid having parameters involving density and velocity. This theory is based on a set of macroscopic equations called the fluid equations, comprising the equation of motion and continuity equation.

The equation of motion says

$$m\frac{d\vec{v}}{dt} = -e\vec{E} - \frac{e}{c}\vec{v}\times\vec{B}, \tag{1.12}$$

where $\vec{E}$ and $\vec{B}$ are the electric and magnetic field; e refers to an electronic charge; $\vec{v}$ refers to the particle velocity; m is the mass of the particle and

the Continuity Equation follows

$$\frac{\partial n}{\partial t} + \nabla.(n\vec{v}) = 0, \tag{1.13}$$

where n refers to the number density.

Both these equations contribute to the description of the behaviour of charged particles in plasmas and will govern the dispersion relation between frequency and wave number.

The dispersion relation consists of two parts i.e., real frequency and imaginary part [76]. The real frequency can be evaluated as

$$\varepsilon_r(\omega,k)\big|_{\omega=\omega_r} = 0. \tag{1.14}$$

and the imaginary part as

$$\omega_i = \left.\frac{-\varepsilon_i(\omega,k)}{\frac{\partial \varepsilon_r(\omega,k)}{\partial \omega}}\right|_{\omega=\omega_r} . \tag{1.15}$$

The appropriate dispersion relation comprises all the information on the wave mode's propagation.

1.7.2 KINETIC THEORY

The kinetic theory is a different theory that is employed in analysis of the waves. Plasma is understood in kinetic theory as a microscopic description of a plasma including the individual motions and interactions of charged particles. The evolution of the distribution function of charged particles in a plasma is described by the Vlasov equation, a key equation in kinetic theory. The Vlasov Equation is as follows

$$\frac{\partial f}{\partial t} + (\vec{v}.\,\Delta)\, f - \frac{e}{m}\left(\vec{E} + \frac{1}{c}\vec{v}\times\vec{B}\right).\frac{\partial f}{\partial \vec{v}} = 0\,, \tag{1.16}$$

where f is the distribution function.

It is possible to study the behaviour of waves using both theories. When a simplified explanation of plasma behaviour is adequate, fluid theory is used and when a more thorough and precise comprehension of plasma behaviour is required, kinetic theory is necessary.

In comparison to fluid theory, kinetic theory provides a more efficient method for solving analytical models as it deals with the interactions of an individual motion and provide in depth understanding of the wave's behaviour.

1.8 APPLICATIONS OF PLASMA

Across many different fields of technology and science, dusty plasmas, an intriguing interdisciplinary area, has a broad spectrum of possibilities. These applications continue to develop and have attracted considerable curiosity from researchers:

- **Nuclear Fusion**

The most demanding use of artificial plasma is to establish controlled thermonuclear fusion, which has enormous potential for power production. The study of dusty plasma is pertinent to nuclear fusion. With the help of high density plasma, we can achieve confinement and the high temperature plasma [16].

❖ **Industrial Plasma**

Plasma processing is the most significant and essential application of industrial plasmas. The best known use of it is in the manufacture of semiconductor gadgets for use in electronics. Other significant uses include those in optics, polymers, bio-medicines, waste management, vehicles, defence, solar energy, among other fields [47]. Surface treatment is a persistent subject in numerous new and present applications. For these applications, plasma enables the conception of novel goods that would be hard to produce using conventional production techniques. Environmental concerns are crucial since plasma-based applications produce relatively little industrial waste, which is beneficial for the environment.

❖ **Dusty Plasma**

In dusty plasma applications and research, plasma plays a very significant role. The addition of dust grains in plasma changes the behaviour of waves. They are employed in many different domains, including materials processing and astronomy. The study of phenomena like dust clouds in space are made possible by plasma's assistance in controlling the dynamics and charge of dust grains.

❖ **Nanostructures**

There are many implications for plasma technology in nanostructures, including carbon nanotubes (CNTs) and graphene. CNTs can have their surfaces functionalized by plasma treatment, which improves their ability to interact with polymers or various other substances for creating composites. It is possible to precisely alter the electrical characteristics of graphene via doping and plasma etching, which makes transistors, graphene-based sensors, and energy storage devices possible. Significant tools for modifying nanostructure characteristics for a range of materials science and electronics applications are provided by these plasma-based methods.

The wide variety of applications including laser produced plasma, plasma processing of materials, welding, medical science etc. as shown in Figure 1.8 emphasises the value of exploring plasmas in both the laboratory and space.

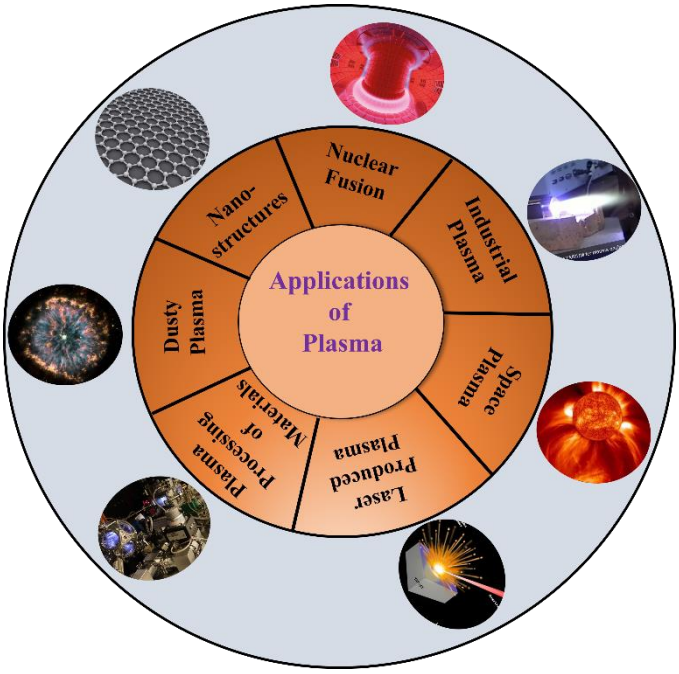

Figure 1.8: Diagram showing various applications of Plasma

1.9 ORGANIZATION OF THE THESIS

The objective of the thesis is deeply driven by the compelling interests of both experimental and theoretical realms. The thesis is motivated to understand the modelling of electrostatic waves in a magnetized dusty plasma. Our research is primarily focused on creating an analytical model for LHWs, EICWs, and IEDDIs driven by different methods, as well as on evaluating frequency and growth rate expressions with various plasma parameters and observing the behaviour of waves and instabilities. By developing our analytical model, we could better comprehend experimental results from many prominent groups of researchers. The thesis is organized into seven chapters, each focused to an investigation of the physical phenomena intrinsic to the waves and instabilities.

- **Chapter 1:** The first chapter delve into the world of plasma and dusty plasma. We provide the basic idea to these topics including information about how dust grains are formed and how they get charged up. Additionally, we explore the electrostatic ion cyclotron waves (EICWs), lower hybrid waves (LHWs) and the inhomogeneous energy density driven instability (IEDDI) that can occur in a magnetized dusty plasma. This chapter cover different mathematical approaches used to determine wave dispersion equation. Furthermore, this chapter discusses beam plasma interaction and thoroughly examines the applications of plasma.

- **Chapter 2:** In this chapter, we have developed a theoretical model of Lower Hybrid Waves (LHWs) driven by an electron beam using a kinetic treatment. The electron beam propagates through a magnetized dusty plasma cylinder which consists of dust grains, electrons, and positively charged potassium ions (K+). The dispersion relation of the same has been developed. The dust grains impact has been discussed on the growth rate of LHWs. The critical drift velocity for excitation of the mode is very essential to understand the unstable mode. The current study has applications in plasma processing of material experiments and has recently received significant attention for affecting the current drive at a very high density.
- **Chapter 3:** We have developed the theoretical model for the electrostatic ion-cyclotron waves (EICWs) in the existence of a transverse direct current (dc) electric field in a collisionless magnetized dusty plasma using the kinetic theory model in this chapter. It is examined that the introduction of dc electric field in the presence of dust grains can alter the dispersion properties of EIC waves. The developed model accounts for the various plasma parameters like electron to ion temperature ratio, and finite gyroradius parameter etc. Moreover, the critical drift velocity for the excitation of the mode with negatively charged dust grains and electron to ion temperature ratio has been studied. The impact of dust grains on the low-frequency waves has also been studied. The present study suggests that after the addition of an electric field, the amplitude of the wave increases. The present work has various applications in space and planetary systems.
- **Chapter 4:** After the analysis of the various plasma parameters on EIC waves in collisionless plasma, this chapter broadens the study by developing the same theoretical model in the collisional plasma for a more comprehensive understanding of the plasma system. The effect of collisions in the occurrence of transverse dc electric field and negatively charged dust grains has been explored using the kinetic theory. The dispersion characteristics of EIC wave alters in the presence of collisions. Plasma parameters such as finite gyro-radius, relative density ratio, magnetic field, dust density and collisional frequency are all taken into account by our model to find out the impact on EIC waves. In addition, the critical drift velocity is studied for the unstable mode. The collisional effects of the particles with various plasma parameters, i.e., gyro-radius, temperature etc. on an EIC wave have been examined. It has been found that the effect of an electron collision destabilizes and is vital for the EIC wave excitation whereas the effect of an ion collision stabilizes the wave. Additionally, the influence of dust particles

was explored. The present study observed that the wave amplitude was lower in collisional plasma than in collisionless plasma. The present study can be applied in various fields, from astrophysics and space physics to laboratory plasma research.

- **Chapter 5:** After studying the effect of collisions on EICWs in a magnetized dusty plasma, in this chapter, we have developed an analytical model in the collisional plasma driven by an ion beam in the presence of a dc electric field using the kinetic treatment. An ion beam parallel to the magnetic field is seen to be the source of ion cyclotron instability with dust particles in a collisional magnetized plasma. The dispersion relation of instability is significantly changed by the interaction of ion beams in a collisional magnetized dusty plasma, relying on properties of the dust grains, beam, and plasma parameters via kinetic theory. The collisional effects of the particles and temperature analysis with various plasma parameters have been examined. Additionally, the influence of dust particles was explored. The observed instability may be related to a bounded dusty plasma system and could be useful in space plasma physics.
- **Chapter 6:** Previously, all theoretical model was developed using the kinetic treatment approach but, in this chapter, we have developed an analytical model of inhomogeneous energy density driven instability (IEDDI) while incorporating the effect of dust particles in a collisional magnetized plasma cylinder using the fluid theory. The localization of the electric field gives rise to IEDDI. Plasma parameters such as relative density ratio, dust density and size are all taken into account to find out the impact on IEDDI. The paper conducted a comparison of the existence and non-existence of dust grains and analyzed their effect on different plasma parameters. The findings revealed that the introduction of dust grains changes the properties of instability and their effect on various parameter. The response of dust grains number density and dust grain size on IEDDI was evaluated. Further, the effects of an electric field on IEDDI were also examined. The present study can explain a wide range of experiments in Earth's ionosphere, and might be beneficial for other space applications. Kinetic theory offers a more effective approach for solving analytical models compared to fluid theory.
- **Chapter 7:** This last chapter provides an overview of the results of the thesis work. Furthermore, the future scope of this work was also been included.

REFERENCES

[1] A. Bouchoule, Dusty Plasmas: Physics, Chemistry and Technological Impacts in Plasma Processing *Wiley* **77,** (1999).

[2] A.A. Mamun, P.K. Shukla, *Physica Scripta* **2002**, 107 (2002).

[3] H. Tanaka, M. Mizuno, K. Ishikawa, S. Toyokuni, H. Kajiyama, F. Kikkawa, M. Hori, *Physics of Plasmas* **1**, 150 (2018).

[4] S.A. Mir, M.A. Shah, M.M. Mir, *Food and Bioprocess Technology* **9**, 734 (2016).

[5] R. Hong, Z. Yang, G. Niu, G. Luo, *Plasma Science and Technology* **15**, 318 (2013).

[6] S. Lee, T.Y. Tou, S.P. Moo, M.A. Eissa, A.V. Gholap, K.H. Kwek, S. Mulyodrono, A.J. Smith, Suryadi, W. Usada, *American Journal of Physics* **56**, 62 (1988).

[7] W. Crookes, *Philosophical Transactions of the Royal Society of London* **170,** 135 (1879).

[8] I. Langmuir, *Physical Review* **33**, 195 (1929).

[9] F.F. Chen, Introduction to Plasma Physics, *Springer Science and Bussiness Media*, (2012).

[10] J.A. Bittencourt, Fundamentals of Plasma Physics, *Springer- Verlag* (2004).

[11] L. Spitzer Jr, *Journal of the Royal Astronomical Society of Canada* **72**, 349 (1978).

[12] B.A. Smith, L. Soderblom, R. Beebe, J. Boyce, G. Briggs, A. Bunker, S.A. Collins, C.J. Hansen, T.V. Johnson, J.L. Mitchell, *Science* **212**, 163 (1981).

[13] B.A. Smith, L. Soderblom, R. Batson, P. Bridges, J.A.Y. Inge, H. Masursky, E. Shoemaker, R. Beebe, J. Boyce, G. Briggs, *Science* **215**, 504 (1982).

[14] G.S. Selwyn, J. Singh, R.S. Bennett, *Journal of Vacuum Science & Technology A* **7**, 2758 (1989).

[15] J.Y.N. Cho, M.C. Kelley, *Reviews of Geophysics* **31**, 243 (1993).

[16] J. Winter, *Plasma Physics and Controlled Fusion* **46**, B583 (2004).

[17] J. Winter, *Physics of Plasmas* **7**, 3862 (2000).

[18] S. Ichimaru, *Reviews of Modern Physics* **54**, 1017 (1982).

[19] J.H. Chu, J.-B. Du, I. Lin, *Journal of Physics D: Applied Physics* **27**, 296 (1994).

[20] Y. Hayashi, K. Tachibana, *Jpn. J. Appl. Phys., Part* **2**, L804 (1994).

[21] A. Melzer, T. Trottenberg, A. Piel, *Physics Letters A* **191**, 301 (1994).

[22] R.L. Merlino, J.A. Goree, *Physics Today* **57**, 32 (2004).

[23] O. Ishihara, *Journal of Physics D: Applied Physics* **40**, R121 (2007).

[24] F.F. Chen, Introduction to Plasma Physics and Controlled Fusion, *Springer* (1984).

[25] P.K. Shukla, A.A. Mamun, Introduction to Dusty Plasma Physics, *CRC Press* (2015).

[26] L. Boufendi, A. Bouchoule, *Plasma Sources Science and Technology* **3**, 262 (1994).

[27] W. Xu, B. Song, R.L. Merlino, N. D'Angelo, *Review of Scientific Instruments* **63**, 5266 (1992).

[28] R.L. Merlino, *Plasma Physics Applied* **5**, 73 (2006).

[29] J.H. Chu, I. Lin, *Physical Review Letters* **72**, 4009 (1994).

[30] E. Thomas Jr, M. Watson, *Physics of Plasmas* **7**, 3194 (2000).

[31] E. Thomas, U. Konopka, D. Artis, B. Lynch, S. Leblanc, S. Adams, R.L. Merlino, M. Rosenberg, *Journal of Plasma Physics* **81**, 345810206 (2015).

[32] A. Barkan, N. D'Angelo, R.L. Merlino, *Physical Review Letters* **73**, 3093 (1994).

[33] E.C. Whipple, T.G. Northrop, D.A. Mendis, *Journal of Geophysical Research: Space Physics* **90**, 7405 (1985).

[34] M.R. Jana, A. Sen, P.K. Kaw, *Physical Review E* **48**, 3930 (1993).

[35] S.V. Vladimirov, *Physics of Plasmas* **1**, 2762 (1994).

[36] C. Cui, J. Goree, *IEEE Transactions on Plasma Science* **22**, 151 (1994).

[37] B. Tian, Y.-T. Gao, *The European Physical Journal D-Atomic, Molecular, Optical and Plasma Physics* **33**, 59 (2005).

[38] R. Bharuthram, P.K. Shukla, *Planetary and Space Science* **40**, 973 (1992).

[39] P.K. Shukla, *Astrophysics and Space Science* **264**, 235 (1998).

[40] L.F. Ziebell, R.d.S. Schneider, M.C. de Juli, R. Gaelzer, *Brazilian Journal of Physics* **38**, 297 (2008).

[41] D.A. Mendis, M. Rosenberg, *Annual Review of Astronomy and Astrophysics* **32**, 419 (1994).

[42] N.N. Rao, P.K. Shukla, M.Y. Yu, *Planetary and Space Science* **38**, 543 (1990).

[43] Z. Donko, J. Goree, P. Hartmann, B. Liu, *Physical Review E* **79**, 026401 (2009).

[44] Z. Donkó, P. Hartmann, *Physical Review E* **69**, 016405 (2004).

[45] J. Ashwin, A. Sen, *Physical Review Letters* **114**, 055002 (2015).

[46] W.-T. Juan, I. Lin, *Physical Review Letters* **80**, 3073 (1998).

[47] R.L. Merlino, *Plasma Physics Applied* **81**, 73 (2006).

[48] M. Cavarroc, M. Mikikian, G. Perrier, L. Boufendi, *Applied Physics Letters* **89**, 013107 (2006).

[49] M. Rosenberg, D.P. Sheehan, P.K. Shukla, *IEEE Transactions on Plasma Science* **34**, 490 (2006).

[50] O. Havnes, L.I. Næsheim, T.W. Hartquist, G.E. Morfill, F. Melandsø, B. Schleicher, J. Trøim, T. Blix, E. Thrane, *Planetary and Space Science* **44**, 1191 (1996).

[51] U. De Angelis, *Physica Scripta* **45**, 465 (1992).

[52] C.K. Goertz, G. Morfill, *Icarus* **53**, 219 (1983).

[53] C.A. McGhee, R.G. French, L. Dones, J.N. Cuzzi, H.J. Salo, R. Danos, *Icarus* **173**, 508 (2005).

[54] D.A. Mendis, *Plasma Sources Science and Technology* **11**, A219 (2002).

[55] G.T. Hoang, A. Bécoulet, J. Jacquinot, J.F. Artaud, Y.S. Bae, B. Beaumont, J.H. Belo, G. Berger-By, J.P.S. Bizarro, P. Bonoli, *Nuclear Fusion* **49**, 075001 (2009).

[56] K. Papadopoulos, P. Palmadesso, *Naval Research Laboratory Report* (1975).

[57] A. Varma, A. Kumar, *Optik* **231**, 166326 (2021).

[58] G. Ganguli, Y.C. Lee, P.K. Chaturvedi, P.J. Palmadesso, S.L. Ossakow, D.C. Naval Research Lab Washington, *Naval Research Lab, Washington DC* (1988).

[59] M.K. Dougherty, N. Achilleos, N. Andre, C.S. Arridge, A. Balogh, C. Bertucci, M.E. Burton, S.W.H. Cowley, G. Erdos, G. Giampieri, *Science* **307**, 1266 (2005).

[60] A. Barkan, N. D'Angelo, R.L. Merlino, *Planetary and Space Science* **43**, 905 (1995).

[61] S.C. Sharma, J. Sharma, *Physics of Plasmas* **17**, 043704 (2010).

[62] F. Verheest, *Space Science Reviews* **77**, 267 (1996).

[63] M.E. Koepke, W.E. Amatucci, J.J. Carroll Iii, V. Gavrishchaka, G. Ganguli, *Physics of Plasmas* **2**, 2523 (1995).

[64] G. Ganguli, Y.C. Lee, P.J. Palmadesso, *The Physics of Fluids* **31**, 823 (1988).

[65] G. Ganguli, P. Palmadesso, Y.C. Lee, *Geophysical Research Letters* **12**, 643 (1985).

[66] M.E. Koepke, J.J. Carroll Iii, M.W. Zintl, C.A. Selcher, V. Gavrishchaka, *Physical Review Letters* **80**, 1441 (1998).

[67] M.E. Koepke, W.E. Amatucci, J.J. Carroll Iii, T.E. Sheridan, *Physical Review Letters* **72**, 3355 (1994).

[68] M.E. Koepke, W.E. Amatucci, *IEEE Transactions on Plasma Science* **20**, 631 (1992).

[69] A.A. Chernyshov, A. Spicher, A.A. Ilyasov, W.J. Miloch, L.B.N. Clausen, Y. Saito, Y. Jin, J.I. Moen, *Physics of Plasmas* **25**, 042902 (2018).

[70] A.M. DuBois, E. Thomas Jr, W.E. Amatucci, G. Ganguli, *Journal of Geophysical Research: Space Physics* **119**, 5624 (2014).

[71] N.J. Sircombe, R. Bingham, M. Sherlock, T. Mendonça, P. Norreys, *Plasma Physics and Controlled Fusion* **50**, 065005 (2008).

[72] D.N. Gupta, A.K. Sharma, *Laser and Particle Beams* **22**, 89 (2004).

[73] J. Lavergnat, R. Pellat, *Journal of Geophysical Research: Space Physics* **84**, 7223 (1979).

[74] S.C. Sharma, M.P. Srivastava, M. Sugawa, V.K. Tripathi, *Physics of Plasmas* **5**, 3161 (1998).

[75] N. Nuwal, I.D. Kaganovich, D.A. Levin, *Physics of Plasmas* **29**, 100702 (2022).

[76] N.A. Krall, A.W. Trivelpiece, R.A. Gross, *American Journal of Physics* **41**, 1380 (1973).

2

Kinetic treatment of lower hybrid waves excitation in a magnetized dusty plasma by electron beam

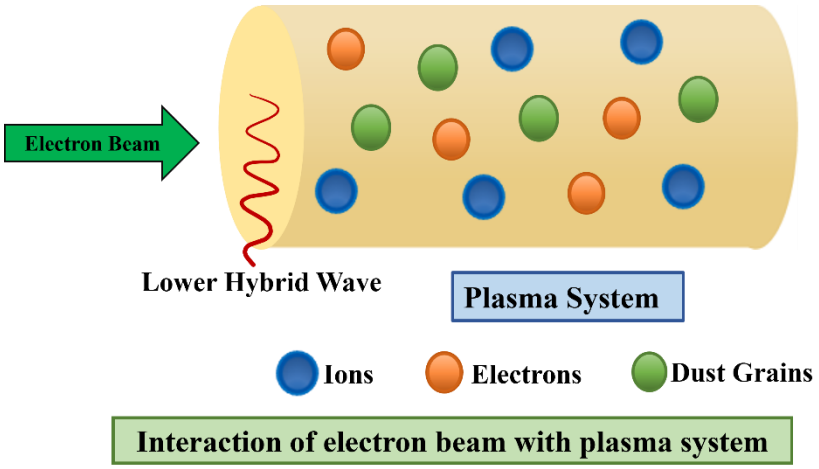

In this chapter, the theoretical model of electrostatic Lower Hybrid Waves (LHWs) has been investigated using a kinetic treatment involving an electron beam. This electron beam propagates through a magnetized dusty plasma cylinder that consists of dust grains, electrons, and positively charged potassium ions (K+). The excitation of LHWs via Cerenkov interaction is driven to instability. The population of charged dust particles affects the growth rate of LHWs in a plasma that has been stimulated by an electron beam, and a dispersion relation has been developed. The dust grain particles impact has been discussed on the growth rate of LHWs. Furthermore, the critical drift velocity for excitation of the mode is derived.

PUBLICATION

Anshu, Jyotsna Sharma, and Suresh C. Sharma, "Kinetic treatment of lower hybrid waves excitation in a magnetized dusty plasma by electron beam", *Indian Journal of Physics* published on 29 August 2023.

2.1 INTRODUCTION

In the captivating realm of beam plasma systems [1,2], a multitude of waves and instabilities exist such as upper hybrid waves [3], ion-cyclotron waves [4], and two-stream instabilities [5] but amongst them, the lower hybrid waves (LHWs) [6] are one of the most prevalent waves. For the last several years, there has been a significant surge of interest in studying quasi-static LHWs. The linear theory of excitation of electrostatic LHWs without charged dust grains by electron beams in plasma has been studied by Papadopoulos and Palmadesso [7]. Lower hybrid waves are electrostatic low-frequency plasma waves due to the longitudinal oscillation of ions in a magnetized plasma. LHWs have been observed in a few experimental and theoretical studies [8,9,10,11,12,13,14,15] by utilizing an ion and a beam of electrons. Thus, these waves are valuable in plasma warming devices to a high degree. Chang [9] had experimentally observed that the maximum growth rate of LHWs was achieved when the phase velocity, together with the magnetic field, was practically identical to the thermal velocity of the electrons. Prakash et al. [10] studied LHWs driven by an electron beam in dusty plasma using the fluid treatment and examined the reliance of the growth rate on the beam velocity. Sharma et al. [11] demonstrated the LHWs excitation in a negative ion plasma via a gyrating ion beam. They observed that the growth rate of negative and positive ion modes, i.e., unstable modes, augments with the relative density ratio of negative ions.

The dust grain charge fluctuations have a significant impact on the growth and damping of the wave [16,17,18]. Lately, extensive work has been done regarding waves and gained a lot of enthusiasm for different waves and instabilities in dusty plasma [19]. A few wave modes have been considered tentatively and analytically, starting with the Bliokh and Yarashenko [20] work by handling waves in Saturn's rings in dusty plasma. Seiler and Yamada [21] have studied the lower hybrid wave instability in a linear Princeton Q-1 device by a spiralling ion beam and reported the results. Barkan et al. [22] have proclaimed exploratory outcomes in a dusty plasma on the current driven Electrostatic Ion Cyclotron (EIC) instability. They reported that the growth rate of the instability was improved in the presence of negatively charged dust grains. Song et al. [23] studied the current-driven EIC instability in negative ion plasmas and found that for the excitation of the wave in a Q-machine, with the increase in the ratio of negative to positive ion density, the critical drift velocity of the electron decreased. The instability growth rate augments with the beam density, as observed by Gupta et al. [24].

Dust grains can acquire charge through various methods, such as energetic ion sputtering, plasma currents, photoelectric effects, auxiliary electron outflow, and other techniques commonly employed in laboratory settings [25]. They are often negatively charged; however, the smaller grains might be positively charged. The presence of charged dust grains in close proximity significantly impacts the properties of the surrounding plasma. D' Angelo [26] investigated the dispersion relation for inhomogeneous dusty plasma immersed in a uniform and steady magnetic field for low-frequency electrostatic waves. Within sight of charged dust grains that are negative, D' Angelo found that the frequency modes increase in a definite proportion to the density ratio of negatively and positively charged ions. The principal distinction of multi-component plasmas from dusty plasmas is that the charges in the dust are not settled but rather preferably controlled by the parameters of plasma in their environment. Here, this impact is considered to define the general active approach [27] for all types of dusty plasma. Chow and Rosenberg [28] observed that the critical drift velocity is reduced for the wave excitation as the relative dust concentration increases, indicating that the wave mode is further destabilized in a negatively charged dusty plasma. Sharma and Sugawa [29] have examined that with the increase in the relative density of negatively charged dust grains, the growth rate and frequency of wave instability increase. Merlino et al. [30] have examined analytically and experimentally the negatively charged dust grains' effect on electrostatic waves of low frequency in a dusty plasma.

In recent years, a kinetic treatment [31] of dusty plasmas has emerged, encompassing the crucial aspect of dust particles absorbing plasma constituents, namely ions and electrons. More recently, Sharma et al. [32] developed a model based on the impact of dust charge fluctuations by relativistic runaway electrons in a tokamak on the parametric decay of lower hybrid wave instability using kinetic theory. They studied the impact of dust charge fluctuations on LHWs instabilities growth rate. Anshu et al. [33] studied the correlation between the growth rate and relative density ratio using the kinetic theory model by the relativistic electron beam on lower hybrid waves. They showed that when the relative density ratio increases, so does the rate of growth increase.

In this present work, the excitation of LHWs is studied via the kinetic theory model by an electron beam in a magnetized dusty plasma. The distribution function of dust is taken to be Maxwellian, as it appears to be a steady arrangement of the present kinetic theory model. Using the Vlasov theory approach [34], the response of the beam electrons has been obtained.

Electrostatic LHWs are driven to instability via Cerenkov interaction by a magnetized dusty plasma interacting with the electron beam. In Section 2.2, the instability of LHWs has been examined, and the outcome of the current work is explained in Section 2.3. Section 2.4 summarizes the conclusion.

2.2 INSTABILITY ANALYSIS

We consider a system filled with plasma that contains electrons and ions with initial densities n_e^0 and n_i^0, respectively, in the existence of an externally applied static magnetic field in the z-direction. Negatively charged dust grains of density n_d^0 are introduced into the system. We examine a lower hybrid low-frequency wave travelling in the x-z plane, which lies firmly perpendicular to the applied magnetic field. An electron beam propagates in the z-direction with an initial velocity as $v_b \hat{z}$ and an initial beam density as n_b^0. A small amplitude perturbed electrostatic potential ϕ is given by

$$\phi = \phi_0 \exp[-i(\omega_l t - k_l x)], \tag{2.1}$$

where (ω_l, k_l) are the frequency and wave vector, and ϕ_0 is the amplitude of the unperturbed electrostatic potential of the lower hybrid wave.

The perturbed density can be evaluated using the Vlasov equation as

$$\frac{\partial F}{\partial t} + \sum_j \left(r_j \nabla f + \frac{\partial}{\partial r_j} . \dot{r}_j F \right) = 0, \tag{2.2}$$

where F is the distribution function, f is the interacting force, r is phase space and $\dot{r}_j$ is the time derivative of phase space of a single particle and $f = ma$, where m and a are the mass and acceleration of the particle, respectively. The expansion of the distribution function of the electron about the equilibrium is as follows $F = f_0 + f_{md}$, where f_0 is the equilibrium distribution function and

$$f_{md} = \frac{\omega_c^e / m_e^2}{\pi^{3/2} v_t^{e^3}} \exp\left(\frac{-\mu_m \omega_c^e + p^2 / 2m_e}{T_e}\right) \tag{2.3}$$

is the perturbed Maxwellian distribution function, $\omega_c^e \left(= \frac{eB_0}{m_e c} \right)$ denotes the cyclotron frequency of the electron, the mass of the electron is m_e, the speed of light is c, e is an electronic charge, p refers to the axial momentum, $v_t^e \left(= \sqrt{\frac{2T_e}{m_e}} \right)$ denotes the thermal velocity of the electron, T_e defines electron temperature, $\mu_m \left(= \frac{m_e v_t^{e^2}}{2\omega_c^e} \right)$ is the electron magnetic moment.

The density perturbation term is evaluated as

$$n = \frac{m_e^2}{\omega_c^e} \iiint f_{md} d^3 \vec{v}. \tag{2.4}$$

Equation (2.4) can be simplified by substituting the expression of f_{md} from Eq. (2.3), and the density perturbation term for electrons and ions can be evaluated as

$$n_{1e} = \frac{n_e^0 e\phi}{T_e}[1 + \frac{\omega_l}{k_l v_t^e} \sum_n Z(\frac{\omega_l + n\omega_c^e}{k_l v_t^e}) I_n(u_e) \exp(-u_e)]. \tag{2.5}$$

$$n_{1i} = \frac{n_i^0 e\phi}{T_i}[1 + \frac{\omega_l}{k_l v_t^i} \sum_n Z(\frac{\omega_l - n\omega_c^i}{k_l v_t^i}) I_n(u_i) \exp(-u_i)]. \tag{2.6}$$

Now, the density perturbation term for the beam is as follows

$$n_{1b} = \frac{-n_b^0 e\phi}{T_b}[1 + \frac{\omega_l - k_z v_b}{k_l v_t^b} \sum_n Z(\frac{\omega_l - k_z v_b}{k_l v_t^b}) I_n(u_b) \exp(-u_b)], \tag{2.7}$$

where n_e^0, n_i^0, n_b^0 is the initial electron, ion and beam density, $\omega_c^i \left(= \frac{eB_0}{m_i c} \right)$ is the ion cyclotron frequency, ion mass is m_i, I_n is the modified Bessel's function, Z denotes the dispersion function of plasma, $\omega_c^b \left(= \frac{eB_0}{m_b c} \right)$ denotes the beam cyclotron frequency, m_b is the beam mass, (T_i, v_t^i) denotes ion temperature and thermal velocity. (T_b, v_t^b) indicates beam temperature and thermal velocity, respectively.

Now, the density perturbation term for dust is given as

$$n_{1d} = \frac{n_d^0 Q_d^0 \phi}{T_d}[1+\frac{\omega_l}{k_l v_t^d}\sum_n Z(\frac{\omega_l - n\omega_c^d}{k_l v_t^d})I_n(u_d)\exp(-u_d)].$$

Here the dust is taken to be unmagnetized, i.e., $\omega_c^d\left(=\frac{Q_d^0 B_0}{m_d c}\right)=0,$ where ω_c^d denotes the dust cyclotron frequency, $Q_d^0\left(=-Z_d e\right)$ refers to the charge of dust grains, Z_d is the dust charge state, m_d is dust grain mass, i.e., $m_d = 10^{12} m_p$, where m_p is the mass of a proton, T_d refers to the temperature of a dust grain, v_t^d is the dust grain thermal velocity. For simplicity, we have taken $n=1$. As we can see that the dust cyclotron frequency varies inversely with the dust grain mass, it becomes negligible and significantly small. Now, the dust density perturbation term becomes

$$n_{1d} = \frac{n_d^0 Q_d^0 \phi}{T_d}[1+\frac{\omega_l}{k_l v_t^d}\sum_n Z(\frac{\omega_l}{k_l v_t^d})]. \tag{2.8}$$

Substituting Eqs. (2.5) - (2.8) in Poisson's Equation

$$\nabla^2\phi = 4\pi\left[en_{1e} - en_{1i} + Q_d^0 n_{1d} + en_{1b}\right]. \tag{2.9}$$

the linear dispersion relation for the electrostatic mode with beam and dust grains is obtained as

$$\varepsilon = 1+\chi_e+\chi_i+\chi_b+\chi_d, \tag{2.10}$$

where χ refers to the susceptibilities. Further, Eq. (2.10) can be simplified as

$$\begin{aligned}\varepsilon = 1 &+ \frac{2\omega_p^{e^2}}{k_l^2 v_t^{e2}}\left[1+\frac{\omega_l}{k_l v_t^e}\sum_n Z\left(\frac{\omega_l}{k_l v_t^e}\right)I_n(u_e)e^{-u_e}\right] \\ &+ \frac{2\omega_p^{i^2}}{k_l^2 v_t^{i2}}\left[1+\frac{\omega_l}{k_l v_t^i}\sum_n Z\left(\frac{\omega_l - n\omega_c^i}{k_l v_t^i}\right)I_n(u_i)e^{-u_i}\right] \\ &+ \frac{2\omega_p^{d^2}}{k_l^2 v_t^{d2}}\left[1+\frac{\omega_l}{k_l v_t^d}\sum_n Z\left(\frac{\omega_l}{k_l v_t^d}\right)\right] \\ &+ \frac{2\omega_p^{b^2}}{k_l^2 v_t^{b2}}\left[1+\frac{\omega_l - k_z v_b}{k_l v_t^b}\sum_n Z\left(\frac{\omega_l - k_z v_b}{k_l v_t^b}\right)I_n(u_b)e^{-u_b}\right],\end{aligned} \tag{2.11}$$

where $\omega_p^{e^2}\left(=\frac{4\pi n_e^0 e^2}{m_e}\right), \omega_p^{i^2}\left(=\frac{4\pi n_i^0 e^2}{m_i}\right), \omega_p^{b^2}\left(=\frac{4\pi n_b^0 e^2}{m_b}\right)$ denotes the plasma frequency of electron, ion and beam responses, respectively, and $\omega_p^{d^2}\left(=\frac{4\pi n_d^0 Q_d^{0^2}}{m_d}\right)$ denotes the dust plasma frequency. For finding the solution of Eq. (2.11), we assume $\left(\frac{\omega_l - n\omega_c^\beta}{k_l v_t^\beta} = \xi\right)$, where $b = d, \alpha(e, i \text{ and } b)$, for dust, electron, ion and beam responses, respectively. Using the expression of plasma dispersion function $Z(\xi)$ from the kinetic theory [35], we obtain

$$Z(\xi) = -\frac{1}{\xi} - \frac{1}{2\xi^3} + ... + i\sqrt{\pi} e^{-\xi^2} \qquad \text{if } \xi >> 1.$$

or

$$Z(\xi) = -2\xi + \frac{2}{3}\xi^3 + ... + i\sqrt{\pi}\, \mathrm{e}^{-\xi^2} \qquad \text{if } \xi << 1,$$

where higher-order terms are neglected. And using conditions $v_t^d << \frac{\omega_l}{k_l} << v_t^i$, Eq. (2.11) can be solved to yield the growth rate and real frequency expression as follows

$$\Gamma = -\sqrt{2\pi}\omega_p^b \left[\frac{\left\{ I_n^2(u_b) e^{-2u_b} \left(X^2 + 16\pi e^{-2\xi^2} \right) + \left(1 - 2I_n(u_b) e^{-u_b} X \right) \right\}^{1/2}}{\left(1 + I_n(u_b) e^{-u_b} X \right)} - \right]^{1/2}, \quad (2.12)$$

where $$X = \frac{\omega_l}{\left(\omega_p^b - k_z v_b\right) \times 0.8 \times \delta} + \frac{\omega_l}{\omega_l - n\omega_c^i} + \frac{\omega_l - k_z v_b}{\omega_l - k_l v_t^b}.$$

$$\omega_r = \omega_p^b \left[\frac{\left\{ I_n^2(u_b) e^{-2u_b} \left(X^2 + 16\pi e^{-2\xi^2} \right) + \left(1 - 2I_n(u_b) e^{-u_b} X \right) \right\}^{1/2}}{\left(1 + I_n(u_b) e^{-u_b} X \right)} + \right]^{1/2}. \quad (2.13)$$

The phase velocity is as follows

$$v_{ph} = \frac{\omega_r}{k_l} = \frac{\omega_p^b \left[\left\{ I_n^2(u_b) e^{-2u_\alpha} \left(X^2 + 16\pi e^{-2\xi^2} \right) + \left(1 - 2I_n(u_b) e^{-u_b} X \right) \right\}^{1/2} + \left(1 + I_n(u_b) e^{-u_b} X \right) \right]^{1/2}}{k_l}. \quad (2.14)$$

Equating the growth rate Eq. (2.12) equal to zero, i.e., $\Gamma = 0$ equates to stability and describes the critical drift velocity u_{cd} as

$$u_{cd} = \log\left(\frac{16 I_n \pi e^{-2\xi^2}}{4X} \right). \quad (2.15)$$

2.3 RESULTS AND DISCUSSION

In this chapter, the analytical model has been developed to study the excitation of LHWs in a magnetized plasma cylinder with negatively charged dust grains by kinetic treatment with an electron beam. The developed model aims to analyse the relationship between various plasma parameters, i.e., real frequency, growth rate etc. The effect of the dust grain size, critical drift velocity and relative density ratio on the wave is studied. The equations that hold accountable for LHWs in Section 2.2 are used to calculate the real frequency and growth rate for the same. In the present calculations, typical dusty plasma parameters have been used. Using the following parameters, i.e., plasma density of ion $n_i^0 = 1\times10^9$ cm^{-3}, plasma density of electron $n_e^0 = (1\times10^9 - 0.2\times10^9)$ cm^{-3}, guide magnetic field $B_0 = 5\times10^4$ gauss, ion mass $m_i^0 = 39\times m_p$ (Potassium-plasma), where $m_p = 1.67\times10^{-24}$ grams, the electron mass $m_e = 9.1\times10^{-28}$ grams, ion temperature $T_i = 0.2$ eV, the temperature of the electron $T_e = 0.2$ eV, the density of the electron beam $n_b^0 = 10^9$ cm^{-3}, density of the dust grains $n_d^0 = 5\times10^4$ cm^{-3}, dust grain mass $m_d = 10^{12} m_p$, and size of the dust grains $a = 5\times10^{-4}$ cm, ion sound speed $C_s = \sqrt{\frac{k_B T_e}{m_i}}$, k_B is the Boltzmann constant. We have plotted the various graphs.

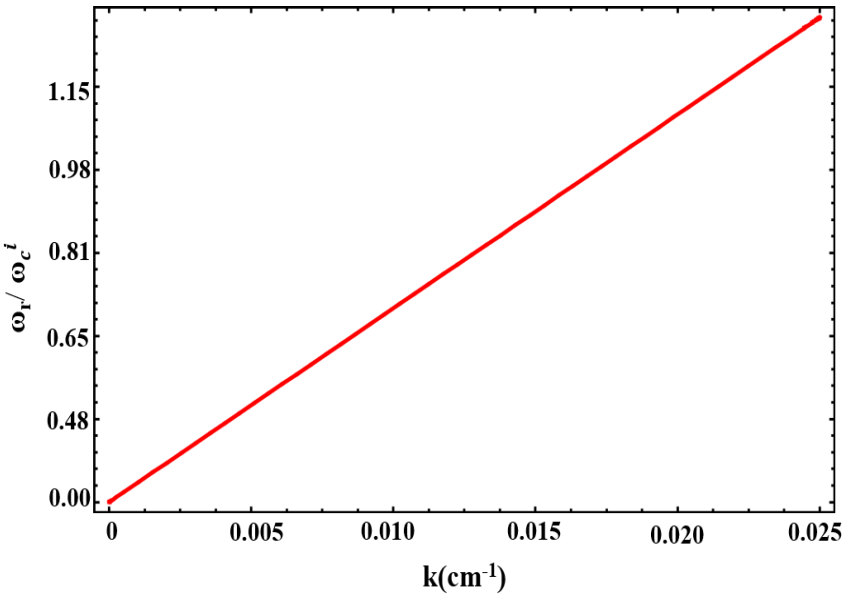

Figure 2.1: Dispersion curve in a magnetized dusty plasma of lower hybrid waves.

In Figure 2.1, the dispersion curve for LHWs has been plotted using Eq. (2.11) for the parameters mentioned above of lower hybrid beam plasma instability. The graph portrays the linear relationship between wavenumber k (cm^{-1}) and the normalized frequency of LHWs, signifying that they are dependent on each other.

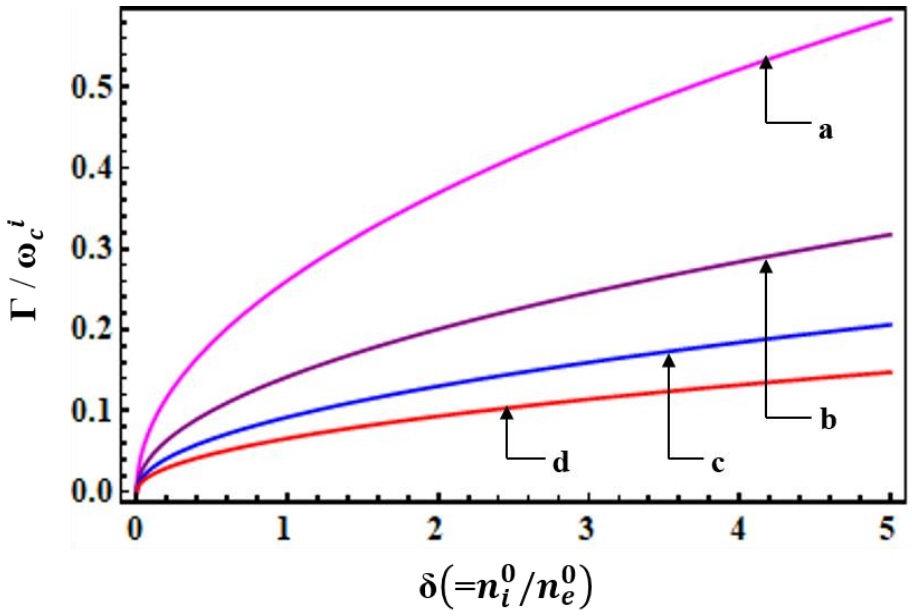

Figure 2.2: Normalized growth rate variation with $\delta\left(=n_i^0/n_e^0\right)$ for the varying value of dust grain size i.e., (a) a = 2 μm, (b) a = 4 μm, (c) a = 6 μm and (d) a = 8 μm.

Figure 2.2 depicts the normalized growth rate variation with a relative density ratio of negatively charged dust grains $\delta\left(=n_i^0/n_e^0\right)$ for different values of dust grain size, (a) a = 2 μm, (b) a = 4 μm, (c) a = 6 μm, (d) a = 8 μm. It is observed from Figure 2. 2 that the value of growth rate is more significant at the lower value of dust grain size. Because of the small dust grain size, the electron density will increase, which further enhances the growth rate. As we augment the density ratio, the rate of growth also increases. Growth rate of LHWs instability in the existence of dust charge stabilizes more as the size of the dust grain increases with $\delta\left(=n_i^0/n_e^0\right)$. The rate of growth gradually decreases as the size of the dust grain augment and the curve flattens. Moreover, it can also be observed that the normalized rate of growth of LHWs upsurges by a factor of~1.75, with the variation of δ from 1 to 3 and by a factor of~2.04 with the variation of δ from 1 to 4. Hence, the obtained result is in line with the theoretical observations of Sharma and Walia [36].

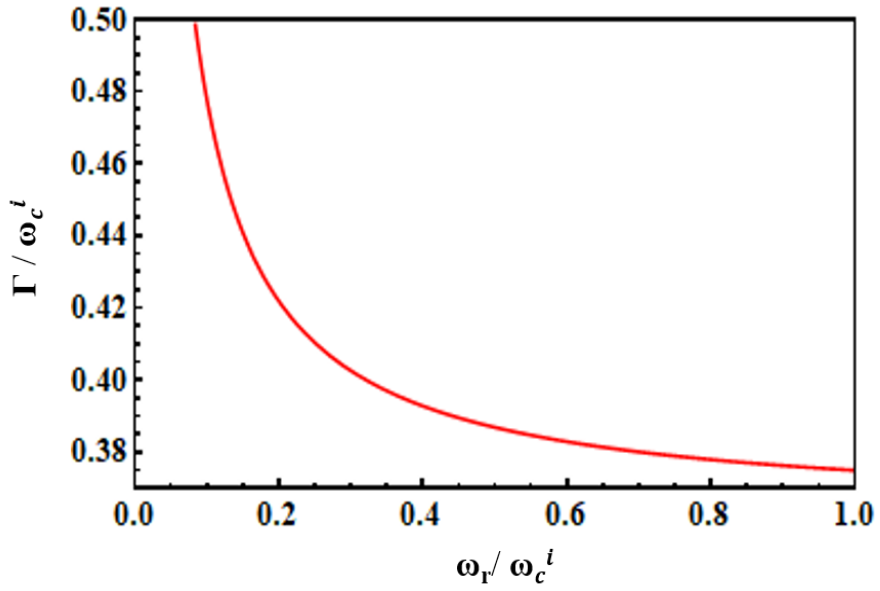

Figure 2.3: Normalized growth rate variation with the normalized frequency of the lower hybrid wave.

We have drawn the graph of normalized growth rate versus normalized frequency ω_r/ω_c^i of LHWs in Figure 2.3 for the same parameters as plotted in Figures 2.1 and 2.2. This graph shows that the normalized growth rate and frequency of LHWs are inversely proportional to each other. With an increase in frequency, the critical drift increases for the excitation of mode and

hence the growth rate decreases. When the frequency of LHWs is more, the growth rate of the wave is more stable.

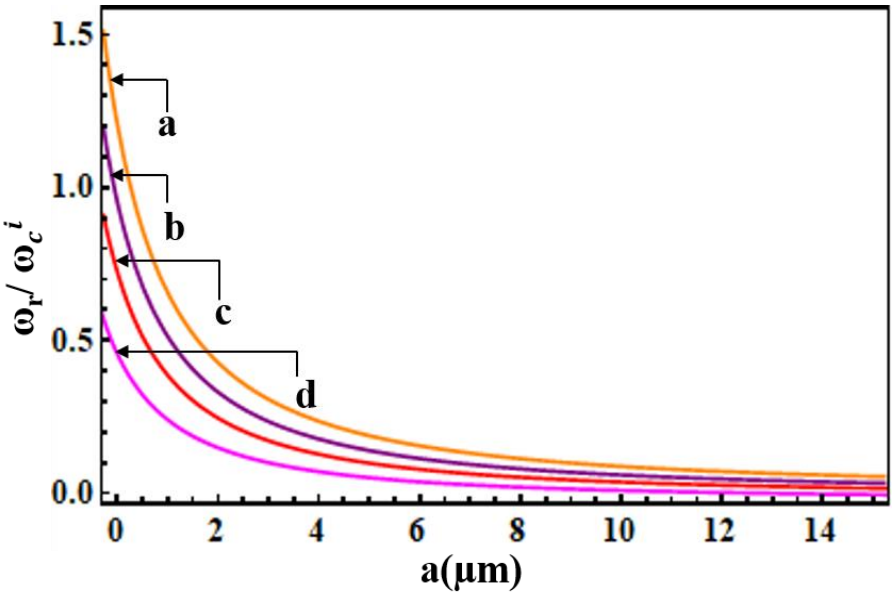

Figure 2.4: The normalized frequency variation with the dust grain size for different relative density ratio $\delta\left(=n_i^0/n_e^0\right)$, i.e., (a) δ = 6, (b) δ = 4, (c) δ = 2, (d) δ = 1.

In Figure 2.4, the normalized lower hybrid wave frequency variation with the dust grain size of negatively charged dust grains for different relative density ratio (a) δ = 6, (b) δ = 4, (c) δ = 2, (d) δ = 1, is shown. As we can see

$$\omega_p^{d^2}\left(=\frac{4\pi n_d^0 Q_d^{0^2}}{m_d}\right), \tag{2.16}$$

where m_d = density x volume, and volume $=\frac{4}{3}\pi a^3$, where a is the radius of the dust grains. Here, we assume that the dust grains are spherical. By putting the expression of mass (m_d) in Eq. (2.16), we can say that frequency scales to 3/2 power of dust grain size, i.e., $\omega_p^d\left(=\left(\frac{1}{a}\right)^{3/2}\sqrt{\frac{3n_d^0 Q_d^{0^2}}{density}}\right)$. From this, we can conclude that as the dust grain size increases, the frequency of the LHWs decreases. As the size of the dust grain increases, volume increases, and hence more electrons will stick to the dust grains. As a result, electron density decreases

sharply, and consequently, wave frequency decreases. Further, with the increase of $\delta\left(=n_i^0/n_e^0\right)$, the frequency augments.

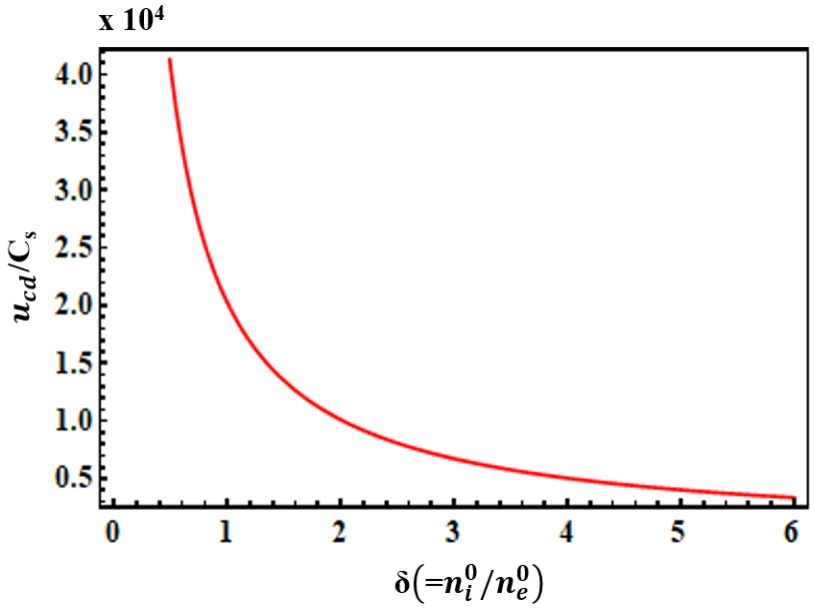

Figure 2.5: The normalized critical drift velocity variation with the relative density ratio $\delta\left(=n_i^0/n_e^0\right)$.

The normalized critical drift velocity versus relative density ratio $\delta\left(=n_i^0/n_e^0\right)$ graph is portrayed in Figure 2.5. From Figure 2.5, we have inferred that with the increase in relative density ratio, the critical drift velocity decreases and can be seen from Eq. (2.15) also. From Figure 2.5, we can say that as δ changes from 4 to 1, the critical drift velocity increases by about 2.97%. Hence, we can say that it is stabilising the growth rate of the wave. For $\delta \geq 2$, the rate of critical drift decreases at a very slow rate.

Figure 2.6 depicts the normalized phase velocity graph of negatively charged dust grains with respect to the relative density ratio $\delta\left(=n_i^0/n_e^0\right)$. The $\delta\left(=n_i^0/n_e^0\right)$ variation from 1 to 5 is shown. In the presence of negatively charged dust grains of LHWs, the phase velocity augments with the relative density ratio. This is because, with the increase in electron density, the real frequency increases, which in turn, increases the phase velocity of the waves. From Figure 2.6, it is clear that as the δ value increases, the phase velocity of the wave also increases. This is because the space occupied by electrons on the dust grains becomes large.

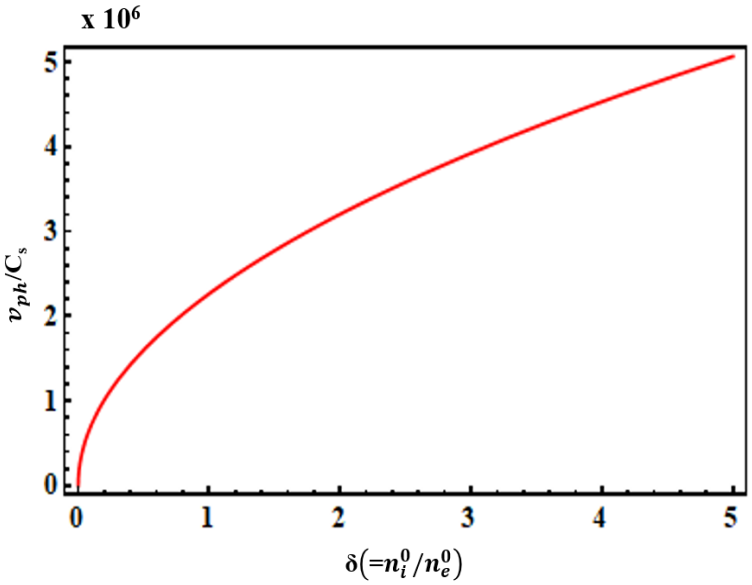

Figure 2.6: Normalized phase velocity v_{ph} as a function of relative density ratio $\delta\left(=n_i^0/n_e^0\right)$

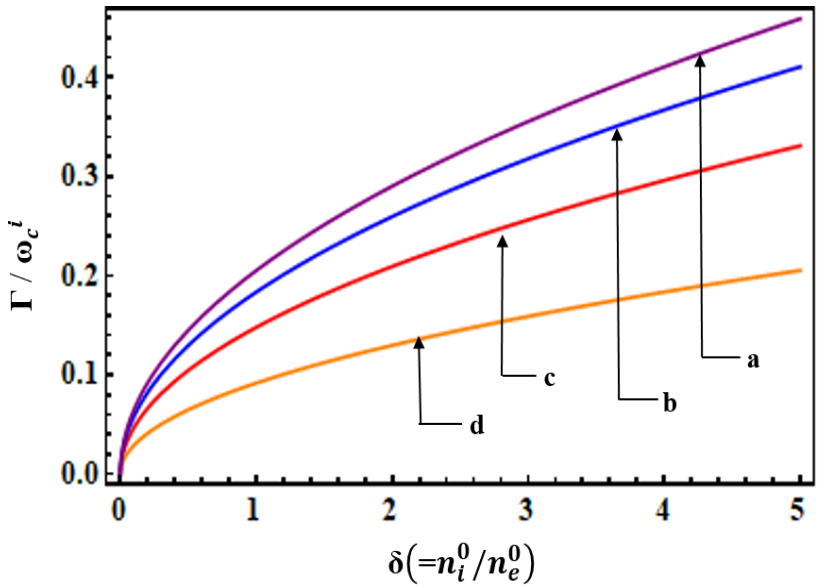

Figure 2.7: Normalized growth rate graph is plotted versus $\delta\left(=n_i^0/n_e^0\right)$ for different beam velocities v_b^0, i.e., (a) $v_b^0=10\times10^8$cm/sec, (b) $v_b^0=8\times10^8$cm/sec, (c) $v_b^0=5.2\times10^8$cm/sec and (d) $v_b^0=2\times10^8\,\mathrm{cm/sec}$.

Figure 2.7 depicts the normalized growth rate variation with the relative density ratio $\delta\left(=n_i^0/n_e^0\right)$ for varying values of beam velocities v_b^0, i.e., (a) $v_b^0 = 10\times10^8 cm/sec$, (b) $v_b^0 = 8\times10^8 cm/sec$, (c) $v_b^0 = 5.2\times10^8 cm/sec$ and (d) $v_b^0 = 2\times10^8 cm/sec$. As we observed, the growth rate of LHWs augments with the velocity of the beam, i.e., beam electrons give energy to the waves, and the wave is growing. As the velocity of the beam augments, the maximum value of the growth rate increases. It is observed that the wave frequency of LHWs increases when the beam velocity and relative density ratio are increased. It can be observed that the normalized growth rate of unstable wave upsurges by a factor of~1.68, with a variation of δ from 1 to 3 and by a factor of~1.93, with the variation of δ from 1 to 4. Our results are in line with Prakash et al. [6].

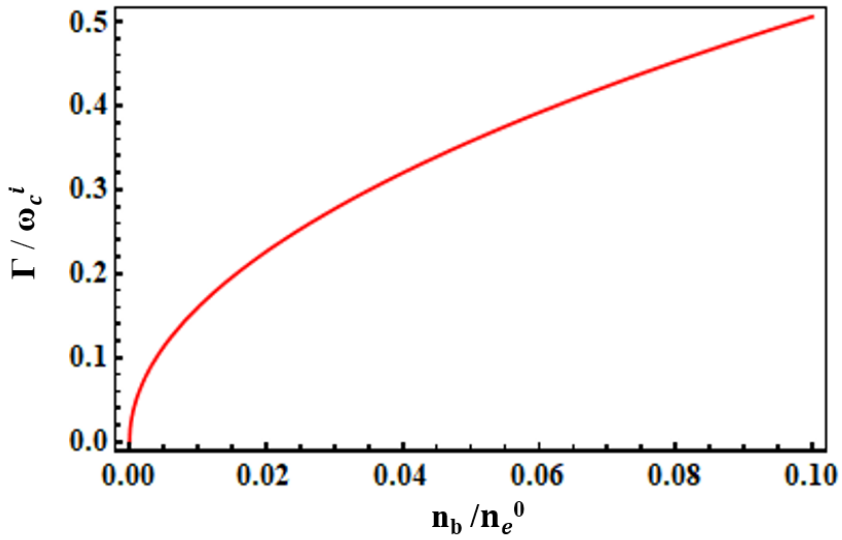

Figure 2.8: The normalized growth rate variation with the beam density.

Figure 2.8 depicts the growth rate of LHWs with respect to beam density. We can conclude that as beam density increases, so does the wave's growth rate. The rate of growth is determined by the square root of the beam's density, as shown by Eq. (2.12). Our theoretical findings are consistent with R.P.H. Chang [9] of experimental observations.

2.4 CONCLUSION

In magnetized dusty plasma, the LHWs excitation has been examined by electron beam using the kinetic treatment. The electrostatic LHWs via Cerenkov interaction are driven to

instability. The outcomes of this work with different plasma parameters were compared and discussed. In magnetized dusty plasma, we investigated the impact of dust grain size on the growth rate and excitation of LHWs. The rate of growth of LHWs augments with the relative density ratio. The growth rate of LHWs increases significantly with a higher population of dust grains. Our growth rate findings are consistent with Sharma et al. [36] theoretical results and Chang [9] experimental observations. The critical drift velocity for mode excitation decreases as the relative density ratio of dust grains increases, resulting in an increase in the phase velocity. Furthermore, it was shown that the growth rate of the unstable mode is proportional to the one-half power of the density of the beam and increases with beam density. LHWs instability driven by an electron beam in plasma processing of material experiments [37] can alter the plasma-surface interactions. Furthermore, in the plasma processing of materials [38,39,40], nano-sized dust particles can be incorporated.

Very few studies have been made so far to derive the relationship among various parameters such as growth rate, frequency and size of dust grains particles etc., using kinetic treatment. This work may serve as a foundation for future studies, where experimentalists and theorists are likely to draw inspiration from its findings. LHWs can be studied in tokamak plasmas [41], lunar dusty plasma [42] and has recently received significant attention for affecting the current drive at a very high density [43].

REFERENCES

[1] M. M. Shoucri and R. R. J. Gagne, *Journal of Plasma Physics* **19,** 281 (1978).

[2] D.N. Gupta and A.K. Sharma, *Laser & Particle Beams* **22,** 89 (2004).

[3] S. C. Sharma and A. Gahlot, *Physics of Plasmas* **16**, 123708 (2009).

[4] M. Yadav & J. Sharma, *Indian Journal of Pure and Applied Physics* **59,** 671 (2021).

[5] P. Yadav, D. N. Gupta, and K. Avinash, *Physics of Plasmas* **24,** 062107 (2017).

[6] V. Prakash, Vijayshri, S. C. Sharma, and R. Gupta, *Physics of Plasmas* **20,** 053701 (2013).

[7] K. Papadopoulos and P. Palmadesso, *Physics of Fluids* **19,** 605 (1976).

[8] O. Koshkarov, A. I. Smolyakov, A. Kapulkin, Y. Raitses, and I. Kaganovich *Physics of Plasmas* **25,** 061209 (2018).

[9] R. P. H. Chang, *Physical Review Letters* **35,** 285 (1975).

[10] V. Prakash, Vijayshri, S. C. Sharma, and R. Gupta, *Physics of Plasmas* **20,** 063701 (2013).

[11] J. Sharma, S. C. Sharma, V. K. Jain, and A. Gahlot, *Physics of Plasmas* **20,** 033706 (2013).

[12] S. C. Sharma, M. P. Srivastava, M. Sugawa and V. K. Tripathi, *Physics of Plasmas* **5,** 3161 (1998).

[13] S. C. Sharma and Ritu Walia, *Physics of Plasmas* **15,** 093703 (2008).

[14] M. M. Shoucri and R. R. J. Gagne, *Journal of Plasma Physics* **19,** 28 (1978).

[15] R. L. Stenzel and W. Gekelman, *Physical Review A* **11,** 6 (1975).

[16] S. V. Vladimirov, K. N. Ostrikov, and M. Y. Yu, *Physical Review E* **60,** 3257 (1999).

[17] M. R. Jana, A. Sen, and P. K. Kaw, *Physical Review E* **48,** 3930 (1993).

[18] S. V. Vladimirov, K. N. Ostrikov, M. Y. Yu, and L. Stenflo, *Physical Review E* **58,** 8046 (1998).

[19] S. V. Vladimirov, K. Ostrikov, M. Y. Yu, and G. E. Morfill, *Physical Review E* **67,** 036406 (2003).

[20] P. V. Bliokh and V. V. Yarashenko, *Soviet Astronomy* **29,** 330 (1985).

[21] S. Seiler and M. Yamada, *Physical Review Letters* **37,** 700 (1976).

[22] A. Barkan, N. D'Angelo, and R. L. Merlino, *Planetary and Space Science* **43,** 905 (1995).

[23] B. Song, D. Suszcynsky, N. D'Angelo, and R. L. Merlino, *Physics of Fluids B* **1,** 2316 (1989).

[24] R. Gupta, S. C. Sharma and V. Prakash, *Physics of Plasmas* **17,** 122105 (2010).

[25] T. K. Baluku and M. A. Hellberg, *Physics of Plasmas* **22,** 083701 (2015).

[26] N. D'Angelo, *Planetary and Space Science* **38,** 1143 (1990).

[27] V. N. Tsytovich, *Physics of Plasmas* **7,** 554 (2000).

[28] V. W. Chow and M. Rosenberg, *Planetary and Space Science* **44,** 465 (1996).

[29] S. C. Sharma and M. Sugawa, *Physics of Plasmas* **6,** 444 (1999).

[30] R. L. Merlino, A. Barkan, C. Thompson, and N. D'Angelo, *Physics of Plasmas* **5,** 1607 (1998).

[31] P. Ricci, G. Lapenta, U. de Angelis, and V. N. Tsytovich*, Physics of Plasmas* **8,** 769 (2001).

[32] J. Sharma, S. C. Sharma and A. Gahlot, *Physics of Plasmas* **28,** 043701 (2021).

[33] Anshu, S. C. Sharma and J. Sharma, *46th EPS Conference on Plasma Physics,* EPS (2019).

[34] C. S. Liu and V. K. Tripathi, *Physics Reports* **130,** 143 (1986).

[35] M. N. Rosenbluth and R. Z. Sagdeev, Handbook of plasma physics, *Elsevier Science Pub*. (1983).

[36] S. C. Sharma, R. Walia, *Physics of Plasmas* **15,** 093703 (2008).

[37] K. Ostrikov, U. Cvelbar, and A. B. Murphy, *Journal of Physics D: Applied Physics* **44,** 174001 (2011).

[38] K. Ostrikov and S. Xu, Plasma-Aided Nanofabrication from Plasma Sources to Nanoassembly (2007).

[39] B. Denysenko, S. Xu, J. D. Long, P. P. Rutkevych, N. A. Azarenkov, and K. Ostrikov*, Journal of Applied Physics* **95**, 2713 (2004).

[40] A. Okita, Y. Suda, A. Ozeki, H. Sugawara, Y. Sakai, A. Oda, and J. Nakamura, *Journal of Applied Physics* **99,** 014302 (2006).

[41] Z. Liu, Z. Gao, A. Zhao, *Physics of Plasmas* **27,** 042503 (2020).

[42] S. I. Popel, A. I. Kassem, Y. N. Izvekova and L. M. Zelenyi, *Physical Letters A* **384,** 126627 (2020).

[43] J. G. Jo, S. H. Kim, *Fusion Engineering and Design Journal* **190,** 113531 (2023).

3

In the existence of a transverse dc electric field, the kinetic theory of current-driven EIC waves excitation in a magnetized dusty plasma

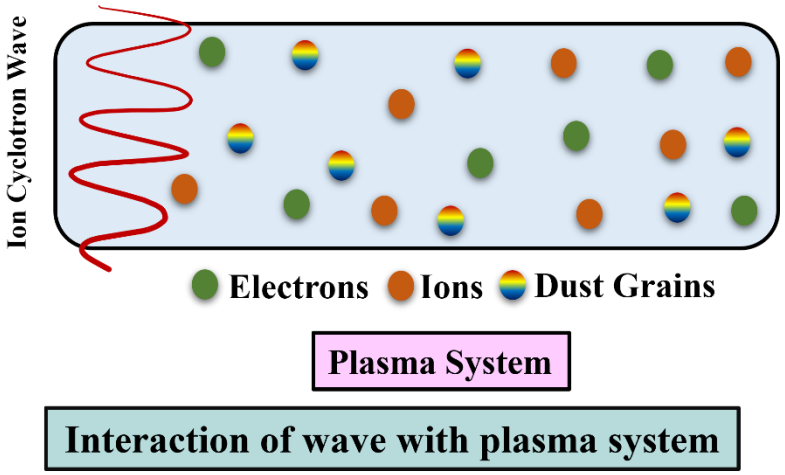

In this chapter, the theoretical model for the Electrostatic Ion Cyclotron Waves (EICWs) in the existence of a transverse direct current (dc) electric field in a collisionless magnetized dusty plasma has been investigated using the kinetic theory model. It is examined that after incorporation of a dc electric field in the presence of dust grains can alter the dispersion properties of EICWs in a magnetized dusty plasma. Our model developed accounts for the critical drift velocity, electron to ion temperature ratio, magnetic field, the number density of dust grains, relative density of negatively charged dust grains, and finite gyroradius parameter. Moreover, the critical drift velocity for the excitation of the mode and the impact of dust grains on the low-frequency waves have been studied.

PUBLICATION

Anshu, Jyotsna Sharma, and Suresh C. Sharma, "In the existence of a transverse dc electric field, the kinetic theory of current-driven electrostatic ion cyclotron waves excitation in a magnetized dusty plasma", *Contributions to Plasma Physics* 62.9, e202200073 (2022).

3.1 INTRODUCTION

The most prevalent state of matter in the cosmos is plasma, with dust being another widespread occurrence. As a result, it's not astonishing that a study of "dusty plasmas" [1-8] is recommended in several astrophysical settings [9-11]. Dust can be observed in the earth's atmosphere and planetary magnetosphere, such as Saturn's ring detected by Voyager spacecraft [12], industry [13-16] and laboratories [3, 7, 15, 17, 18]. Because of the existence of dust in a plasma environment, the dust is electrically charged [19, 20], thereby affecting the overall charge neutrality condition. Properties of plasma and wave behaviours are modified after the addition of dust and result in additional wave modes [21-24]. Waves in dusty plasmas have been theoretically investigated for over an era [1, 22, 24-28]. These waves have been briefly examined by Goertz [25], who refers to previous work by Papadopoulos and Palmadesso [26]. They studied the excitation by electron beams in plasma on the lower hybrid waves. Electrostatic waves in Saturn's rings were studied by Bliokh and Yarashenko [27]. In dusty plasma, D'Angelo [1] considered the low-frequency electrostatic waves. Low-frequency instabilities can be induced by drifting electrons in a plasma. The Electrostatic Ion-Cyclotron Instability [29] (EICI) is one of the fundamental modes when the plasma is magnetized, and the electrons drift along magnetic field lines. The EICWs propagates approximately perpendicular to the magnetic field B and has a small but limited wave number along the field, allowing electrons travelling along B to destabilize it. The EIC is a field-aligned current-driven instability [30] with one of the lowest threshold drift velocities among current-driven instabilities. This type of wave has been found to be crucial in fusion plasma heating [31-34], fundamental collective wave lab experiments [3, 35-37], and space plasmas [38-41]. Several computer simulations [41-43] of the EICI have been conducted in this regard. The EICWs have also been the subject of many purely theoretical studies [44-49]. EICWs have been detected in many satellite measurements, including S3–3, ISEE-1 [40], Viking [50], FAST, and THEMIS [51]. Because of this, the EICWs have recently gained broad attention from researchers [22, 38, 40, 51, 52]. Drummond et al. [45] analytically observed that the oscillations were caused by current-driven electrostatic ion–cyclotron instability. The value of electron drift velocity at equal electron and ion temperature for EIC wave was examined by them. Many theoretical and experimental works [46, 48, 53-57] have been studied on the EICI. D′Angelo [1] studied the ion cyclotron waves using fluid treatment in dusty plasma. He depicted that with the gradual

increase in the frequencies of the positive ion EIC mode, the concentration of negatively charged dust grains gets enhanced. A study of EIC wave in a Q-machine is reported by Barkan et al. [3] They predicted that with a large amount of negatively charged dust, the instability growth rate enhanced. Koepke et al. [55] studied the experimental EICWs in a WVU Q-machine. They observed that with the inclusion of a transverse, localized dc electric field in EICWs, the instability threshold decreases. Song et al. [57] studied the EIC wave modes (positive and negative ion modes) in a plasma. They observed that the frequencies of both the modes increase and critical drift decrease with an increase in the percentage of negative ions. Chow and Rosenberg [8] observed that the critical drift velocity decreases for the EIC wave excitation as the relative dust concentration increases, indicating that the wave mode is further destabilized in a negatively charged dusty plasma using the kinetic theory. Sharma et al. [49] investigated the excitation of EICWs in a magnetized plasma. They found that the wave's growth rate augments as the mode frequency augments, and the real frequency is almost directly proportional to the transverse dc electric field using fluid treatment in the existence of the electric field.

Much research has been done on EIC instability, emphasizing the importance of Drummond and Rosenbluth's work [45] (and its extensions [29]) in understanding various elements of plasma settings. However, to our knowledge, the previous works have not studied the impact of temperature, critical drift velocity, dust and various other parameters that affect the instability of waves in the existence of an electric field in a collisionless dusty magnetized plasma. As a result, we have extended previous work on the excitation of current-driven EICWs in a magnetized plasma [49] in the occurrence of a transverse dc electric field to highlight the role of temperature, dust and other parameters by using the kinetic treatment. Kinetic treatment involves the distribution function of each species (electrons, ions, etc.) distinctively, and our results can be calculated more precisely than using the fluid treatment.

In this chapter, we study the excitation of current-driven electrostatic ion cyclotron waves in a collisionless magnetized dusty plasma in the existence of a transverse dc electric field. Kinetic theory is used to investigate the effect of frequency, growth rate, critical drift and temperature with different parameters on EICWs. This chapter is organized as follows. The instability analysis and dispersion relation derivation of EICWs using the Vlasov equation is described in

Section 3.2. Results and discussion, and comparisons with theoretical and experimental models are presented in Section 3.3. The key findings are summarized in Section 3.4.

3.2 INSTABILITY ANALYSIS

A collisionless magnetized dusty plasma is considered, which is contained in a static uniform magnetic field B_0 in the z-direction. This system comprises three species, i.e., ions, electrons and negatively charged dust grains with equilibrium densities n_i^0, n_e^0 and n_d^0 and their respective velocities v_i, v_e and v_d. The mass, charge and temperature of ions, electrons and dust grains are denoted by $(m_i, e \text{ and } T_i)$, $(m_e, -e \text{ and } T_e)$ and $(m_d, Q_d \text{ and } T_d)$, respectively. In the x-direction, the system is introduced with a transverse direct current (dc) electric field E_0. This causes $\vec{E} \times \vec{B}$ flows of electrons and ions as well as the drift of magnitude $v_E \left(= \frac{cE_0}{B_0}\right)$ in the y-direction. Furthermore, the electrons are assumed to have a drift velocity u_{de} in the direction of the applied magnetic field, i.e., the z-axis. An EIC wave propagates approximately perpendicular to the applied magnetic field in the y-z plane with wave frequency ω and propagation vector k.

The drifting Maxwellian distribution function for electrons is stated by

$$f_e^0 = n_e^0 \left(\frac{m_e}{2\pi K T_e} \right)^{3/2} \exp\left[\frac{-1}{2} \frac{m_e}{K T_e} \left\{ v_x^2 + \left(v_y - v_E \right)^2 + \left(v_z - u_{de} \right)^2 \right\} \right], \tag{3.1}$$

where f_e^0 is the equilibrium Maxwellian distribution function, the Boltzmann constant is K, v_x, v_y and v_z denotes the velocities in the x, y and z - direction, respectively. In contrast, the ions (and dust) distribution function can be obtained by replacing the $\left(n_e^0, m_e, T_e\right)$ by $\left(n_i^0, m_i, T\right)$ and $\left(n_d^0, m_d, T_d\right)$ and considering u_{de} equals zero in the above equation.

In equilibrium, the quasi-neutrality condition follows,

$$e n_i^0 = e n_e^0 + Q_d n_d^0 . \tag{3.2}$$

An electrostatic potential perturbation is defined by

$$\phi_1 = \phi_0 \exp\left[-i\left(\omega t - k_y y - k_z z\right)\right], \tag{3.3}$$

where ϕ_0 is unperturbed electrostatic potential.

The Vlasov equation has been employed to estimate the perturbed densities of ions, electrons and dust particles and can be written as

$$\frac{\partial f}{\partial t} + \left(\vec{v}.\,\Delta\right) f - \frac{e}{m}\left(\vec{E} + \frac{1}{c}\vec{v}\times\vec{B}\right).\frac{\partial f}{\partial \vec{v}} = 0, \tag{3.4}$$

where the speed of light is c, $\vec{E}$ and $\vec{B}$ are electric and magnetic fields, $f = f_0 + f_1$ is the distribution function, where f_0 is unperturbed and f_1 is perturbed distribution function.

The density perturbation response can be governed by

$$n_\alpha^1 = \frac{m_\alpha^2}{\omega_{c\alpha}} \iiint f_\alpha^0 d^3\vec{v}, \tag{3.5}$$

where α refers to the ions, electrons and dust grains, respectively and $\omega_{c\alpha}\left(=\frac{eB_0}{m_\alpha c}\right)$ refers to the cyclotron frequency.

Equation (3.5) can be simplified and density perturbation terms for electrons, ions and dust grains can be written as

$$n_e^1 = \frac{n_e^0 e\phi}{T_e}\left[1 + \frac{\omega_1}{k_z v_{te}} \sum_n Z\left(\frac{\omega_1}{k_z v_{te}}\right)\Gamma_n^e\right]. \tag{3.6}$$

$$n_i^1 = \frac{n_i^0 e\phi}{T_i}\left[1 + \frac{\omega_2}{k_z v_{ti}} \sum_n Z\left(\frac{\omega_2 - n\omega_{ci}}{k_z v_{ti}}\right)\Gamma_n^i\right]. \tag{3.7}$$

$$n_d^1 = \frac{n_d^0 Q_d \phi}{T_d}\left[1 + \frac{\omega}{k v_{td}} \sum_n Z\left(\frac{\omega - n\omega_{cd}}{k v_{td}}\right)\right], \tag{3.8}$$

where $\omega_1 = \omega - k_y v_E - k_z u_{de}$ and $\omega_2 = \omega - k_y v_E$; $v_{te}\left(=\sqrt{\frac{2KT_e}{m_e}}\right)$, $v_{ti}\left(=\sqrt{\frac{2KT_i}{m_i}}\right)$ and $v_{td}\left(=\sqrt{\frac{2KT_d}{m_d}}\right)$ represents the electron, ion and dust grain's thermal velocities, respectively;

$\Gamma_n^{\alpha} = I_n(b_\alpha)\exp(-b_\alpha)$, where $b_\alpha\left(=\frac{k_y^2\rho_\alpha^2}{2}\right)$, $\rho_\alpha\left(=\sqrt{\frac{v_{t\alpha}^2}{\omega_{c\alpha}^2}}\right)$ denotes the gyroradius, I_n represents the modified Bessel function of n[th] order and $\omega_{dc}\left(=\frac{Q_d^0 B}{m_d c}\right)$ is the dust cyclotron frequency. As we know dust mass is very large i.e., $m_d = 10^{12} m_p$. Hence, dust cyclotron frequency becomes very small and can be neglected. So, Eq. (3.8) becomes

$$n_d^1 = \frac{n_d^0 Q_d \phi}{T_d}\left[1+\frac{\omega}{k v_{td}}\sum_n Z\left(\frac{\omega}{k v_{td}}\right)\right]. \tag{3.9}$$

Substituting Eqs. (3.6), (3.7) and (3.9) in Poisson's equation

$$\nabla^2\phi = 4\pi\left[e n_e^1 - e n_i^1 + Q_d n_d^1\right]. \tag{3.10}$$

and simplifying this expression leads to the dispersion relation. The EIC wave linear dispersion relation is given by

$$\varepsilon(\omega,k) = 1+\chi_\alpha\ , \tag{3.11}$$

where χ are the susceptibilities.

$$\chi_e = \frac{2\omega_{pe}^2}{k^2 v_{te}^2}\left[1+\frac{\omega_1}{k_z v_{te}}\Gamma_n^e\sum_n Z\left(\frac{\omega_1}{k_z v_{te}}\right)\right]. \tag{3.12}$$

$$\chi_i = \frac{2\omega_{pi}^2}{k^2 v_{ti}^2}\left[1+\frac{\omega_2}{k_z v_{ti}}\Gamma_n^i\sum_n Z\left(\frac{\omega_2 - n\omega_{ci}}{k_z v_{ti}}\right)\right]. \tag{3.13}$$

$$\chi_d = \frac{2\omega_{pd}^2}{k^2 v_{td}^2}\left[1+\frac{\omega}{k v_{td}}\sum_n Z\left(\frac{\omega}{k v_{td}}\right)\right], \tag{3.14}$$

where $\omega_{pe}\left(=\sqrt{\frac{4\pi n_e^0 e^2}{m_e}}\right)$, $\omega_{pi}\left(=\sqrt{\frac{4\pi n_i^0 e^2}{m_i}}\right)$ and $\omega_{pd}\left(=\sqrt{\frac{4\pi n_d^0 Q_d^2}{m_d}}\right)$ are the plasma frequency of electrons, ions and dust grains, respectively.

The EIC wave can be studied analytically in the phase velocity region (Drummond and Rosenbluth)[45]

$$\frac{\omega_1}{k_z v_{te}} << 1 \tag{3.15}$$

$$\frac{\omega_2 - n\omega_{ci}}{k_z v_{ti}} >> 1 \tag{3.16}$$

corresponds to the small ion cyclotron damping term and

$$\frac{\omega}{k v_{td}} >> 1 \tag{3.17}$$

agrees to Landau damping for dust.

In Eq. (3.12), we have considered the small electron gyroradius, i.e., $b_e << 1$ and utilized only $n = 0$ term because $\Gamma_0^e = 1$ and $\Gamma_n^e = 0$ when $n \neq 0$. This supposition makes it possible to expand the plasma dispersive function, i.e., $Z(\xi)$ in the kinetic theory [58] as follows

$$Z(\xi_\alpha) = -2\xi_\alpha + \frac{2}{3}\xi_\alpha^3 + ... + i\sqrt{\pi}\, \mathrm{e}^{-\xi_\alpha^2} \quad \text{if } \xi_\alpha << 1 \tag{3.18}$$

$$Z(\xi_\alpha) = -\frac{1}{\xi_\alpha} - \frac{1}{2\xi_\alpha^3} + ... + i\sqrt{\pi}\, \mathrm{e}^{-\xi_\alpha^2} \quad \text{if } \xi_\alpha >> 1, \tag{3.19}$$

where $\xi_e = \frac{\omega_1}{k_z v_{te}}$, $\xi_i = \frac{\omega_2 - n\omega_{ci}}{k_z v_{ti}}$ and $\xi_d = \frac{\omega}{k v_{td}}$.

Introducing the expression (3.15) and (3.18), the Eq. (3.12) modifies to

$$\chi_e = \frac{2\omega_{pe}^2}{k^2 v_{te}^2}\left[1 + i\sqrt{\pi}\,\frac{\omega_1}{k_z v_{te}}\right]. \tag{3.20}$$

Similarly, in Eq. (3.13), we have considered that EIC wave having frequency $\omega \approx \omega_{ci}$ and using the recursive relation [59]

$$\sum_{n \neq 1} \Gamma_n^i \frac{1}{1-n} = \frac{1}{b_i}\left[1 - \Gamma_0^i\right]. \tag{3.21}$$

the Eq. (3.13) reduces to

$$\chi_i = \frac{2\omega_{pi}^2}{k^2 v_{ti}^2}\left[1-\Gamma_1^i \frac{\omega_2}{\omega_2-\omega_{ci}} - \frac{1-\Gamma_0^i}{b_i} + i\sqrt{\pi}\,\frac{\omega_2}{k_z v_{ti}}\Gamma_0^i\, e^{-\xi_i^2}\right]. \tag{3.22}$$

Using Eq. (3.17) limit and Eq. (3.19) expansion, the Eq. (3.14) modifies to

$$\chi_d = -\frac{\omega_{pd}^2}{\omega^2}, \tag{3.23}$$

where $\omega_{pd} = \sqrt{\frac{4\pi n_d^0 Q_d^2}{m_d}}$. As we know, dust mass is very large. So, here we can neglect this term $\frac{\omega_{pd}^2}{\omega^2} << 1$. Also, $\frac{\omega_{pd}^2}{\omega^2} << \chi_i$.

Substituting Eqs. (3.20), (3.22) and (3.23) in Eq. (3.11), we get

$$\varepsilon(\omega,k) = 1 + \frac{2\omega_{pe}^2}{k^2 v_{te}^2}\left[1 + i\sqrt{\pi}\,\frac{\omega_1}{k_z v_{te}}\right] + \frac{2\omega_{pi}^2}{k^2 v_{ti}^2}\left[1-\Gamma_1^i \frac{\omega_2}{\omega_2-\omega_{ci}} - \frac{1-\Gamma_0^i}{b_i} + i\sqrt{\pi}\,\frac{\omega_2}{k_z v_{ti}}\Gamma_0^i\, e^{-\xi_i^2}\right]. \tag{3.24}$$

This leads to the dispersion relation for EIC waves.

$$\varepsilon_r(\omega,k) + i\varepsilon_i(\omega,k) = 0, \tag{3.25}$$

where
$$\varepsilon_r(\omega,k) = 1 + \frac{2\omega_{pe}^2}{k^2 v_{te}^2} + \frac{2\omega_{pi}^2}{k^2 v_{ti}^2} - \Gamma_1^i \frac{2\omega_{pi}^2}{k^2 v_{ti}^2}\frac{\omega_2}{\omega-\omega_{ci}} - \frac{2\omega_{pi}^2}{k^2 v_{ti}^2}\left(\frac{1-\Gamma_0^i}{b_i}\right). \tag{3.26}$$

corresponds to the real part and

$$\varepsilon_i(\omega,k) = \sqrt{\pi}\left[\frac{\omega_1}{k_z v_{te}}\left(\frac{2\omega_{pe}^2}{k^2 v_{te}^2}\right) + \frac{2\omega_{pi}^2}{k^2 v_{ti}^2}\Gamma_0^i\left(\frac{\omega_2}{k_z v_{ti}}\right) e^{-\xi_i^2}\right]. \tag{3.27}$$

corresponds to the imaginary part.

The wave is either growing or damped, the solution for the EICWs can be obtained from the dispersion relation i.e., Eq. (3.24). The real part of frequency i.e., ω_r is obtained by

$$\varepsilon_r(\omega,k) = 0\big|_{\omega=\omega_r}. \tag{3.28}$$

The frequency imaginary part is defined by [60]

$$\omega_i = \left.\frac{-\varepsilon_i(\omega,k)}{\frac{\partial \varepsilon_r(\omega,k)}{\partial \omega}}\right|_{\omega=\omega_r} . \tag{3.29}$$

Solving for real and imaginary part of the Eqs. (3.28) and (3.29), it gives

$$\omega_r = \omega_{ci}(1+\Delta) + k_y v_E , \tag{3.30}$$

where

$$\Delta = \frac{\Gamma_1^i}{1-\Gamma_1^i - \frac{1-\Gamma_0^i}{b_i} + \frac{T_i}{T_e}\left(1+\frac{k^2 T_e}{4\pi n_i e^2}\right)}$$

$$\omega_i = -\sqrt{\pi}\frac{\left(\omega_r - k_y v_E - \omega_{ci}\right)^2}{\Gamma_1^i \omega_{ci}}\left[\frac{\left(\omega_r - k_y v_E - k_z u_{de}\right)}{k_z v_{te}}\frac{T_i}{T_e} + \Gamma_0^i \frac{\left(\omega_r - k_y v_E\right)}{k_z v_{ti}} e^{-\xi_i^2}\right]. \tag{3.31}$$

Equations (3.30) and (3.31) represent the real frequency and growth rate of EICWs in the existence of a transverse dc electric field. These analytical expressions are analogous to the expression of Chow and Rosenberg [8, 61] when there is no transverse dc electric field, i.e., $v_E \to 0 (E_0 = 0)$.

If we take into account the dust contribution, i.e., Eq. (3.23), the growth rate of the waves, i.e., Eq. (3.31), modifies to

$$\omega_i = -\sqrt{\pi}\left[\frac{\frac{2\omega_{pe}^2}{k^2 v_{te}^2}\frac{\left(\omega_r - k_y v_E - k_z u_{de}\right)}{k_z v_{te}} + \frac{2\omega_{pi}^2}{k^2 v_{ti}^2}\frac{\left(\omega_r - k_y v_E\right)}{k_z v_{ti}}\Gamma_o^i e\left(-\xi^2\right)}{\frac{2\omega_{pi}^2}{k^2 v_{ti}^2}\Gamma_1^i \frac{\omega_{ci}}{\left(\omega_r - k_y v_E - \omega_{ci}\right)^2} + \frac{2\omega_{pd}^2}{\omega_r^3}}\right]. \tag{3.32}$$

The critical drift velocity u_{de} is defined by the condition $\omega_i = 0$ which corresponds to the marginal stability. The expression is as follows

$$u_{de} = \frac{1}{k_z}\left[\left(\omega_r - k_y v_E\right)\left(1+\Gamma_0^i\, e^{-\xi_i^2}\,\delta\sqrt{\frac{m_i}{m_e}}\left(\frac{T_e}{T_i}\right)^{3/2}\right)\right]. \qquad (3.33)$$

3.3. RESULTS AND DISCUSSION

We have studied the excitation of EICWs in a collisionless magnetized dusty plasma in the occurrence of a transverse dc electric field. The present analysis would help accomplish the waves' real frequency and growth rate. The analytical expression for dispersion relation is derived for EICWs. The outcome of the magnetic field, electric field and temperature on the waves are examined. The equations discussed in Sec. 3.2. that are solved for frequency and growth rate of the waves, considering the experimentally acquired plasma parameters anticipated from various kinds of literature [3, 55, 61], are mentioned in Table 3.1.

The normalized real frequency of EIC wave with the finite gyroradius parameter in the presence of an electric field is illustrated in Figure 3.1(a). It can be observed from the graph that the frequency of the wave first increases as the gyroradius augments, attains a maximum value and then reduces for all values of δ. Variation in the frequency is also analyzed for different values of relative density ratio δ . As seen from the graph, frequency also increases with the increase in δ. This result is consistent with Chow and Rosenberg [8, 61]. The maximum frequency value is observed at $b_i = 0.84$ for $\delta = 4.0$ and the corresponding real frequency $\omega_r = 4.5\times10^6\, rad./\sec$. When $v_E \to 0$ in Eq. (3.30), the frequency decreases and its corresponding value $\omega_r = 1.05\times10^6\, rad./\sec$ for $\delta = 4.0$. This result is analogous to Chow and Rosenberg's [8] theoretical conclusion (cf. Figure no. 1(a)). We have shown this result when $v_E \to 0$ for real frequency in Figure 3.1(b), and the frequency results of Chow and Rosenberg [8] are shown in the inset of Figure 3.1(b). Hence, we can say that there is a significant increase in the wave frequency by a factor of ~ 4.3 as v_E included for $\delta = 4.0$ as compared to the wave frequency without the presence of v_E, and it can also be seen from Eq. (3.30). This is because the introduction of an electric field causes $\vec{E}\times\vec{B}$ drift, which produces the doppler effect, and so the frequency of the waves increases when a dc transverse electric field is present.

Table 3.1: Plasma parameters mentioned in the model.

Terms	Values
e (Electronic charge)	$4.8\times10^{-10}\,statcoul$
m_i (Ion mass)	$39\times1.67\times10^{-24}\,gm$
m_e (Electron mass)	$9.1\times10^{-28}\,gm$
m_d (Dust mass)	$10^{12}\times1.67\times10^{-24}\,gm$
c (Speed of light)	$3\times10^{10}\,cm/\mathrm{s}$
n_e^0 (Initial electron density)	$\left(1\times10^{9}-0.2\times10^{9}\right)cm^{-3}$
n_i^0 (Initial ion density)	$10^{9}\,cm^{-3}$
n_d^0 (Dust density)	$5\times10^{4}\,cm^{-3}$
u_{de} (Critical electron drift velocity)	$6\times10^{7}\,cm/\mathrm{sec}$
T_e (Electron temperature)	$0.2\ eV$
T_i (Ion temperature)	$0.2\ eV$
B_0 (Magnetic field)	$\left(0.1-4.5\right)kG$
E_0 (Electric field)	$0.35\ stat\ V\ cm^{-1}$
$\delta\left(=n_i/n_e\right)$ (Relative density ratio	$1-12$
K (Boltzmann constant)	$1.38\times10^{-16}\,erg/Kel$
k_z	$0.1\ cm^{-1}$
k_y	$1\ cm^{-1}$

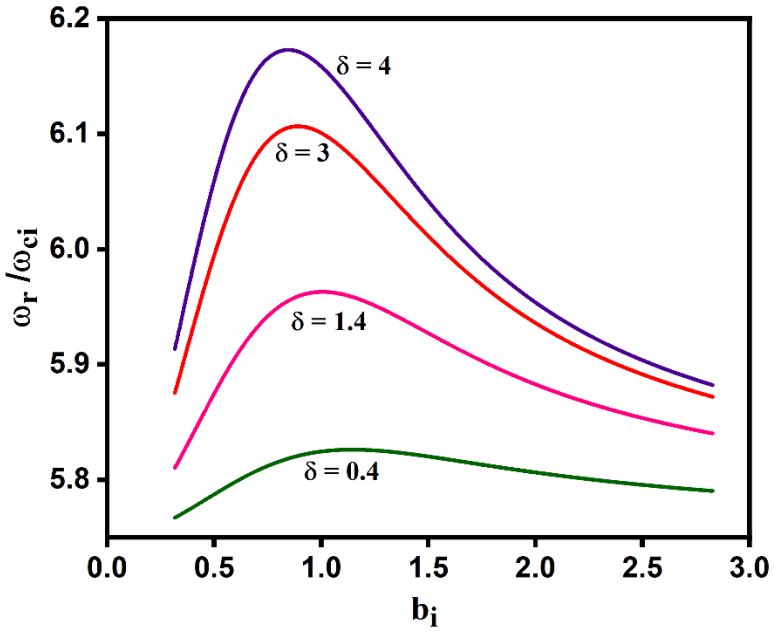

Figure 3.1 (a): The normalized real frequency as a function of finite gyroradius parameter for different relative densities of negatively charged dust grains in the existence of an electric field.

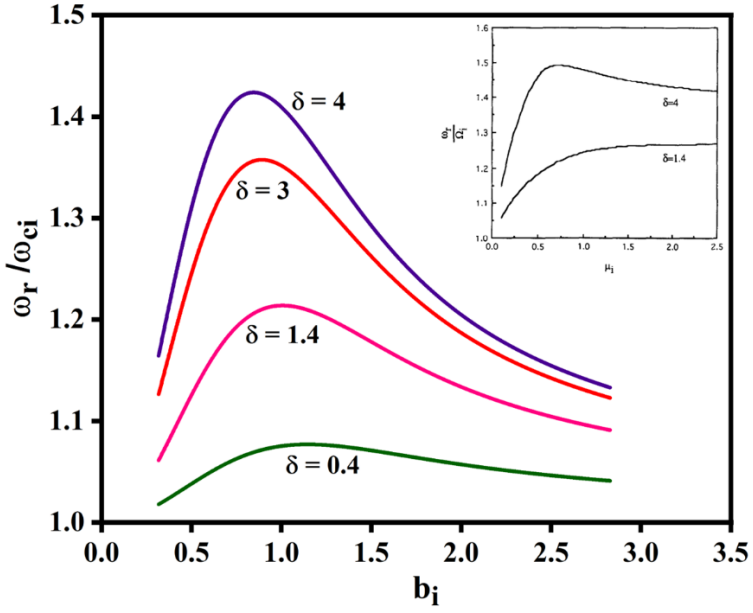

Figure 3.1(b): The normalized real frequency as a function of finite gyroradius parameter b_i for different relative densities of negatively charged dust grains in the absence of an electric field, inset of Figure 3.1(b) displays the results of Chow and Rosenberg [8].

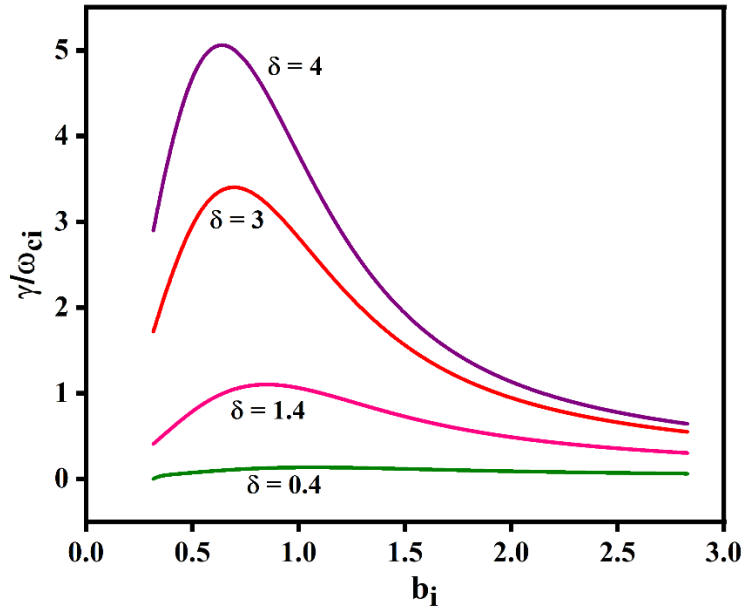

Figure 3.2: The normalized growth rate γ/ω_{ci} versus finite gyroradius parameter b_i for varying values of relative densities ratio $\delta\left(=n_i^0/n_e^0\right)$.

Figure 3.2 depicts the variation of normalized growth rate as a function of finite gyroradius for different values of relative density ratio. It can be concluded from the graph that with the increase in gyroradius, the growth rate of the EIC wave first increases, reaches a maximum value and then reduces for all values of δ. Variation in the growth rate is also evaluated for different relative density values of negatively charged dust grains. It can be seen from the graph that the growth rate also augments with an increase in δ. The maximum growth rate value is observed at $b_i = 0.63$ for $\delta = 4.0$ and the corresponding $\gamma = 3.7\times10^5\,\text{sec}^{-1}$. From Eq. (3.31), it can be seen that there is a small contribution from the electric field. Hence, we can conclude that there is a small change in the rate of growth after the inclusion of the electric field. This result is in line with the observations of Chow and Rosenberg [8] (cf. Figure no. 1(b)).

Figure 3.3 (a) show the variation of normalized real frequency of the wave with the relative density ratio δ for a fixed b_i in the presence of an electric field. As the amount of charge that dust carries augments, the frequency of the wave's augments. In the electric field's presence,

the maximum real frequency value is observed at $\omega_r = 4.45\times10^6 rad./\sec$. As $v_E \to 0$ in Eq. (3.31), the maximum real frequency value corresponds to $\omega_r = 9.5\times10^5 rad./\sec$.

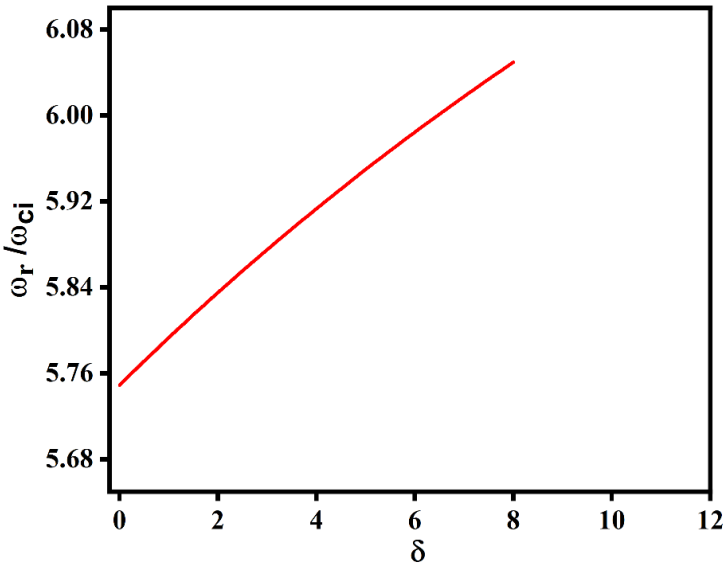

Figure 3.3 (a): The normalized real frequency ω_r/ω_{ci} is plotted with the relative density of negatively charged dust grains $\delta\left(=n_i^0/n_e^0\right)$ for $b_i = 0.1$ in the existence of an electric field.

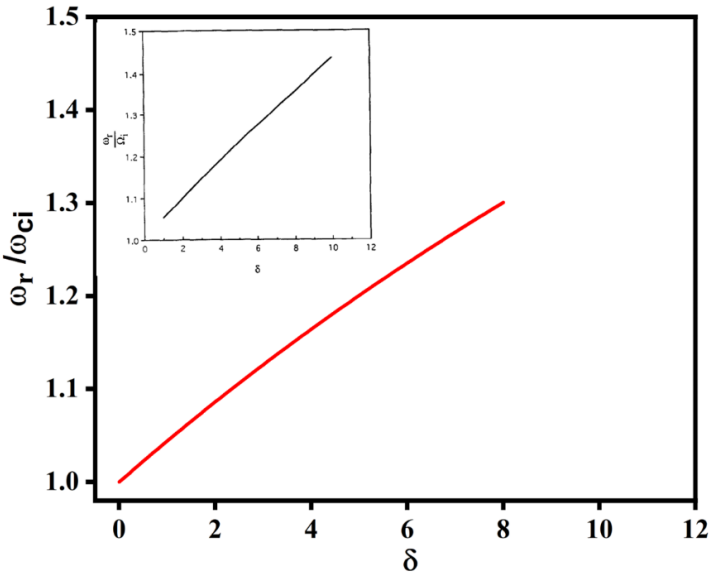

Figure 3.3 (b): The normalized real frequency ω_r/ω_{ci} variation with respect to the relative density of negatively charged dust grains $\delta\left(=n_i^0/n_e^0\right)$ for $b_i = 0.1$ and the inset of Figure 3.3 (b) shows the results of Chow and Rosenberg[8] in the absence of an electric field.

Figure 3.3 (b) show the variation of normalized real frequency of the wave with the relative density ratio δ for a fixed b_i in the absence of an electric field. As the amount of charge that dust carries augments, the frequency of the wave's augments. In the absence of an electric field, our result is in line with the theoretical conclusion of Chow and Rosenberg [8] (cf. Figure no. 2(a)) and the same is shown in the inset of Figure 3.3(b). As a result, it can be observed from the graphs that the frequency of the wave gets enhanced with the inclusion of an electric field.

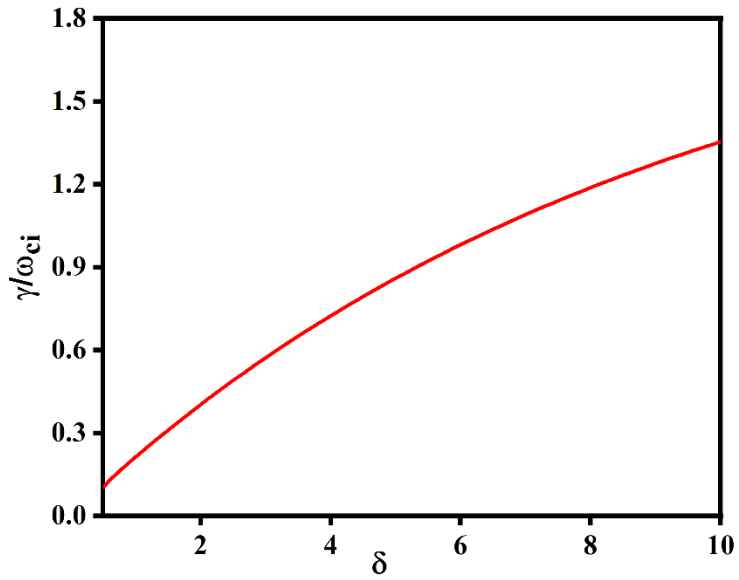

Figure 3.4: The normalized growth rate γ/ω_{ci} as a function of relative density of negatively charged dust grains $\delta\left(=n_i^0/n_e^0\right)$ for $b_i = 0.1$.

Figure 3.4 shows the dependence of normalized growth rate with respect to the relative density of negatively charged dust grains for a fixed b_i. It can be figured out from the graph that the growth rate increases with the increase in δ. It could be explained by the fact that when δ grows, the electron plasma density falls in comparison to the ion plasma density. The effective mass $m_{ieff} = \frac{m_i}{\delta}$ of an ion is smaller than m_i for greater values of δ, and as a result of their greater movement, wave generation gets enhanced.

We have plotted a normalized critical drift velocity graph with the negatively charged dust grain's relative density δ in Figure 3.5. We have inferred from the graph that as the relative density ratio increases, the critical electron drift velocity decreases, which can also be seen

from Eq. (3.33). This result is in line with Chow and Rosenberg [8] (cf. Figure no. 2(b)). Hence, we can say that it stabilizes the wave as the negatively charged dust grains increase. The rate of decrease of critical drift becomes relevant for $\delta \geq 1.65$. Also, our result complies with the experimental observation of Barkan et al. [3]

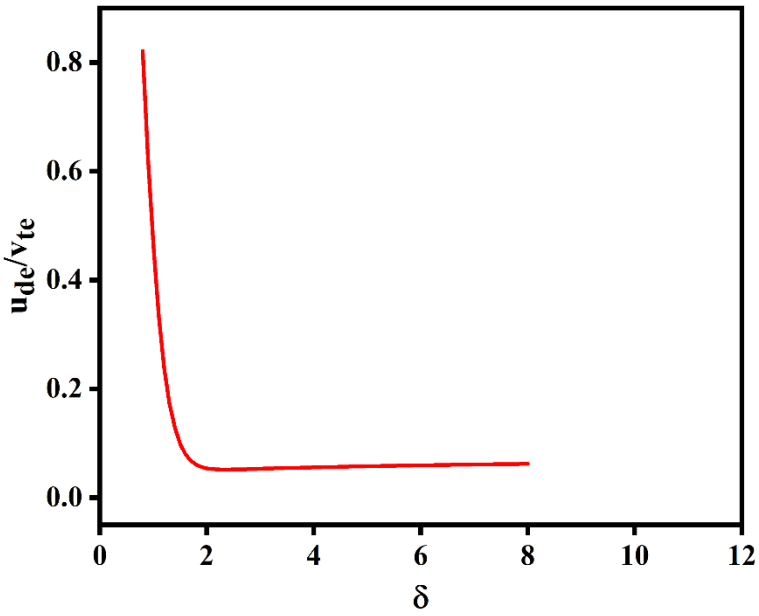

Figure 3.5: The normalized critical electron drift velocity u_{de}/v_{te} as a function of relative density of negatively charged dust grains $\delta\left(=n_i^0/n_e^0\right)$.

Figures 3.6 (a) and (b) illustrate the normalized frequency and growth rate, respectively, as a function of the magnetic field for $\delta = 2$. The figures show the linear relationship of the magnetic field with the frequency and growth rate of the EIC wave. Both the real frequency and growth rate of the waves increases as the magnetic field increases. It can be concluded that with the inclusion of an electric field in the EIC wave in a magnetized dusty plasma, the frequency of the mode and growth rate of the instability increase. This result is analogous to the Koepke and Amatucci [55] outcomes (cf. Figure no. 3) and Motley and Angelo [36] (cf. Figure no. 3). The experimental data of Koepke and Amatucci [55] shows a better result with the kinetic theory than the fluid theory.

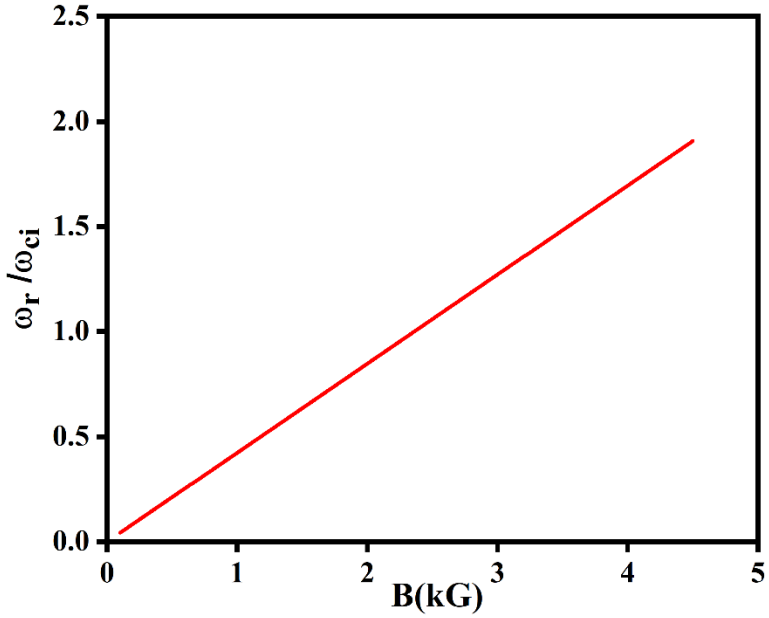

Figure 3.6 (a): The normalized real frequency ω_r/ω_{ci} variation of the EIC wave with the magnetic field $B(kG)$ for relative density ratio $\delta = 2$.

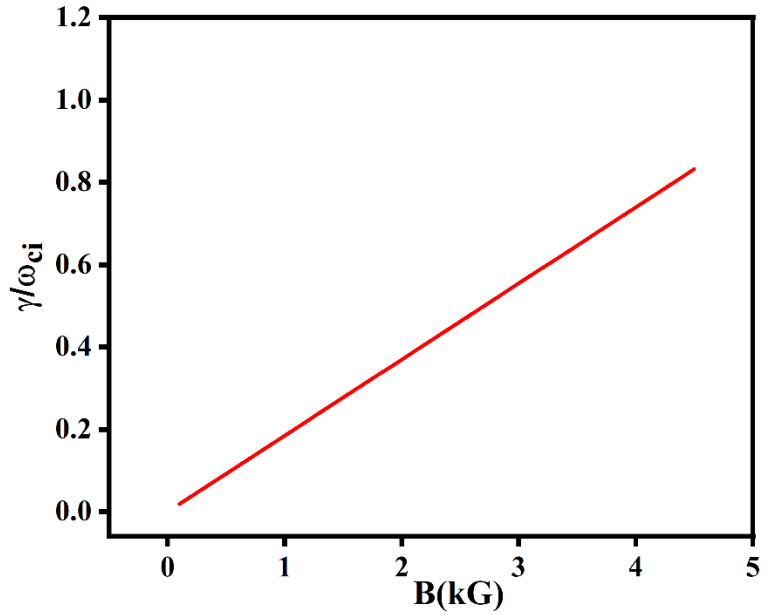

Figure 3.6 (b): The normalized growth rate γ/ω_{ci} of EIC wave with respect to the magnetic field $B(kG)$ for relative density ratio $\delta = 2$.

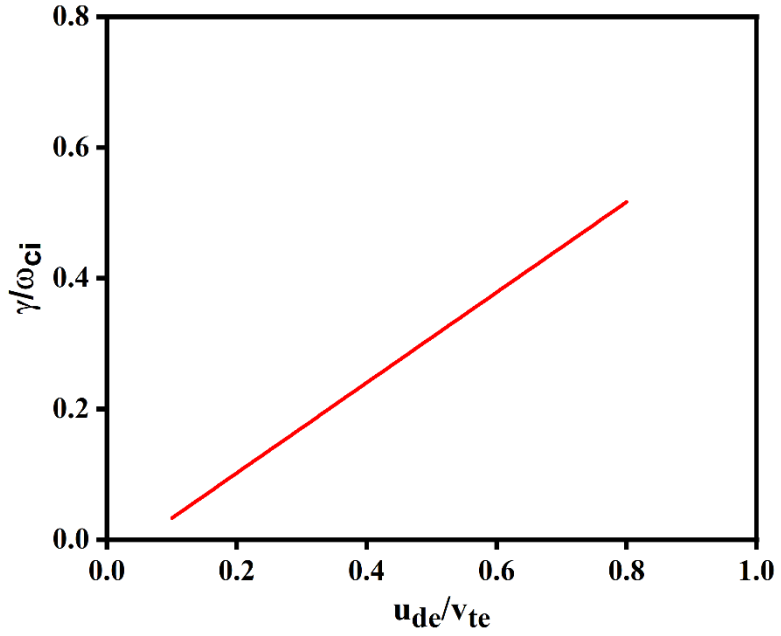

Figure 3.7: The normalized growth rate γ/ω_{ci} as a function of normalized critical electron drift velocity u_{de}/v_{te} for $B = 3.3\ kG$.

The graph between normalized growth rate and critical drift velocity for $B = 3.3\ kG$ is shown in Figure 3.7. It can be observed from the graph as the critical drift velocity increases, the growth rate of the instability increases. This result is consistent with the experimental observations of Correll et al. [37] (cf. Figure no. 6) for electrostatic ion cyclotron instability.

The dependence of normalized real frequency is plotted as a function of an electron to ion temperature ratio in Figure 3.8. As the electron to ion temperature ratio increases, the normalized frequency of the wave increases. It can be seen from Eq. (3.30) that as the T_e / T_i increases, the value of Δ increases, which increases the frequency. This result is in line with the Kindel and Kennel [46] (cf. Figure no. 1(b)).

The normalized growth rate graph as a function of an electron to ion temperature ratio of the EIC wave is explained in Figure 3.9. It indicates that the growth rate gradually decreases with the rise in the electron to ion temperature ratio for all values of δ and can be verified from Eq. (3.31).

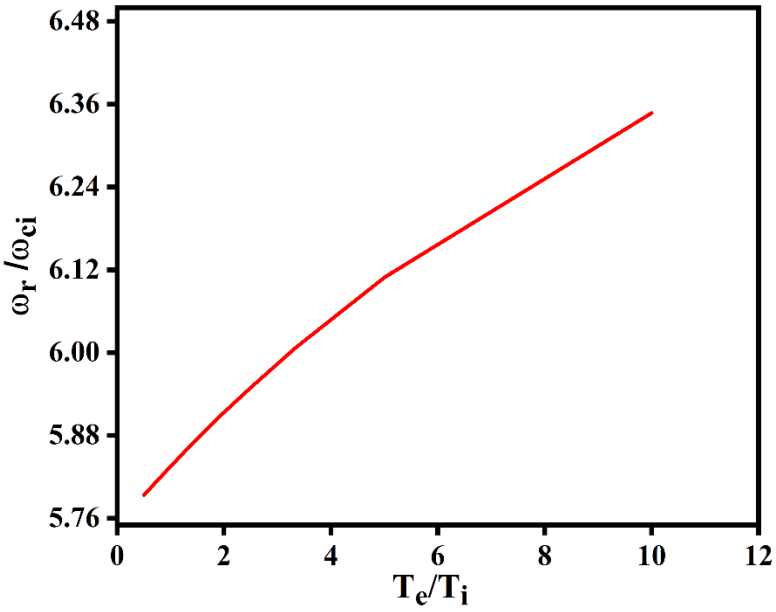

Figure 3.8: The normalized real frequency ω_r/ω_{ci} variation with the normalized temperature ratio (T_e/T_i) of an electron to ion.

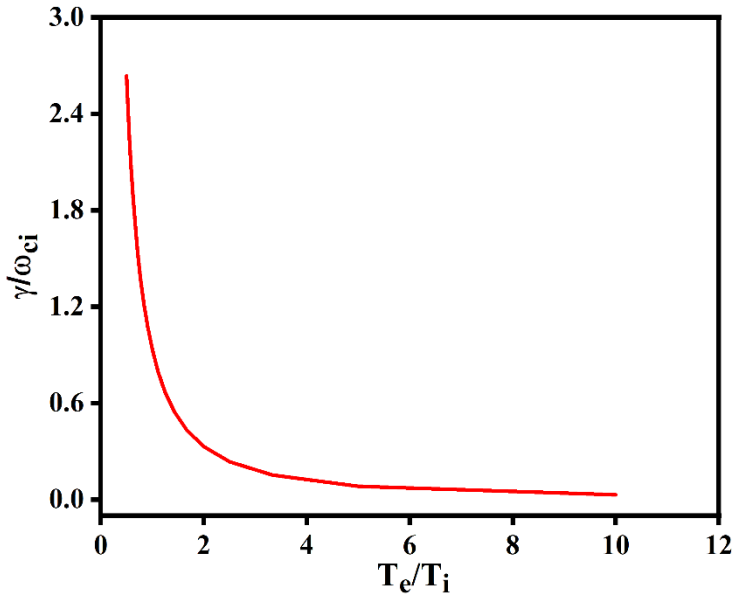

Figure 3.9: The normalized growth rate γ/ω_{ci} variation with the normalized temperature ratio T_e/T_i.

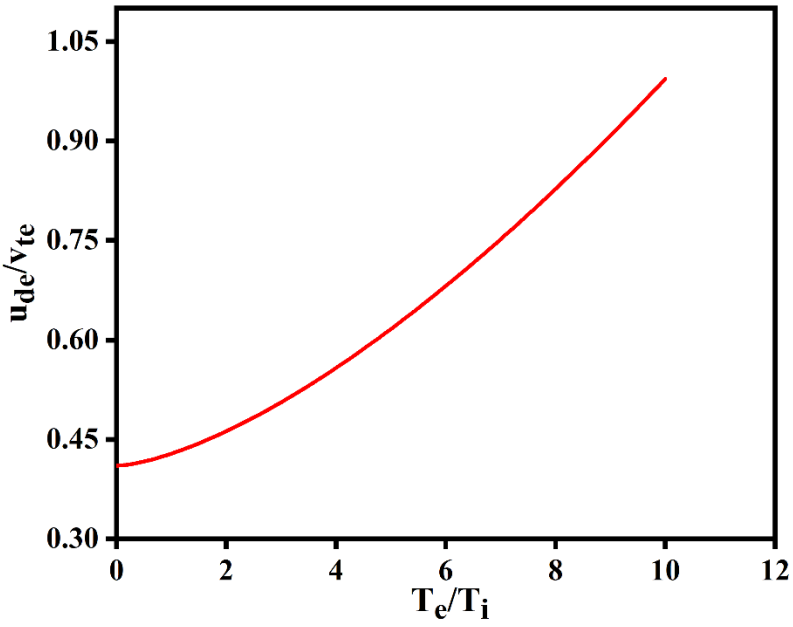

Figure 3.10: The normalized critical electron drift velocity variation with temperature ratio.

We have also plotted the normalized critical drift velocity variation with respect to electron to ion temperature ratio, which is displayed in Figure 3.10. It can be observed from the graph that critical drift increases as we augment the electron to ion temperature ratio, which can also be seen from Eq. (3.33). Levine and Kuckes [35] also showed in their experiment that critical electron drift velocity increases with the rise in electron to ion temperature ratio.

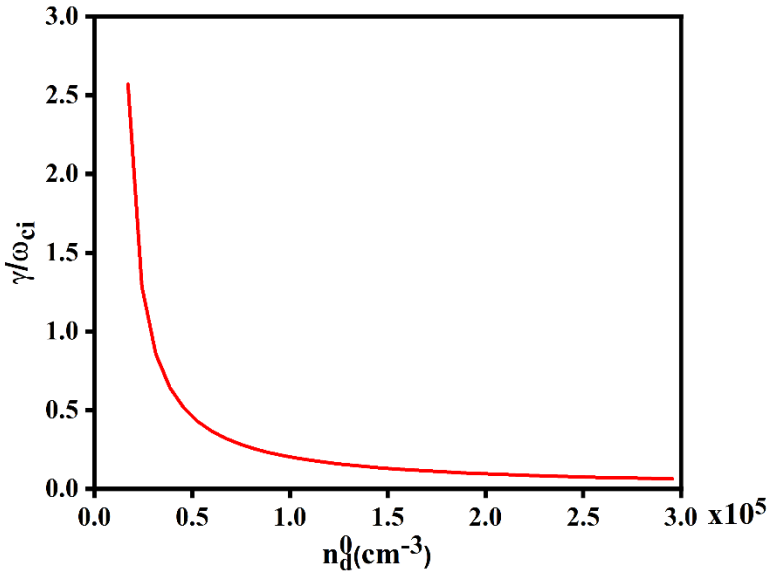

Figure 3.11: The normalized growth rate γ/ω_{ci} variation with the dust grain number density.

Figure 3.11 depicts the variation between normalized growth rate with respect to dust particle number density. It can be observed from the graph that the normalized growth rate is inversely proportional to the dust number density, which can also be seen from Eq. (3.32). As the number of dust particles augments, the number of accessible electrons per dust grain falls, implying that the dust particles collectively have a huge demand for electrons. The average dust grain charge Q_d is reduced, and as a result, the growth rate decrease.

3.4 CONCLUSION

An analytical model to study the excitation of current-driven EICWs in a magnetized dusty plasma in the existence of a transverse dc electric field has been developed, and the frequency, growth rate and other parameters of the EICWs have been investigated. The dispersive relation for the same has been inferred. From the study of the growth rate and frequency of the waves, it was found that the growth rate and frequency first increase with the increase in finite gyroradius parameter and then start decreasing with the gyroradius parameter in the presence and absence of an electric field. The maximum value of $\gamma = 3.7\times10^{5}\,\mathrm{sec}^{-1}$ at $b_i = 0.63$ and the $\omega_r = 4.5\times10^{6}\,rad./\mathrm{sec}$ at $b_i = 0.84$ for $\delta = 4.0$ when the electric field is present. When there is no electric field, our results are analogous to Chow and Rosenberg [8]. With the increase in relative density of negatively charged dust grains, both the growth rate and frequency of the EIC mode increase. The critical drift plays a vital role in the excitation of the mode, and it was found that with an augment in relative density ratio, the critical drift reduces. It was also observed that the magnetic field is directly proportional to both the growth rate and frequency of the waves. The effect of an electron to ion temperature ratio on various parameters of EICWs has also been examined. The frequency and critical drift are found to increase with an augment in electron to ion temperature ratio while the growth rate decreases with an augment in temperature ratio. Our theoretical results are consistent with many experimental studies [3, 46, 55]. It was observed that in spite of the small effect of dust grains on EICWs, it modifies the properties of EICWs. The growth rate of the wave decreases as the dust grains number density increases.

Our findings could benefit near-earth space environments [62] as it comprises a considerable amount of negatively charged dust grains, ions, electrons and a current-driven electric field.

These findings are also relevant to the ionosphere's EICWs excitation. The present work has various applications in space and planetary systems, e.g., in the study of the magnetosphere of Uranus [63].

REFERENCES

[1] N. D'Angelo, *Planetary and Space Science* **38**, 1143 (1990).

[2] A. Barkan, N. D'Angelo, R.L. Merlino, *Planetary and Space Science* **44**, 239 (1996).

[3] A. Barkan, N. D'Angelo, R.L. Merlino, *Planetary and Space Science* **43**, 905 (1995).

[4] A.M. Ignatov, *Plasma Physics Reports* **31**, 46 (2005).

[5] P.K. Shukla, *Physics of Plasmas* **8**, 1791 (2001).

[6] P.K. Shukla, A. Mamun, Introduction to Dusty Plasma Physics, *CRC Press* (2015).

[7] R.L. Merlino, A. Barkan, C. Thompson, N. D'Angelo, *Physics of Plasmas* **5**, 1607 (1998).

[8] V.W. Chow, M. Rosenberg, *Planetary and Space Science* **44**, 465 (1996).

[9] L. Spitzer Jr, *Journal of the Royal Astronomical Society of Canada* **72**, 349 (1978).

[10] J. Glanz, *Science* **264**, 28 (1994).

[11] D.A. Mendis, M. Rosenberg, *Annual Review of Astronomy and Astrophysics* **32**, 419 (1994).

[12] Bradford et al., *Science* **215**, 504 (1982).

[13] J. Winter, *Physics of Plasmas* **7**, 3862 (2000).

[14] G.S. Selwyn, J.E. Heidenreich, K.L. Haller, *Applied Physics Letters* **57**, 1876 (1990).

[15] R.L. Merlino, J.A. Goree, *Physics Today* **57**, 32 (2004).

[16] R.L. Merlino, *Plasma Physics Applied* **81**, 73 (2006).

[17] J. Pavlů, J. Šafránková, Z. Němeček, I. Richterová, *Contributions to Plasma Physics* **49**, 169 (2009).

[18] S.H. Kim, J.R. Heinrich, R.L. Merlino, *Planetary and Space Science* **56**, 1552 (2008).

[19] V.N. Tsytovich, O. Havnes, *Comments on Plasma Physics and Controlled Fusion* **15**, 267 (1993).

[20] S.K. El-Labany, W.M. Moslem, A.E. Mowafy, *Physics of Plasmas* **10**, 4217 (2003).

[21] M.-m. Lin, W.-s. Duan, *Chaos, Solitons & Fractals* **33**, 1189 (2007).

[22] A. Kumar, R. Gupta, J. Sharma, *AIP Advances* **12**, 035026 (2022).

[23] F. Verheest, *Space Science Reviews* **77**, 267 (1996).

[24] V. Prakash, S.C. Sharma, V. Vijayshri, R. Gupta, *Progress in Electromagnetics Research M* **36**, 161 (2014).

[25] C.K. Goertz, *Reviews of Geophysics* **27**, 271 (1989).

[26] K. Papadopoulos, P. Palmadesso, *Naval Research Laboratory Report* (1975).

[27] P.V. Bliokh, V.V. Yaroshenko, *Soviet Astronomy* **29**, 330 (1985).

[28] N.N. Rao, P.K. Shukla, M.Y. Yu, *Planetary and Space Science* **38**, 543 (1990).

[29] J.J. Rasmussen, R.W. Schrittwieser, *IEEE Transactions on Plasma Science* **19**, 457 (1991).

[30] G. Ganguli, Y. Lee, P. Chaturvedi, P. Palmadesso, S. Ossakow, Naval Research Lab Washington DC (1988).

[31] T.F.R. Group, *Physical Review Letters* **41**, 113 (1978).

[32] R.E. Waltz, R.R. Dominguez, *The Physics of Fluids* **24**, 1575 (1981).

[33] Zhang et al., *Nuclear Fusion* **52**, 032002 (2012).

[34] R.J. Dumont, D. Zarzoso, *Nuclear Fusion* **53**, 013002 (2012).

[35] A.M. Levine, A.F. Kuckes, *The Physics of Fluids* **9**, 2263 (1966).

[36] R.W. Motley, N. D'Angelo, *The Physics of Fluids* **6**, 296 (1963).

[37] D.L. Correll, N. Rynn, H. Böhmer, *The Physics of Fluids* **18**, 1800 (1975).

[38] K.-y. Yi, Z.-a. Wei, J.X. Ma, Q. Liu, Z.-y. Li, *Physics of Plasmas* **27**, 082103 (2020).

[39] Cattell et al., *Geophysical Research Letters* **25**, 2053 (1998).

[40] C.A. Cattell, F.S. Mozer, I. Roth, R.R. Anderson, R.C. Elphic, W. Lennartsson, E. Ungstrup, *Journal of Geophysical Research: Space Physics* **96**, 11421 (1991).

[41] J.R. Kan, H. Okuda, *Journal of Geophysical Research: Space Physics* **88**, 6339 (1983).

[42] P.L. Pritchett, M. Ashour-Abdalla, J.M. Dawson, *Geophysical Research Letters* **8**, 611 (1981).

[43] C.E. Seyler, J. Providakes, *The Physics of Fluids* **30**, 3113 (1987).

[44] G. Ganguli, P. Bakshi, *The Physics of Fluids* **25**, 1830 (1982).

[45] W.E. Drummond, M.N. Rosenbluth, *The Physics of Fluids* **5**, 1507 (1962).

[46] J.M. Kindel, C.F. Kennel, *Journal of Geophysical Research* **76**, 3055 (1971).

[47] K.F. Lee, *Journal of Plasma Physics* **8**, 379 (1972).

[48] G. Ganguli, Y.C. Lee, P. Palmadesso, *The Physics of Fluids* **28**, 761 (1985).

[49] S.C. Sharma, M. Sugawa, V.K. Jain, *Physics of Plasmas* **7**, 457 (2000).

[50] M. André, H. Koskinen, G. Gustafsson, R. Lundin, *Geophysical Research Letters* **14**, 463 (1987).

[51] X. Tang, C. Cattell, R. Lysak, L.B. Wilson Iii, L. Dai, S. Thaller, *Journal of Geophysical Research: Space Physics* **120**, 3380 (2015).

[52] M.F. Bashir, R. Ilie, G. Murtaza, *Physics of Plasmas* **25**, 052114 (2018).

[53] D.M. Suszcynsky, N. D'Angelo, R.L. Merlino, *Journal of Geophysical Research: Space Physics* **94**, 8966 (1989).

[54] M. Rosenberg, R.L. Merlino, *Journal of Plasma Physics* **75**, 495 (2009).

[55] M.E. Koepke, W.E. Amatucci, *IEEE Transactions on Plasma Science* **20**, 631 (1992).

[56] G. Ganguli, P.J. Palmadesso, *Geophysical Research Letters* **15**, 103 (1988).

[57] B. Song, D. Suszcynsky, N. D'Angelo, R.L. Merlino, *Physics of Fluids B: Plasma Physics* **1**, 2316 (1989).

[58] A. Bers, M.N. Rosenbluth, R.Z. Sagdeev, *MN Rosenbluth and RZ Sagdeev eds* **1**, (1983).

[59] D.B. Melrose, Instabilities in Space and Laboratory Plasmas (1986).

[60] N.A. Krall, A.W. Trivelpiece, *American Journal of Physics* **41**, 1380 (1973).

[61] V.W. Chow, M. Rosenberg, *Planetary and Space Science* **43**, 613 (1995).

[62] P.M. Kintner, M.C. Kelley, F.S. Mozer, *Geophysical Research Letters* **5**, 139 (1978).

[63] R.S. Pandey, M. Kumar, *East European Journal of Physics* **1,** 32 (2022).

4

Investigating EIC Waves in Magnetized Dusty Plasmas: Unveiling the Impact of Collisions in the Presence of DC Electric Field

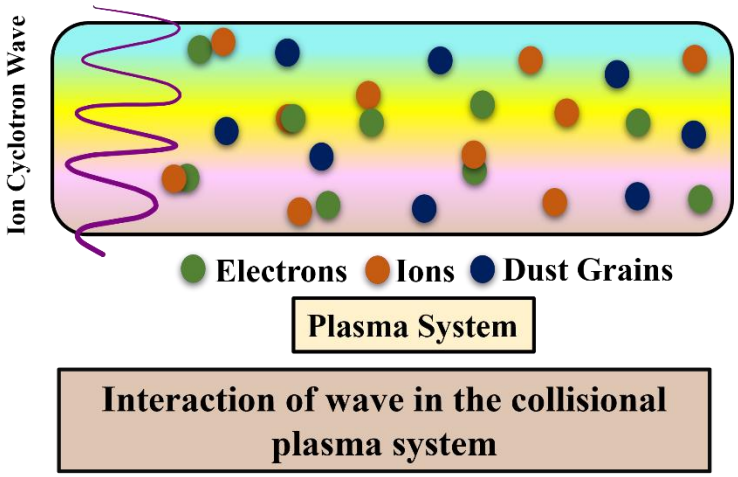

After the analysis of the various plasma parameters on Electrostatic Ion Cyclotron Waves (EICWs) in collisionless plasma, this chapter broadens the study by developing the same theoretical model in the collisional plasma for a more comprehensive understanding of the plasma system. The dispersion characteristics of EICWs alters in the presence of collisions. The collisional effects of the particles with various plasma parameters, i.e., gyro-radius, temperature etc. on an EIC wave have been examined. It has been found that the effect of an electron collision destabilizes and is vital for the EIC wave excitation whereas the effect of an ion collision stabilizes the wave. In addition, the critical drift velocity and temperature analysis has also been studied for the wave. Additionally, the influence of dust particles was explored.

PUBLICATION

Anshu, Jyotsna Sharma, and Suresh C. Sharma, "Investigating EIC Waves in Magnetized Dusty Plasmas: Unveiling the Impact of Collisions in the Presence of DC Electric Field". (Communicated)

4.1 INTRODUCTION

The study of plasma has become indispensable due to its pervasive nature. Therefore, it is not surprising that research into "plasmas" [1-6] is proposed in several waves [7-12] and astrophysical phenomena [13-17]. EICWs in plasma have been investigated by numerous researchers [18-21] through diverse methods, including kinetic theory, kappa distribution and fluid theory in many experimental and theoretical studies [7, 8, 22-25]. Observations of electrostatic ion-cyclotron EICWs have been made in various kinds of environments, from fusion heating [26-28], space plasmas to laboratory experiments [29-34]. The initial experimental findings of EIC oscillations in lab plasmas were presented by D'Angelo and Motley [35]. The oscillations that were observed were identified to be current driven electrostatic ion cyclotron (EIC) instability which is theoretically anticipated by Drummond and Rosenbluth [36]. A well-known low-frequency field-aligned phenomenon which has received a lot of interest from the plasma physics field is the current-driven EIC instability [3]. In contrast to other current-driven instabilities, this one has a strikingly low threshold electron drift velocity [18]. The electron current, which is indicated by the electron drift velocity, across the lines of the magnetic field can make the EIC wave unstable since it flows roughly perpendicular to the direction of the magnetic field [37]. The comprehension of the fundamental process that causes these ion-cyclotron instabilities in collisional plasma has been given by Chaturvedi and Kaw [38] using fluid treatment. Drummond and Rosenbluth [36] carried out a mathematical investigation and found that the oscillations were related to the current-driven EIC instability. They specifically looked at the value of electron drift velocity for EICWs under the assumption of identical electron and ion temperatures. D'Angelo [3] investigated in his studies the interaction between the plasma's charged dust particles and ion cyclotron waves. He showed that as the positive ion EIC mode's frequency gradually rises, the amount of negatively charged particles augments. In a Q-machine, the study on EICWs was reported by Barkan et al. [31] and it was observed that the growth rate of the wave was increased in the presence of a substantial amount of negatively charged dust particles. Chow and Rosenberg [39] concluded in their research using the kinetic theory, as the relative dust concentration augments, the critical drift velocity falls during the excitation of EICWs and observed that in a plasma with plenty of negatively charged dust particles, the wave mode is further destabilised. Chaturvedi and Kaw [38] studied the collisional effects of EICWs in a fully ionised collisional plasma and observed the stability of obliquely propagating EIC wave to current flow across the lines of the magnetic field via fluid theory. Satyanarayana et al. [40] theoretically studied the collisional effects of EICWs in bottomside ionosphere and it was discovered that electron collisions are unstable and

are essential for causing the EIC instability to arise. Suszcynsky et al. [34] conducted an experimental study on EICWs in laboratory plasma in an auroral ionosphere regime and demonstrated the effects of collisions between neutral particles and waves in a Q-machine. Bharuthram et al. [41] examined the collisional effects on EICWs in plasma via kinetic theory in the absence of a transverse electric field and concluded that the wave behaviour is altered by the presence of collisions. In a magnetized plasma, Sharma et al. [8] using fluid treatment examined the excitation of EICWs. They found a strong relationship between the wave's frequency and rate of growth in presence of an electric field, where the frequency rises as the growth rate lowers. Anshu et al. [21] studied the EICWs in a collisionless plasma via kinetic treatment. They found that with an addition of an electric field, the dispersion relation modifies and it would further affect the frequency and the growth rate of the wave.

A theoretical model has not been proposed, as far as the authors are aware to study the combined effect of collision, temperature and dust in the transverse dc electric field in a dusty magnetized plasma via kinetic theory. Therefore, we have expanded earlier research [8, 21] to understand the role of plasma parameters, i.e., dust density, relative density ratio, and gyroradius parameter etc. on the EIC wave in a collisional magnetized plasma having negatively charged dust particles in the existence of a transverse dc electric field via kinetic theory. Moreover, this current model shows the effect of collision frequency with different plasma parameters to study the behaviour of the waves i.e., frequency and the growth rate.

This chapter is organized as follows for the succeeding sections: the detailed analysis of electrostatic ion cyclotron wave for solving the expression of growth rate, frequency and critical drift is delineated in Section 4.2. In Section 4.3, the outcomes of the theoretical modelling of the EIC wave have been compared with the results of the existing observations. The conclusion is outlined in Section 4.4.

4.2 INSTABILITY ANALYSIS

In this chapter, we studied the collisional multispecies magnetized dusty plasma that is enclosed in a uniform and static magnetic field B oriented along the z-direction. The proposed system consists of three species: electrons, ions and dust particles, and their notations can be tabulated in Table 4.1. An EIC wave exhibits a characteristic frequency ω and propagation vector k oriented in the y-z plane and its alignment is roughly perpendicular to the applied magnetic field. In addition, we provide proposed system with a transverse dc electric field E in

the direction of x. This introduction of an electric field induces $\vec{E}\times\vec{B}$ drift causing excitation of a wave and has a magnitude $v_E\left(=\frac{cE}{B}\right)$, oriented in the y-direction and c is the speed of light.

Table 4.1: Species and their notations considered in the model.

S. No.	Species	Equilibrium density	Drift Velocity	Velocity	Mass	Charge	Temperature	Collisional Frequency
1.	Electrons	n_e^0	$u_{ed} \parallel \hat{z}$	v_e	m_e	$-e$	T_e	υ_e
2.	Ions	n_i^0	0	v_i	m_i	e	T_i	υ_i
3.	Dust Particles	n_d^0	0	v_d	m_d	Q_d^0	T_d	υ_d

We have also taken into consideration the appropriate drifting Maxwellian distribution function for the electrons and is as follows

$$f_e^0 = n_e^0\left(\frac{m_e}{2\pi KT_e}\right)^{3/2}\exp\left[\frac{-1}{2}\frac{m_e}{KT_e}\left\{v_x^2+\left(v_y-v_E\right)^2+\left(v_z-u_{ed}\right)^2\right\}\right], \qquad (4.1)$$

where K = Boltzmann constant,

f_e^0 = Maxwellian distribution function at equilibrium,

v_x, v_y and v_z represents the velocities in their respective directions.

On the other hand, by changing $\left(n_e^0, m_e, T_e\right)$ with $\left(n_d^0, m_d, T_d\right)$ and $\left(n_i^0, m_i, T\right)$ and taking $u_{ed}=0$ in Eq. (4.1), the dust (and ions) distribution function can be obtained.

In equilibrium, the quasi-neutrality condition says

$$en_i^0 = en_e^0 + Q_d^0 n_d^0 . \qquad (4.2)$$

For frequencies in the same range as the ion gyrofrequency, $\omega \approx \omega_{ic} \gg \omega_{dc}$, where $\omega_{ic}\left(=\frac{eB}{m_i c}\right)$ represents the ion cyclotron frequency and $\omega_{dc}\left(=\frac{Q_d^0 B}{m_d c}\right)$ is the dust cyclotron frequency. So, it is possible to consider the dust particles to be non-magnetized.

Applying the BGK collision model [19, 42] the following is the expression for the kinetic dispersion relation that governs the behaviour of electrostatic modes in a collisional dusty plasma with dust particles to be non-magnetized and is expressed as follows

$$\varepsilon(\omega,k)=1+\sum_{\alpha}\chi_{\alpha}=0\,, \tag{4.3}$$

where χ are the susceptibilities and α refers to the electrons, ions and dust grains, respectively.

The electron, ion and dust grains susceptibilities are given as follows

$$\chi_e=\frac{2\omega_{ep}^2}{k^2v_{et}^2}\left[1+\frac{\omega_1+i\upsilon_e}{k_zv_{et}}\sum_n\Gamma_n^eZ\left(\frac{\omega_1+i\upsilon_e}{k_zv_{et}}\right)\right]\left[1+\frac{i\upsilon_e}{k_zv_{et}}\sum_n\Gamma_n^eZ\left(\frac{\omega_1+i\upsilon_e}{k_zv_{et}}\right)\right]^{-1}. \tag{4.4}$$

$$\chi_i=\frac{2\omega_{ip}^2}{k^2v_{it}^2}\left[1+\frac{\omega_2+i\upsilon_i}{k_zv_{it}}\sum_n\Gamma_n^iZ\left(\frac{\omega_2-n\omega_{ic}+i\upsilon_i}{k_zv_{it}}\right)\right]\left[1+\frac{i\upsilon_i}{k_zv_{it}}\sum_n\Gamma_n^iZ\left(\frac{\omega_2-n\omega_{ic}+i\upsilon_i}{k_zv_{it}}\right)\right]^{-1}. \tag{4.5}$$

$$\chi_d=\frac{2\omega_{dp}^2}{k^2v_{dt}^2}\left[1+\frac{\omega+i\upsilon_d}{kv_{dt}}Z\left(\frac{\omega+i\upsilon_d}{kv_{dt}}\right)\right]\left[1+\frac{i\upsilon_d}{kv_{td}}Z\left(\frac{\omega+i\upsilon_d}{kv_{dt}}\right)\right]^{-1}, \tag{4.6}$$

where $\omega_1=\omega-k_yv_E-k_zu_{ed}$ and $\omega_2=\omega-k_yv_E$; k_y and k_z are the wave vector oriented along y and z-direction; $\Gamma_n^{\alpha}=I_n(\mu_{\alpha})\exp(-\mu_{\alpha})$, where $\mu_{\alpha}\left(=\frac{k_y^2\rho_{\alpha}^2}{2}\right)$, $\rho_{\alpha}\left(=\sqrt{\frac{v_{\alpha t}^2}{\omega_{\alpha c}^2}}\right)$ denotes the gyroradius, I_n represents the modified n[th] order Bessel function; Z depicts the plasma dispersion function [43] and other parameters are tabulated in Table 4.2.

Table 4.2: Notations and their formulas

S. No.	Notations	Terms	Formula
1.	ω_{ep}	Electron plasma frequency	$\sqrt{\frac{4\pi n_e^0e^2}{m_e}}$
2.	ω_{ip}	Ion plasma frequency	$\sqrt{\frac{4\pi n_i^0e^2}{m_i}}$
3.	ω_{dp}	Dust plasma frequency	$\sqrt{\frac{4\pi n_d^0Q_d^2}{m_d}}$
4.	v_{et}	Electron thermal velocity	$\sqrt{\frac{2KT_e}{m_e}}$
5.	v_{it}	Ion thermal velocity	$\sqrt{\frac{2KT_i}{m_i}}$
6.	v_{dt}	Dust thermal velocity	$\sqrt{\frac{2KT_d}{m_d}}$

Analytical solutions of Eq. (4.3) are possible in some regimes by introducing some simplifying conditions. We are only concerned with the phase-velocity regime for the EICWs (Drummond and Rosenbluth). [36]

$$\frac{\omega_1 + i\upsilon_e}{k_z v_{et}} << 1 . \tag{4.7}$$

$$\frac{\omega_2 - n\omega_{ic} + i\upsilon_i}{k_z v_{it}} >> 1, \tag{4.8}$$

refers to the small ion cyclotron damping term and

$$\frac{\omega + i\upsilon_d}{k v_{dt}} >> 1, \tag{4. 9}$$

agrees to Landau damping for dust.

Equation (4.4) can be simplified by assuming $\mu_e << 1$, and utilized only $n = 0$ term because $\Gamma_0^e = 1$ and $\Gamma_n^e = 0$ when $n \neq 0$. This presumption allows us to conveniently expand the plasma dispersive function $Z(\xi)$ within the framework of kinetic theory [44] as follows:

$$Z(\xi_\alpha) = -2\xi_\alpha + \frac{2}{3}\xi_\alpha^3 + ... + i\sqrt{\pi}\, \mathrm{e}^{-\xi_\alpha^2} \qquad \text{if } \xi_\alpha << 1 \tag{4.10}$$

$$Z(\xi_\alpha) = -\frac{1}{\xi_\alpha} - \frac{1}{2\xi_\alpha^3} + ... + i\sqrt{\pi}\, \mathrm{e}^{-\xi_\alpha^2} \qquad \text{if } \xi_\alpha >> 1 , \tag{4.11}$$

where $\xi_e = \frac{\omega_1 + i\upsilon_e}{k_z v_{et}}$, $\xi_i = \frac{\omega_2 - n\omega_{ic} + i\upsilon_i}{k_z v_{it}}$ and $\xi_d = \frac{\omega + i\upsilon_d}{k v_{dt}}$.

So, Eq. (4.4) can be rewritten after substituting Eqs. (4.7) and (4.10)

$$\chi_e = \frac{2\omega_{ep}^2}{k^2 v_{et}^2}\left[1 + \frac{\sqrt{\pi}\upsilon_e}{k_z v_{et}} + i\sqrt{\pi}\,\frac{\omega_1}{k_z v_{et}}\left(1 + \frac{\sqrt{\pi}\upsilon_e}{k_z v_{et}}\right)\right] . \tag{4.12}$$

For the ions, we can approximate the Eq. (4.5) by retaining only n=0 and n=1 terms in the χ_i summation; including ions-neutral collisions and further assuming $\omega \approx \omega_{ci}$, $\frac{\upsilon_i}{\omega} \ll 1$ and $\frac{\upsilon_i}{\omega - \omega_{ic}} \ll 1$, the Eq. reduces to

$$\chi_i = \frac{2\omega_{ip}^2\left(\omega_2 + i\upsilon_i\right)\left(1-\frac{1-\Gamma_0^i}{\mu_i}-\Gamma_1^i\right)-\omega_{ic}\left(1-\Gamma_0^i\right)}{k^2 v_{it}^2\left(\omega_2-\omega_{ic}\right)-i\upsilon_i\left[\frac{\omega_2-\omega_{ic}}{\omega_2}\Gamma_0^i-\left(1-\Gamma_1^i\right)\right]}\,. \tag{4.13}$$

Equation (4.6) can be solved by substituting Eqs. (4.9) and (4.11), here we have neglected the dust collision frequency because the mass of dust is very large and hence, this Eq. abridges to

$$\chi_d = -\frac{\omega_{dp}^2}{\omega^2}\,. \tag{4.14}$$

In this context, we can ignore this term $\frac{\omega_{dp}^2}{\omega^2} << 1$. Also, $\frac{\omega_{dp}^2}{\omega^2} << \chi_i$.

Substituting Eqs. (4.12), (4.13) and (4.14) in Eq. (4.3), we get

$$\begin{aligned}\varepsilon\left(\omega,k\right) = 1 &+ \frac{2\omega_{ep}^2}{k^2 v_{et}^2}\left[1+\frac{\sqrt{\pi}\upsilon_e}{k_z v_{et}}+i\sqrt{\pi}\,\frac{\omega_1}{k_z v_{et}}\left(1+\frac{\sqrt{\pi}\upsilon_e}{k_z v_{et}}\right)\right] \\ &+ \frac{2\omega_{ip}^2\left(\omega_2+i\upsilon_i\right)\left(1-\frac{1-\Gamma_0^i}{\mu_i}-\Gamma_1^i\right)-\omega_{ic}\left(1-\Gamma_0^i\right)}{k^2 v_{it}^2\left(\omega_2-\omega_{ic}\right)-i\upsilon_i\left[\frac{\omega_2-\omega_{ic}}{\omega_2}\Gamma_0^i-\left(1-\Gamma_1^i\right)\right]}\,.\end{aligned} \tag{4.15}$$

This results in the EICWs dispersion relation for collisional plasma.

The wave is either growing or damped, the dispersion relation is used to determine the solutions for the EICWs. The following equations determine the real and imaginary components of the frequency

$$\varepsilon_r\left(\omega,k\right) = 0\big|_{\omega=\omega_r}\,, \tag{4.16}$$

where ε_r is the real part of Eq. (4.15)

The frequency imaginary part is defined by [45]

$$\gamma = \left.\frac{-\varepsilon_i\left(\omega,k\right)}{\frac{\partial\varepsilon_r\left(\omega,k\right)}{\partial\omega}}\right|_{\omega=\omega_r}\,, \tag{4.17}$$

where ε_i denotes the imaginary part of Eq. (4.15)

Determining the real and imaginary parts of the Eqs. (4.16) and (4.17), and leading to

$$\omega_r = \omega_{ic}\left(1+\Delta\right)+k_y v_E\,, \tag{4.18}$$

where

$$\Delta = \frac{\Gamma_1^i}{1-\Gamma_1^i-\dfrac{1-\Gamma_0^i}{\mu_i}+\dfrac{T_i}{T_e}\left(1+\dfrac{k^2T_e}{4\pi n_e e^2}+\dfrac{1}{1+\left(P_e+P_i\right)}\right)},$$

where $$P_e = \frac{\sqrt{\pi}\upsilon_e}{k_z v_{et}}\,.$$

$$P_i = \upsilon_i \frac{\omega_2\left(1-\dfrac{1-\Gamma_0^i}{\mu_i}-\Gamma_1^i\right)-\omega_{ic}\left(1-\Gamma_0^i\right)}{\left(\omega_2-\omega_{ic}\right)^2}\,.$$

$$\gamma = -\sqrt{\pi}\frac{\left(\omega_r-k_y v_E-\omega_{ic}\right)^2}{\Gamma_1^i\omega_{ic}}\frac{T_i}{T_e}\left[\frac{\left(\omega_r-k_y v_E-k_z u_{ed}\right)}{k_z v_{et}}\left(1+\frac{\sqrt{\pi}\upsilon_e}{k_z v_{et}}\right)\right]-\upsilon_i\left[1-\Gamma_1^i\right]. \tag{4.19}$$

The analytical expressions for the real frequency and growth rate are given in Eqs. (4.18) and (4.19) of the EICWs in the presence of a transverse dc electric field If $v_E \to 0$ and $\upsilon_i = \upsilon_e = 0$, these mathematical formulations are similar to the results that Chow and Rosenberg reported in their prior works [39, 46]. Moreover, we replicate the expressions of Anshu et al. [21] in the absence of collisions.

The wave growth rate, given by Eq. (4.19), changes to Eq. (4.20), if we account for the dust component.

$$\gamma = -\sqrt{\pi}\left[\frac{\dfrac{2\omega_{ep}^2}{k^2v_{et}^2}\dfrac{\left(\omega_r-k_y v_E-k_z u_{ed}\right)}{k_z v_{et}}\left(1+\dfrac{\sqrt{\pi}\upsilon_e}{k_z v_{et}}\right)}{\dfrac{2\omega_{ip}^2}{k^2v_{it}^2}\Gamma_1^i\dfrac{\omega_{ic}}{\left(\omega_r-k_y v_E-\omega_{ic}\right)^2}+\dfrac{2\omega_{dp}^2}{\omega_r^3}}\right]-\upsilon_i\left[1-\Gamma_1^i\right]. \tag{4.20}$$

The criterion $\gamma = 0$, which pertains to the point of marginal stability, is referred to as the critical drift velocity, u_{ed}. The expression for u_{ed} is provided as follows

$$u_{ed} = \frac{1}{k_z}\left[\left(\omega_r - k_y v_E\right) + \frac{\omega_{ic}\Gamma_1^i \upsilon_i\left[1-\Gamma_1^i\right]}{\sqrt{\pi}\left(\omega_r - k_y v_E - \omega_{ic}\right)^2}\frac{T_e}{T_i}\frac{k_z v_{et}}{\left(1+\frac{\sqrt{\pi}\upsilon_e}{k_z v_{et}}\right)}\right]. \qquad (4.21)$$

4.3 RESULTS AND DISCUSSION

In this chapter, the analytical model has been developed in a collisional magnetized plasma to study the EIC wave excitation with negatively charged dust grains while incorporating an electric field using the kinetic theory. The developed model aims to analyse the relationship between various plasma parameters, i.e., real frequency, growth rate, etc. The effect of the collisions, temperature, gyro-radius and relative density ratio on the wave is studied. The equations that hold accountable for the EIC wave in Sec. 4.2 are used to calculate the frequency, the rate of growth and critical drift for the same. The graphs have been plotted using the MATLAB program for the analytically solved equations i.e., for real frequency and the growth rate. The modified plasma parameters used in our calculation are obtained from various experimental and theoretical papers [7, 31, 46, 47] and are tabulated in Table 4.3.

Figure 4.1 portrays the plot of normalized growth rate as a function of the gyro-radius parameter for varying δ i.e., (a) $\delta = 0.4$, (b) $\delta = 1.4$, (c) $\delta = 3$, and (d) $\delta = 4$, respectively. From Figure 4.1, it can be observed that with an increase in values of the gyro-radius parameter, the rate of growth of the instability first augments and then attains a maximum value, i.e., $\gamma = 2.19\times10^4$ sec^{-1} for $\mu_i = 0.96$ at $\delta = 4$. After attaining maximum value, the instability's growth rate decreases. It can also be inferred that with the increase in the relative density ratio, the growth rate of the unstable wave augments. When $\upsilon_e = \upsilon_i \to 0$ in Eq. (4.20), the growth rate increases and its corresponding value $\gamma = 2.5\times10^5$ sec^{-1} for $\delta = 4$. This result is in good agreement with the experimental observation of Chow and Rosenberg in the absence of collisions [39].

Table 4.3: Plasma parameters are specified in this model.

Terms	Values
e (Electronic charge)	$4.8\times10^{-10}\,statcoul$
Q_d^0 (Dust charge)	$\left(10^3-10^4\right)e$
m_d (Dust mass)	$10^{12}\times1.67\times10^{-24}\,gm$
m_e (Electron mass)	$9.1\times10^{-28}\,gm$
m_i (Ion mass)	$39\times1.67\times10^{-24}\,gm$
T_e (Electron temperature)	$0.2\ eV$
T_i (Ion temperature)	$0.2\ eV$
n_i^0 (Initial ion density)	$10^9\,cm^{-3}$
n_e^0 (Initial electron density)	$\left(1\times10^9-0.2\times10^9\right)cm^{-3}$
n_d^0 (Dust density)	$(1-5)\times10^4\,cm^{-3}$
c (Speed of light)	$3\times10^{10}\,cm/\mathrm{s}$
B (Magnetic field)	$\left(0.1-4.5\right)kG$
$\delta\left(=n_i/n_e\right)$ (Relative density ratio)	$1-10$
$\mu_i(=k_y\rho_i)^2$ (Gyro-radius parameter)	$0-3.5$
K (Boltzmann constant)	$1.38\times10^{-16}\,erg/Kel$
k_z	$0.1\ cm^{-1}$
k_y	$1\ cm^{-1}$
υ_e (Electron collisional frequency)	$4\times10^5\,\mathrm{sec}^{-1}$
υ_i (Ion collisional frequency)	$1\times10^3\,\mathrm{sec}^{-1}$
u_{ed} (Critical electron drift velocity)	$6\times10^7\,cm/\mathrm{sec}$
E (Electric field)	$0.35\ stat\ V\ cm^{-1}$

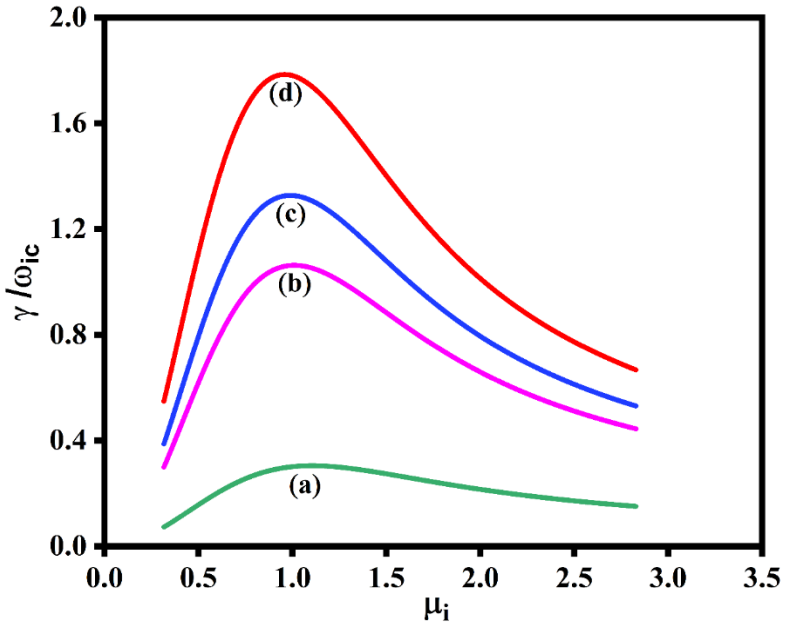

Figure 4.1: Variation in normalized growth rate γ/ω_{ic} with the finite gyro-radius parameter μ_i of EIC wave for varying δ i.e., (a) $\delta = 0.4$, (b) $\delta = 1.4$, (c) $\delta = 3$, and (d) $\delta = 4$.

The normalized real frequency variation corresponding to the gyro-radius parameter has been plotted in Figures 4.2 (a) and (b) for different sets of relative density ratios i.e., δ (a) $\delta = 0.4$, (b) $\delta = 1.4$, (c) $\delta = 3$, and (d) $\delta = 4$, in the presence and absence of electric field, respectively. From the plots, it can be noted that the frequency value rises with increasing gyro-radius parameters until they reach their peak value, after which there is a decline in magnitude for all values of the relative density ratio. In addition, with the rise in the relative density ratio, the real frequency augments. We can conclude that after the inclusion of the electric field, the real frequency follows a similar trend as in the case of the absence of the electric field despite the rise in their values. This is because of the reason that the Doppler effect is caused by $\vec{E} \times \vec{B}$ drift among particles, which is induced by the occurrence of an electric field. As a result, the waves' frequency grows when a dc transverse electric field is applied. The inset of Figure 4.2 (b) shows the result of $\upsilon_e = \upsilon_i \to 0$. We can say that the frequency, in collisionless case, is more as compared to collisional plasma because the charged particles can react more swiftly to an external perturbation than in collisional plasma. This result matches with the experimental paper of Chow and Rosenberg [39].

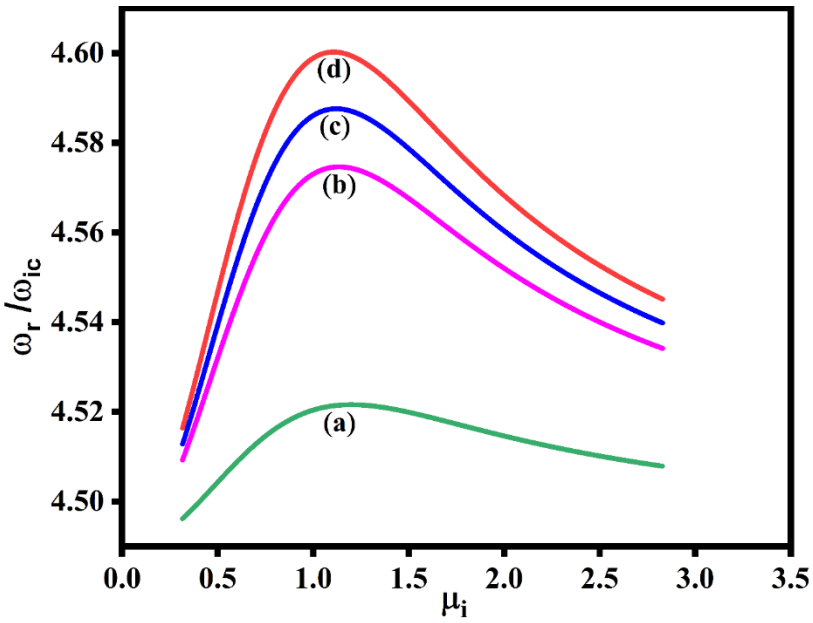

Figure 4.2 (a): Variation in normalized real frequency ω_r/ω_{ic} with the finite gyro-radius parameter μ_i of EIC wave with the electric field for varying δ i.e., (a) $\delta = 0.4$, (b) $\delta = 1.4$, (c) $\delta = 3$, and (d) $\delta = 4$.

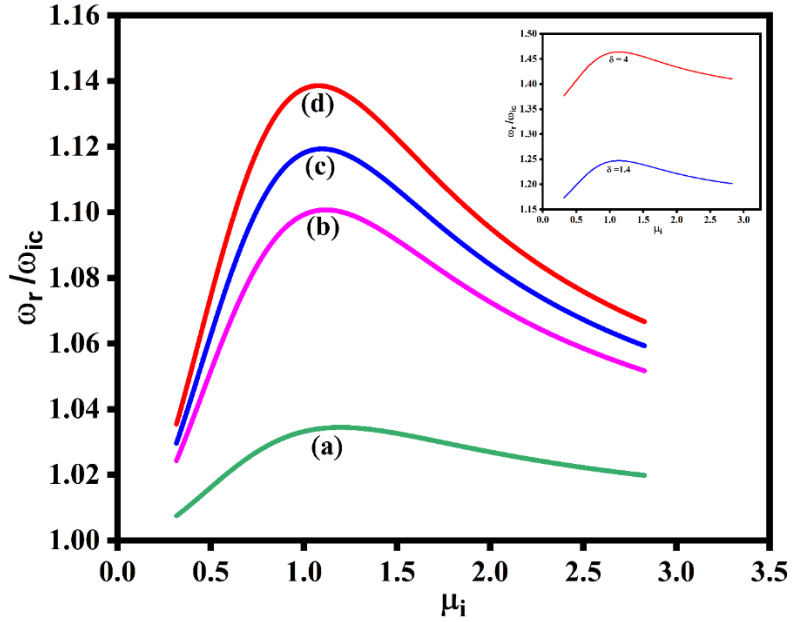

Figure 4.2 (b): Variation in normalized real frequency ω_r/ω_{ic} with the finite gyro-radius parameter μ_i without the electric field for varying δ in the presence of collisions and inset of Figure 4.2 (b) portrays the collisionless case.

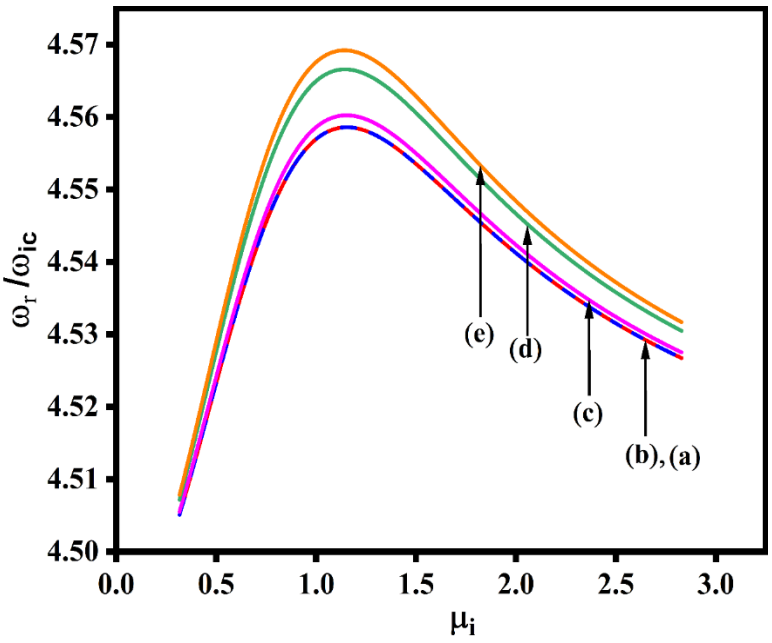

Figure 4.3 (a): The normalized real frequency variation for the case $\delta = 1$ corresponding to the finite gyro-radius parameter for different electron collisional frequencies υ_e i.e., (a) $\upsilon_e = 0$, (b) $\upsilon_e = 1\times10^5$ rad/sec , (c) $\upsilon_e = 2\times10^5$ rad/sec , (d) $\upsilon_e = 4\times10^5$ rad/sec , (e) $\upsilon_e = 7\times10^5$ rad/sec.

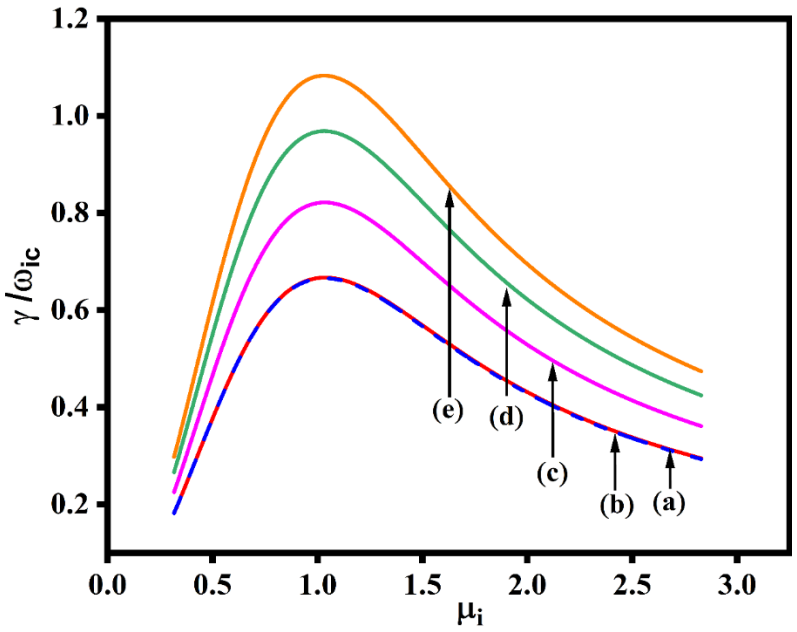

Figure 4.3 (b): The normalized growth rate γ/ω_{ic} variation for the case $\delta = 1$ corresponding to the finite gyro-radius parameter μ_i for different electron collisional frequencies υ_e i.e., $\upsilon_e = 0$, (b) $\upsilon_e = 1\times10^5$ rad/sec , (c) $\upsilon_e = 2\times10^5$ rad/sec , (d) $\upsilon_e = 4\times10^5$ rad/sec , (e) $\upsilon_e = 7\times10^5$ rad/sec.

For the case $\delta = 1$ (no dust particles), Figures 4.3 (a) and 4.3 (b) depict the impact of variation in electron collision frequency on the real frequency and growth rate, respectively. From plots, it can be noted that the frequency and growth rate values rise with increasing gyro-radius parameter until they reach their peak value, after which there is a decline in magnitude. In both the graphs, the dash curve (a) corresponds to the collisionless case ($\upsilon_e = \upsilon_i \to 0$) and other solid curves corresponds to the collisional case for $\upsilon_i = 1\times10^3$ rad/sec and varying υ_e i.e. (b) $\upsilon_e = 1\times10^5$ rad/sec, (c) $\upsilon_e = 2\times10^5$ rad/sec, (d) $\upsilon_e = 4\times10^5$ rad/sec, (e) $\upsilon_e = 7\times10^5$ rad/sec. It can be seen that the real frequency and growth rate (for curve (b)) for the chosen fixed plasma parameters is nearly equal to the collisionless case i.e., curve (a). This is because ion collisions have a stabilising effect whereas electron collisions have a destabilising effect [40]. For the limit, $\frac{\upsilon_e}{k_z v_{et}} << 1$, the ion collisions dominate electron collisions destabilising effects. As the υ_e increases to the higher value, the electron collisions start to dominate and an enhancement of the real frequency and rate of growth is observed. We can infer that the wave's frequency has slightly increased while the growth rate has increased considerably when electron collision frequency augments. Our result is analogous to the Bharuthram et al. [41] findings.

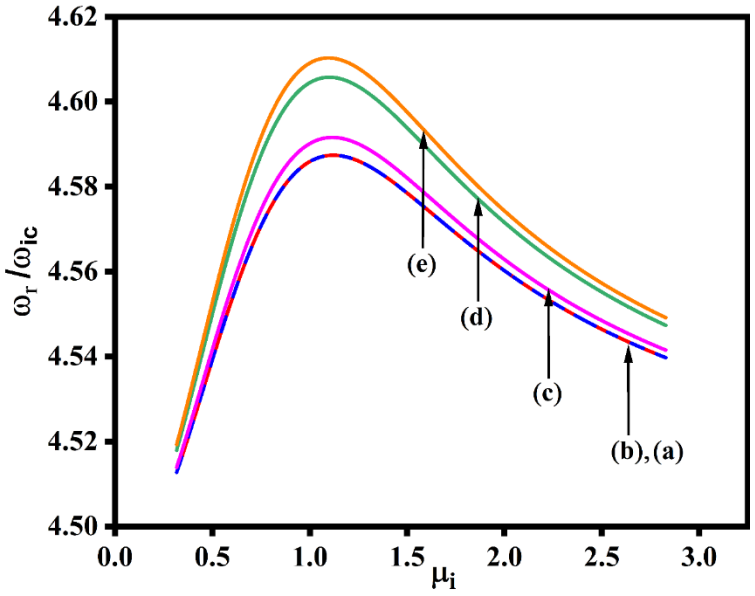

Figure 4.4 (a): The normalized real frequency variation for the case $\delta = 3$ corresponding to the finite gyro-radius parameter μ_i for different electron collisional frequencies i.e., (a) $\upsilon_e = 0$, (b) $\upsilon_e = 1\times10^5$ rad/sec, (c) $\upsilon_e = 2\times10^5$ rad/sec, (d) $\upsilon_e = 4\times10^5$ rad/sec, (e) $\upsilon_e = 7\times10^5$ rad/sec.

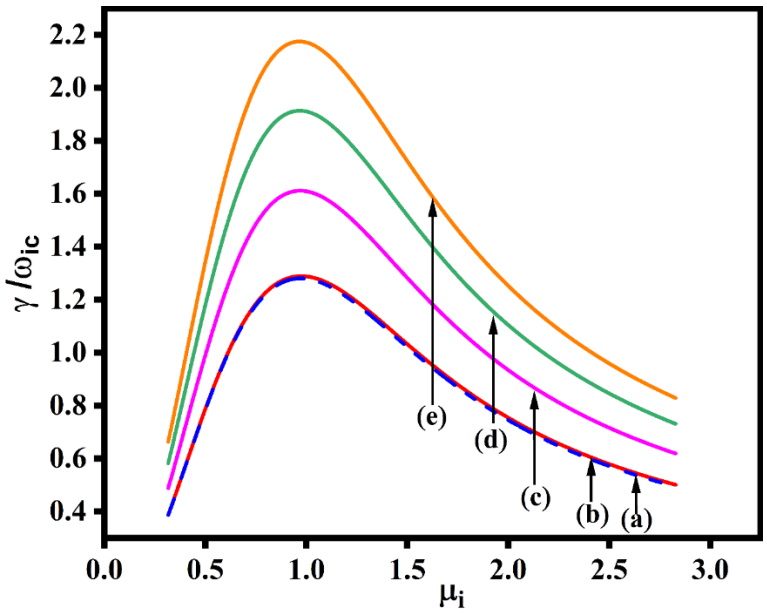

Figure 4.4 (b): The normalized growth rate variation for the case $\delta = 3$ corresponding to the finite gyro-radius parameter μ_i for different electron collisional frequencies υ_e e.g., (a) $\upsilon_e = 0$, (b) $\upsilon_e = 1\times10^5$ rad/sec , (c) $\upsilon_e = 2\times10^5$ rad/sec , (d) $\upsilon_e = 4\times10^5$ rad/sec , (e) $\upsilon_e = 7\times10^5$ rad/sec.

The existence of negatively charged dust particles with $\delta = 3$ is the next aspect we take into account for $n_d^0 = 5\times10^4\,\text{cm}^{-3}$ in Figures 4.4 (a) and 4.4 (b). Figures 4.4 (a) and 4.4 (b) depict the impact of variation of electron collision frequencies υ_e i.e. (b) $\upsilon_e = 1\times10^5$ rad/sec , (c) $\upsilon_e = 2\times10^5$ rad/sec , (d) $\upsilon_e = 4\times10^5$ rad/sec , (e) $\upsilon_e = 7\times10^5$ rad/sec on real frequency and growth rate with gyro-radius parameter of the wave for $\upsilon_i = 1\times10^3$ rad/sec . From the plots, it can be noted that it follows the same trend as in the above-mentioned graphs i.e., absence of dust particles with gyro-radius parameter and electron collision frequency. Moreover, we can conclude that after the addition of the dust grains in these graphs, the growth rate and frequency for both the cases i.e., collisionless (Figure 4.4 curve (a)) and collisional (Figure 4.4 curve (b), (c), (d), and (e)) gets enhanced as compared to the previous graphs i.e., Figures 4.3 (a) and (b). This is because the addition of the dust grains modifies the properties of the EIC wave and the collective effect of charged particles (electrons, ions and dust particles) becomes more intricate and their interaction leads to the augmentation in frequency and growth rate of the wave. Our findings matches with Chow and Rosenberg's [46] for a collisionless dusty plasma. Moreover, our results are also analogous to the Bharuthram et al. [41].

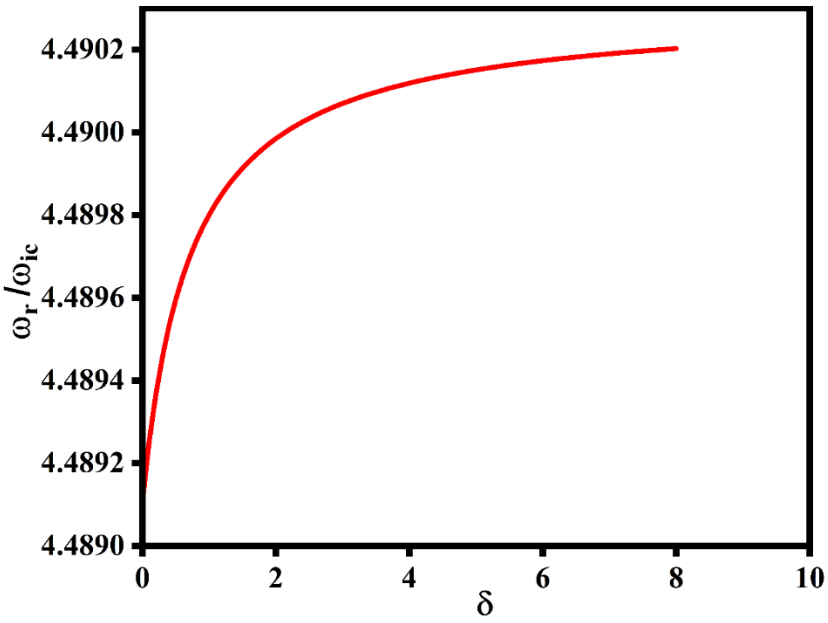

Figure 4.5 (a): The normalized real frequency ω_r/ω_{ic} versus relative density ratio $\delta\left(=n_i^0/n_e^0\right)$.

Figure 4.5 (a) illustrates the impact of the relative density ratio on the normalized real frequency of the wave. We observed that the normalized real frequency is in a direct relationship with respect to the $\delta\left(=n_i^0/n_e^0\right)$, and it can be verified from our Eq. (4.18). Our outcome aligns with Chow and Rosenberg's theoretical conclusion [39] in the absence of an electric field and Anshu et al. results in the absence of collisions [21].

Figure 4.5 (b) illustrates the impact of normalized growth rate for varying υ_e i.e., (a) $\upsilon_e = 4\times10^5$ rad/sec, (b) $\upsilon_e = 6\times10^5$ rad/sec, (c) $\upsilon_e = 8\times10^5$ rad/sec on the relative density ratio of the wave. As the relative density ratio augment in plasma, the growth rate of instability increases. It might be because as δ increases, the plasma density of electrons decreases relative to the plasma density of ions. For increasing the values of δ, an ion's effective mass $\mathrm{m_{ieff}}\left(=\frac{\mathrm{m_i}}{\delta}\right)$ is smaller than m_i, and because of its higher mobility, the growth rate of the instability gets enhanced. Figure 4.5 (b) demonstrates unequivocally that, in accordance with the growth rate expression i.e., Eq. (4.19), the normalised growth rate increases linearly with an increase in υ_e. It is well known that electron collisions can cause the destabilization of EICWs as shown by numerous studies [38, 40, 48]. Our results matches with the experimental paper of Sharma et al. [47].

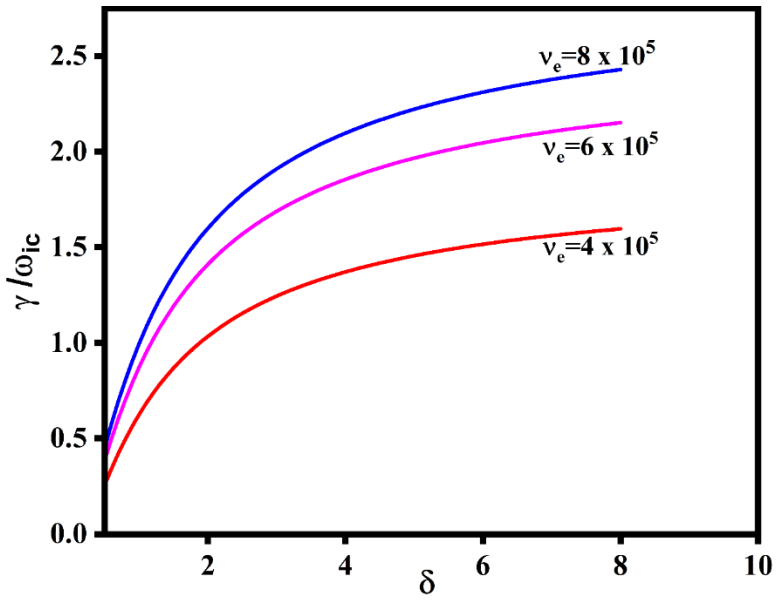

Figure 4.5 (b): Variation in the normalized growth rate γ/ω_{ic} with relative density ratio $\delta\left(=n_i^0/n_e^0\right)$ for varying electron collisional frequencies υ_e i.e., (a) $\upsilon_e = 4\times10^5$ rad/sec, (b) $\upsilon_e = 6\times10^5$ rad/sec and (c) $\upsilon_e = 8\times10^5$ rad/sec.

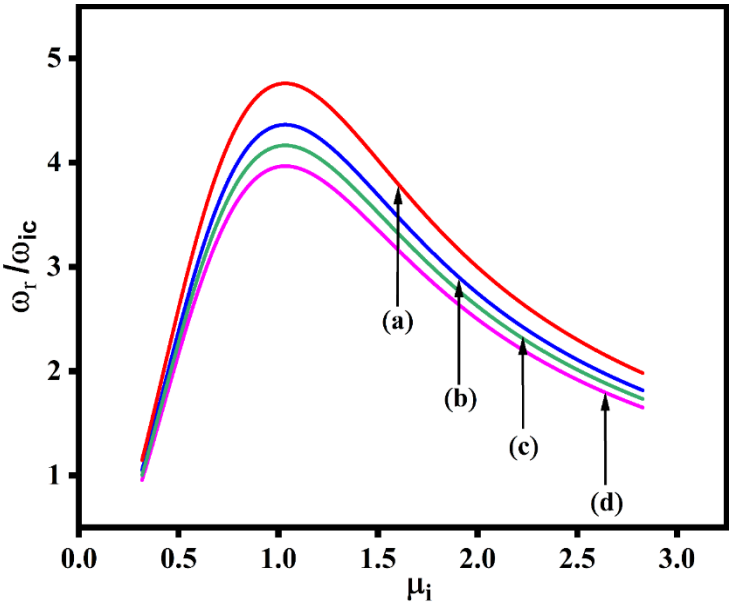

Figure 4.6 (a): The normalized real frequency ω_r/ω_{ic} variation for case $\delta = 1$ corresponding to the finite gyro-radius parameter μ_i for different ion collisional frequencies υ_i i.e. (a) $\upsilon_i = 2\times10^3$ rad/sec, (b) $\upsilon_i = 4\times10^3$ rad/sec, (c) $\upsilon_i = 6\times10^3$ rad/sec, (d) $\upsilon_i = 8\times10^3$ rad/sec.

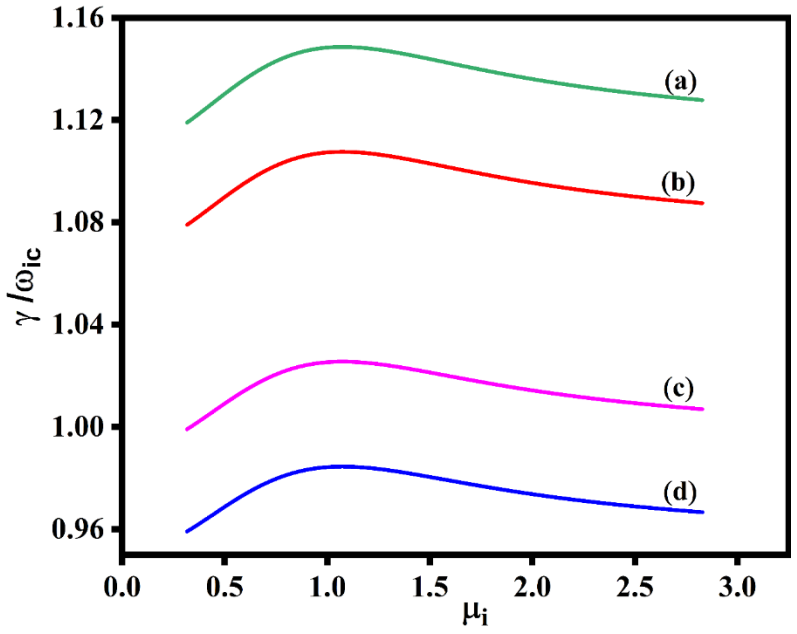

Figure 4.6 (b): The normalized growth rate γ/ω_{ic} variation for the case $\delta=1$ corresponding to the finite gyro-radius parameter μ_i for different ion collisional frequencies υ_i i.e. (a) $\upsilon_i=2\times10^3$ rad/sec, (b) $\upsilon_i=4\times10^3$ rad/sec, (c) $\upsilon_i=6\times10^3$ rad/sec, (d) $\upsilon_i=8\times10^3$ rad/sec.

For the case $\delta=1$ (no dust particles), Figures 4.6 (a) and 4.6 (b) depict the impact of variation in ion collision frequency on the real frequency and growth rate, respectively. From plots, it can be noted that the frequency and growth rate values rise with increasing gyro-radius parameters until they reach their peak value, after which there is a decline in magnitude. In both the graphs, the curves correspond to the $\upsilon_e=4\times10^5$ rad/sec for varying υ_i i.e. (a) $\upsilon_i=2\times10^3$ rad/sec, (b) $\upsilon_i=4\times10^3$ rad/sec, (c) $\upsilon_i=6\times10^3$ rad/sec, (d) $\upsilon_i=8\times10^3$ rad/sec. It can be seen that the real frequency and growth rate reduce for increasing values of υ_i, the ion collision frequency. Further, for fixed υ_e, it is found that a rise in ion collision frequency results in the expected stabilising effect. Our results are analogous to the findings of Bharuthram et al. [41].

The relationship of normalized frequency and the growth rate are depicted in Figures 4.7 (a) and (b), respectively with the magnetic fields. The graphs demonstrate that the frequency and growth rate of the EIC wave correlate linearly to the magnetic field. As the magnetic field grows, so do the waves' frequency and growth rate. It can be concluded that with the addition of collisions, the frequency and growth rate decrease as compared to collisionless case [21]. The outcomes of Koepke and Amatucci [7] as well as Motley and D' Angelo [33] are

comparable to this outcome without collisions. The kinetic theory yields better results than the fluid theory, according to the experimental evidence of Koepke and Amatucci [7].

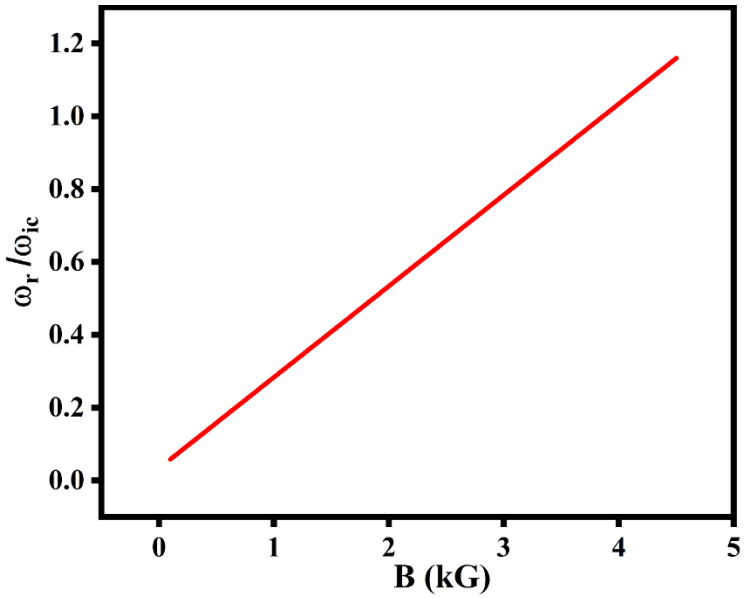

Figure 4.7 (a): The normalized real frequency ω_r/ω_{ic} versus magnetic field $B(\text{in kG})$ of EIC wave.

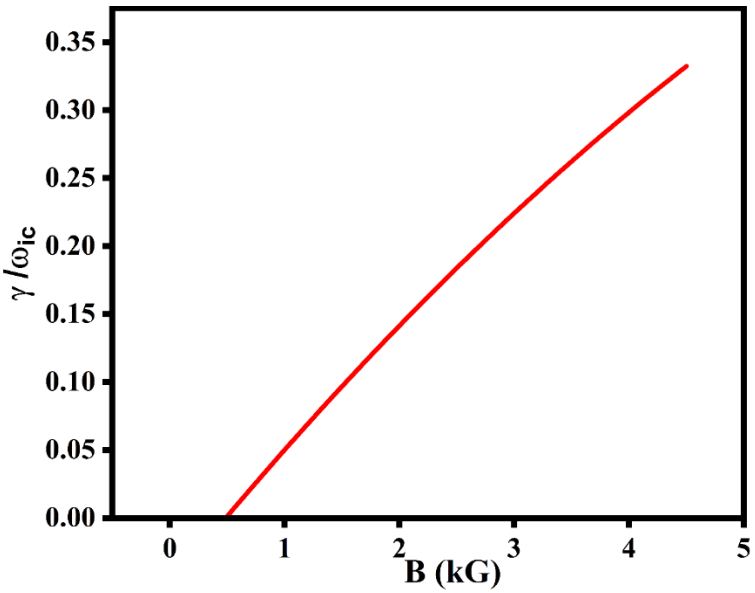

Figure 4.7 (b): The normalized growth rate γ/ω_{ic} with respect to the magnetic field $B(\text{in kG})$ of the EIC wave.

In Figure 4.8, we have displayed a normalized critical drift velocity u_{ed}/v_{et} curve with the relative density of the negatively charged dust grains. According to the graph and Eq. (4.21), the critical electron drift velocity u_{ed}/v_{et} reduces as the relative density ratio rises. Thus, as the

amount of negatively charged dust particles rises, it stabilizes the EIC wave. This outcome aligns with Chow and Rosenberg [39].

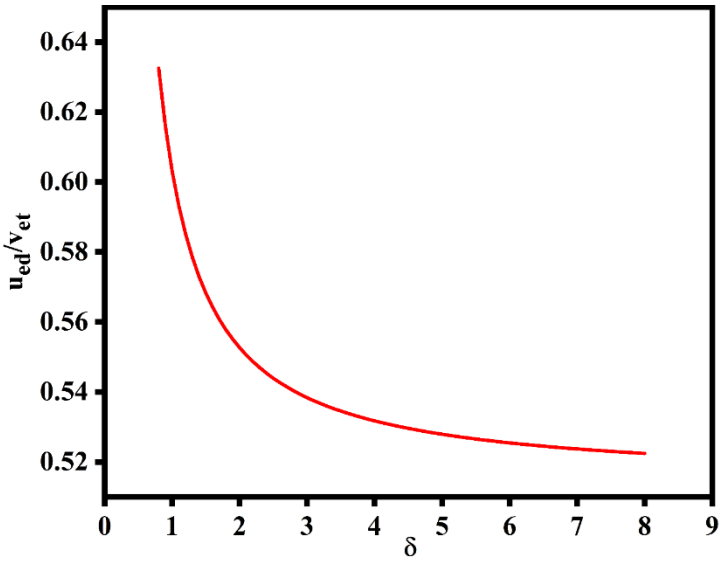

Figure 4.8: The normalized critical electron drift velocity u_{ed}/v_{et} in relation to the relative density of negatively charged dust particles $\delta\left(=n_i^0/n_e^0\right)$.

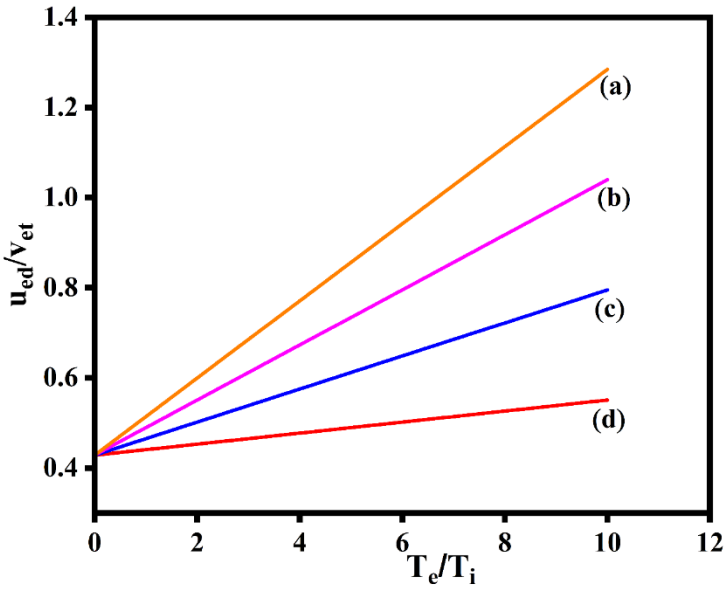

Figure 4.9: The normalized critical electron drift velocity for different electron collision frequencies i.e., (a) $\upsilon_e = 2\times10^5$ rad/sec, (b) $\upsilon_e = 4\times10^5$ rad/sec, (c) $\upsilon_e = 6\times10^5$ rad/sec, and (d) $\upsilon_e = 8\times10^5$ rad/sec as a function of temperature ratio (T_e/T_i).

As shown in Figure 4.9, we have presented the normalized critical electron drift velocity graph for fixed $\upsilon_i = 1\times10^3$ rad/sec for varying electron collision frequency υ_e i.e., (a)

$\upsilon_e = 2\times10^5$ rad/sec , (b) $\upsilon_e = 4\times10^5$ rad/sec , (c) $\upsilon_e = 6\times10^5$ rad/sec , and (d) $\upsilon_e = 8\times10^5$ rad/sec in relation to the electron to ion temperature ratio. As we increase the T_e / T_i, critical drift rises, as seen in the graph and verified by Eq. (4.21). Furthermore, with the augment in electron collision frequency, the critical drift of the EIC wave reduces [40]. This is due to the fact that numerous electron collisions might result in more effective energy dissipation and thermalization, changing the behaviour of the system as a whole and possibly stabilizing the system at lower critical electron drift velocities. We can conclude that higher temperature further enhances the critical drift of the wave. Additionally, our result aligns with the Levine and Kuckes [49] experimental observation in the absence of collisions.

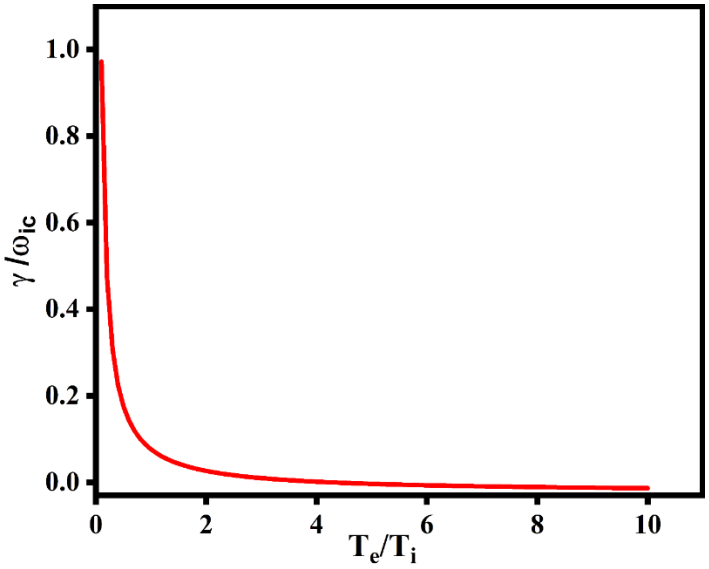

Figure 4.10: The normalized growth rate γ/ω_{ic} as a function of temperature ratio (T_e / T_i).

In Figure 4.10, the electron to ion temperature ratio in relation to the normalized growth rate graph is discussed for the EICWs. It shows that the growth rate gradually lowers as the electron to ion temperature ratio rise and this conclusion is supported by Eq. (4.19).

We have plotted the relationship between normalized real frequency and the temperature ratio for varying υ_i i.e. (a) $\upsilon_i = 2\times10^3$ rad/sec , (b) $\upsilon_i = 4\times10^3$ rad/sec , (c) $\upsilon_i = 6\times10^3$ rad/sec , (d) $\upsilon_i = 8\times10^3$ rad/sec in Figure 4.11. The normalized frequency of the wave augments with the rise in T_e / T_i. Using Eq. (4.18), it is clear that when T_e / T_i rises, Δ value rises which in turn increases the frequency. This outcome is consistent with the findings of Kindel and Kennel in the absence of collisions [19]. Moreover, higher ion collisional frequencies typically result in a reduction in EIC wave frequency.

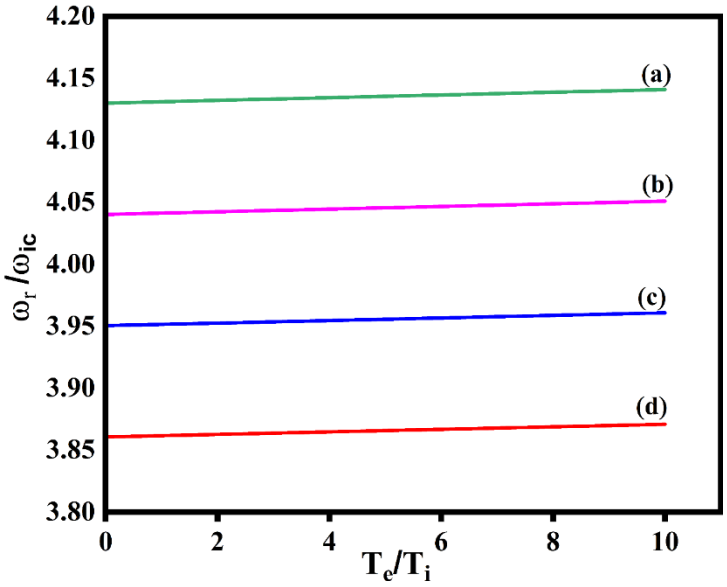

Figure 4.11: The normalized real frequency with varying ion collision frequency υ_i i.e., (a) $\upsilon_i = 2\times10^3$ rad/sec, (b) $\upsilon_i = 4\times10^3$ rad/sec, (c) $\upsilon_i = 6\times10^3$ rad/sec, (d) $\upsilon_i = 8\times10^3$ rad/sec as a function of temperature ratio (T_e / T_i).

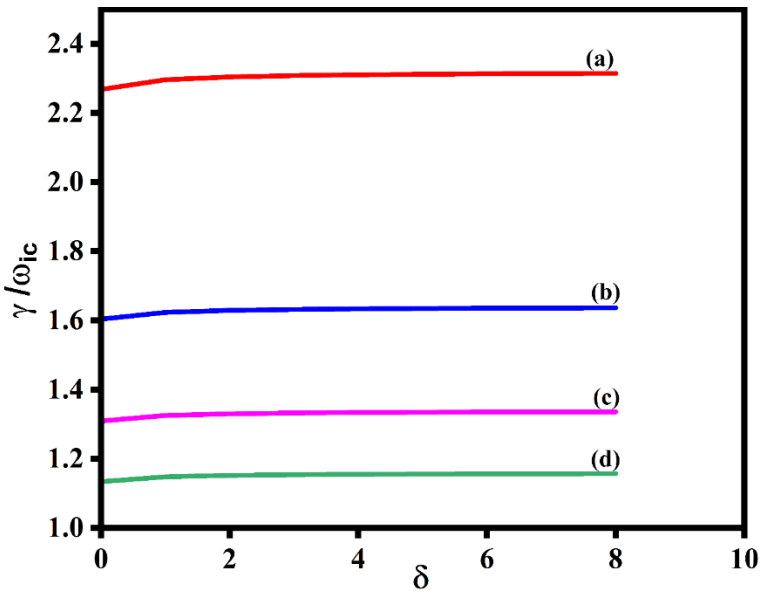

Figure 4.12: The normalized growth rate γ/ω_{ic} variation with $\delta\left(=n_i^0/n_e^0\right)$ for varying dust grain number density i.e., (a) $n_d^0 = 2\times10^4\,\text{cm}^{-3}$, (b) $n_d^0 = 4\times10^4\,\text{cm}^{-3}$, (c) $n_d^0 = 6\times10^4\,\text{cm}^{-3}$ and (d) $n_d^0 = 8\times10^4\,\text{cm}^{-3}$ of the wave.

The normalized growth rate graph versus δ for varying the values of dust number density i.e., (a) $n_d^0 = 2\times10^4\,\text{cm}^{-3}$, (b) $n_d^0 = 4\times10^4\,\text{cm}^{-3}$, (c) $n_d^0 = 6\times10^4\,\text{cm}^{-3}$, and (d) $n_d^0 = 8\times10^4\,\text{cm}^{-3}$ is

illustrated in Figure 4.12. It is found that as the relative density ratio rises, the growth rate of the wave grows. According to the graphical analysis, the normalized growth rate and dust number density have an inverse relationship, which is consistent with Eq. (4.20). This is because the rise in dust particles reduces the number of readily available electrons per dust grain. In turn, this leads to an increased need for electrons among the dust particles as a whole. This increased electron demand from the numerous dust particles leads to a fall in average dust grain charge Q_d^0, which, in turn, lowers the growth rate of the wave.

4.4 CONCLUSION

The EIC wave excitation in the collisional magnetized dusty plasma under the outcome of an electric field has been presented via kinetic theory. The study of collisional effects has been examined for various plasma parameters like gyro-radius, growth rate and frequency etc. The wave's dispersive relationship has been deduced. The real frequency and growth rate augment with an augment in the relative density ratio. The impact of the gyro-radius parameter on the frequency and the growth rate of wave for varying electron and ion collision frequencies was also examined. It was discovered that the frequency and the rate of growth first rise as the gyroradius parameter augments before starting to fall as the gyroradius parameter further augments. Furthermore, it has been found that the effect of an electron collision destabilizes the mode whereas the effect of an ion collision stabilizes the mode and the growth rate. The growth rate and frequency of the waves rise along with the magnetic field strength, emphasizing the stronger connection between the plasma particles and the magnetic fields. It was also discovered that as the relative density ratio rises, the critical drift reduces, which is essential for the mode's excitation. According to the study, the temperature analysis was also examined on the EIC wave and it was found that as the electron to ion temperature ratio rises, both the critical electron drift velocity and frequency rise. On the other hand, as the temperature ratio rises, the wave's growth rate reduces. It was also examined that with the increasing values of dust density, the growth rate of wave decreases. The acquired results were compared to the already existing observations [7, 19, 21, 41, 46] and are in good agreement.

The present work can be applied in various fields, from astrophysics [50] and space physics [51, 52] to laboratory plasma research [34]. These studies improve our knowledge of plasma phenomena and have the potential to have an impact on a variety of areas, including fusion energy research, tokamak and plasma heating [53, 54].

REFERENCES

[1] A. Barkan, N. D'Angelo, R.L. Merlino, *Planetary and Space Science* **44**, 239 (1996).

[2] P.V. Bliokh, V.V. Yaroshenko, *Soviet Astronomy* **29**, 330 (1985).

[3] N. D'Angelo, *Planetary and Space Science* **38**, 1143 (1990).

[4] M.E. Koepke, *Physics of Plasmas* **9**, 2420 (2002).

[5] P.K. Shukla, *Physics of Plasmas* **8**, 1791 (2001).

[6] P.K. Shukla, A.A. Mamun, Introduction to Dusty Plasma Physics, *CRC Press* (2015).

[7] M.E. Koepke, W.E. Amatucci, *IEEE transactions on Plasma Science* **20**, 631 (1992).

[8] S.C. Sharma, M. Sugawa, V.K. Jain, *Physics of Plasmas* **7**, 457 (2000).

[9] J. Sharma, S.C. Sharma, V.K. Jain, A. Gahlot, *Physics of Plasmas* **20**, 033706 (2013).

[10] J. Sharma, S.C. Sharma, *Physics of Plasmas* **17**, 123701 (2010).

[11] M.E. Koepke, J.J. Carroll Iii, M.W. Zintl, *Physics of Plasmas* **5**, 1671 (1998).

[12] V. Prakash, S.C. Sharma, V. Vijayshri, R. Gupta, *Progress in Electromagnetics Research M* **36**, 161 (2014).

[13] M.E. Koepke, J.J. Carroll Iii, M.W. Zintl, *Journal of Geophysical Research: Space Physics* **104**, 14397 (1999).

[14] A.A. Chernyshov, A. Spicher, A.A. Ilyasov, W.J. Miloch, L.B.N. Clausen, Y. Saito, Y. Jin, J.I. Moen, *Physics of Plasmas* **25**, 042902 (2018).

[15] J. Jyoti, S.C. Sharma, R.P. Sharma, *Physics of Plasmas* **30**, 022904 (2023).

[16] R. Gueroult, J.-M. Rax, N.J. Fisch, *Plasma Physics and Controlled Fusion* **65**, 034006 (2023).

[17] N. Villarroel-Sepúlveda, R.A. López, P.S. Moya, *arXiv preprint arXiv:2306.01880* (2023).

[18] G. Ganguli, Y.C. Lee, P.K. Chaturvedi, P.J. Palmadesso, S.L. Ossakow, D.C. Naval Research Lab Washington, *Naval Research Lab, Washington DC* (1988).

[19] J.M. Kindel, C.F. Kennel, *Journal of Geophysical Research* **76**, 3055 (1971).

[20] G. Ganguli, Y.C. Lee, P. Palmadesso, *The Physics of Fluids* **28**, 761 (1985).

[21] Anshu, J. Sharma, S.C. Sharma, *Contributions to Plasma Physics* **62**, e202200073 (2022).

[22] G. Ganguli, P.J. Palmadesso, *Geophysical Research Letters* **15**, 103 (1988).

[23] B. Song, D. Suszcynsky, N. D'Angelo, R.L. Merlino, *Physics of Fluids B: Plasma Physics* **1**, 2316 (1989).

[24] C.A. Cattell, F.S. Mozer, I. Roth, R.R. Anderson, R.C. Elphic, W. Lennartsson, E. Ungstrup, *Journal of Geophysical Research: Space Physics* **96**, 11421 (1991).

[25] H. Sugai, H. Kojima, T. Okuda, *Physics Letters A* **92**, 392 (1982).

[26] T.F.R. Group, *Physical Review Letters* **41**, 113 (1978).

[27] R.E. Waltz, R.R. Dominguez, *The Physics of Fluids* **24**, 1575 (1981).

[28] R.J. Dumont, D. Zarzoso, *Nuclear Fusion* **53**, 013002 (2012).

[29] Kai-yang Yi, Zi-an Wei, J.X. Ma, Qi Liu, Zheng-yuan Li, *Physics of Plasmas* **27**, 082103 (2020).

[30] C. Cattell, R. Bergmann, K. Sigsbee, C. Carlson, C. Chaston, R. Ergun, J. McFadden, F.S. Mozer, M. Temerin, R. Strangeway, *Geophysical Research Letters* **25**, 2053 (1998).

[31] A. Barkan, N. D'Angelo, R.L. Merlino, *Planetary and Space Science* **43**, 905 (1995).

[32] D.L. Correll, N. Rynn, H. Böhmer, *The Physics of Fluids* **18**, 1800 (1975).

[33] R.W. Motley, N. D'Angelo, *The Physics of Fluids* **6**, 296 (1963).

[34] D.M. Suszcynsky, S.L. Cartier, R.L. Merlino, N. D'Angelo, *Journal of Geophysical Research: Space Physics* **91**, 13729 (1986).

[35] N. D'Angelo, R.W. Motley, *The Physics of Fluids* **5**, (1962).

[36] W.E. Drummond, M.N. Rosenbluth, *The Physics of Fluids* **5**, 1507 (1962).

[37] J.J. Rasmussen, R.W. Schrittwieser, *IEEE Transactions on Plasma Science* **19**, 457 (1991).

[38] P.K. Chaturvedi, P.K. Kaw, *Plasma Physics* **17**, 447 (1975).

[39] V.W. Chow, M. Rosenberg, *Planetary and Space Science* **44**, 465 (1996).

[40] P. Satyanarayana, P.K. Chaturvedi, M.J. Keskinen, J.D. Huba, S.L. Ossakow, *Journal of Geophysical Research: Space Physics* **90**, 12209 (1985).

[41] R. Bharuthram, P. Singh, M. Rosenberg, V.W. Chow, *Physica Scripta* **1998**, 223 (1998).

[42] S.L. Ossakow, K. Papadopoulos, J. Orens, T. Coffey, *Journal of Geophysical Research* **80**, 141 (1975).

[43] B.D. Fried, S.D. Conte, The plasma dispersion function: the Hilbert transform of the Gaussian, *Academic Press* (2015).

[44] A. Bers, M.N. Rosenbluth, R.Z. Sagdeev, *MN Rosenbluth and RZ Sagdeev eds* **1**, (1983).

[45] N.A. Krall, A.W. Trivelpiece, R.A. Gross, *American Journal of Physics* **41**, 1380 (1973).

[46] V.W. Chow, M. Rosenberg, *Planetary and Space Science* **43**, 613 (1995).

[47] S.C. Sharma, K. Sharma, A. Gahlot, *Physics of Plasmas* **20**,053704 (2013).

[48] B. Milić, *The Physics of Fluids* **15**, 1630 (1972).

[49] A.M. Levine, A.F. Kuckes, *The Physics of Fluids* **9**, 2263 (1966).

[50] P.M. Kintner, M.C. Kelley, F.S. Mozer, *Geophysical Research Letters* **5**, 139 (1978).

[51] J. Providakes, C.E. Seyler, *Journal of Geophysical Research: Space Physics* **95**, 3855 (1990).

[52] R.S. Pandey, M. Kumar, *East European Journal of Physics* **1**, 32 (2022).

[53] S. Sumida, K. Shinohara, M. Ichimura, T. Bando, A. Bierwage, T. Kobayashi, H. Yamazaki, S. Moriyama, S. Ide, *Plasma Physics and Controlled Fusion* **65**, 075002 (2023).
[54] J. Hillairet, *Reviews of Modern Plasma Physics* **7**, 16 (2023).

5

Kinetic Theory of Resonant Ion-Cyclotron Instability Induced by Ion Beams in Collisional Magnetized Dusty Plasmas Under the Influence of DC Electric Field

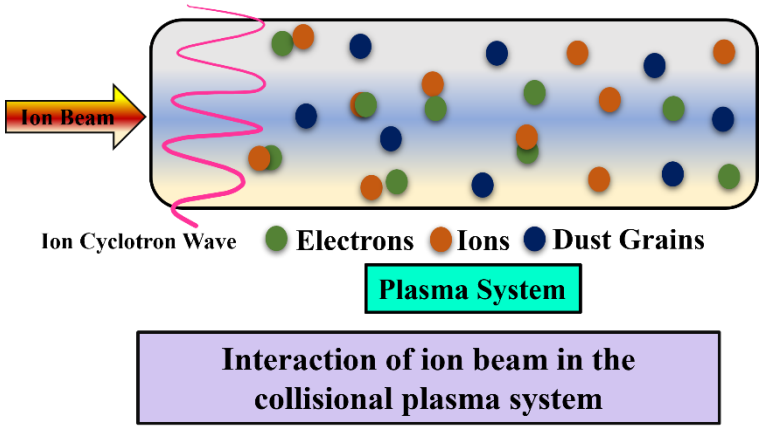

After studying the effect of collisions on Electrostatic Ion Cyclotron Waves (EICWs) in a magnetized dusty plasma, in this chapter, we have developed an analytical model driven by an ion beam in the collisional magnetized dusty plasma in the presence of a dc electric field using the kinetic treatment. An ion beam parallel to the magnetic field is seen to be the source of ion cyclotron instability with dust particles. The dispersion relation of instability is significantly changed by the interaction of ion beams. The effect of ion beam with various plasma parameters i.e., gyro-radius, relative density ratio etc. on an EICWs have been examined. The temperature analysis and the effect of dust grains was also examined on the EICWs.

PUBLICATION

Anshu, Jyotsna Sharma, and Suresh C. Sharma, "Kinetic Theory of Resonant Ion-Cyclotron Instability Induced by Ion Beams in Collisional Magnetized Dusty Plasmas Under the Influence of DC Electric Field". (Communicated)

5.1 INTRODUCTION

The interconnection between a magnetized plasma and an ion beam gives rise to numerous instabilities [1-7]. These phenomena provide a valuable understanding of the basic mechanisms governing plasma confinement, heating, and stability. EICWs with distinctive properties, particularly a significant parallel phase velocity, appear when an ion beam is introduced in parallel alignment with the magnetic field [8]. In such circumstances, these waves are frequently subject to destabilization. EICWs have been seen in a wide range of applications including space plasmas and laboratory studies [9-18]. The ions and electrons are heated by electrostatic waves through cyclotron damping and Landau damping, respectively.

In plasma environments, wave phenomena have been thoroughly investigated through theoretical analysis and experimental observations, including both scenarios with [14, 19-24] and without [17, 25-30] particulate entities known as dust grains. The emerging collective characteristics displayed by the plasma medium are significantly influenced by the addition of dust grains [31, 32]. The initial experimental findings of EIC oscillations in lab plasmas were presented by D'Angelo and Motley [10]. In a Q-machine, the study on EIC wave was reported by Barkan et al. [14] and it was observed that the growth rate of the wave was increased in the presence of a substantial amount of negatively charged dust particles. Chow and Rosenberg [33] concluded in their research using the kinetic theory in a collisionless plasma that in a plasma with plenty of negatively charged dust particles, the wave mode is destabilised. In a plasma medium including negatively charged dust particles, Merlino et al. [19] have presented both experimental and theoretical evidence for low frequency electrostatic waves. The characteristics of the current-driven EIC instability are altered by the existence of dust particles despite the fact that the dust particles themselves are not actively participating in the wave dynamics. Yamada et al. [34] have investigated theoretically and experimentally the occurrence of instabilities produced by an ion beam in parallel alignment with a magnetic field. These instabilities include a resonant ion cyclotron instability as well as a non-resonant ion cyclotron drift wave induced by the beam density gradient. Bharuthram et al. [35] examined the collisional effects on EICWs in plasma via kinetic theory in the absence of a transverse electric field and concluded that the wave behaviour is altered by the presence of collisions. A study was done by Sugawa [29] to determine how the interaction of beam ions in a ion beam plasma system affects the EICWs. A theoretical framework for the excitation of EICWs through the interaction with a spiralling ion beam has been developed by Sharma and Sharma [4] and the study was carried out in a cylindrical dusty magnetized plasma system. In a magnetized dusty

plasma environment, Prakash et al. [8, 36, 37] have investigated lower hybrid waves driven by ion and electron beams and resonant ion cyclotron instability driven by an ion beam. Anshu et al. [38] studied the EIC wave in a collisionless plasma via kinetic treatment. They found that with an addition of an electric field, the dispersion relation modifies and it would further affect the growth rate and frequency of the wave.

As far as authors are aware, it is important to highlight that prior studies did not explore the implications of variables like temperature, collisional effects, dust particles, and other parameters on instability in the transverse dc electric field in a collisional dusty magnetized plasma. Therefore, we have expanded earlier research [8, 28] to understand the role of dust, temperature, and other parameters on the EIC wave driven by an ion beam in a collisional magnetized plasma having negatively charged dust particles in the existence of a transverse dc electric field via kinetic theory.

In the present chapter, we establish a kinetic approach to demonstrate the impact on ion cyclotron instability induced by ion beams. Moreover, this current model shows the effect of collision frequency and beam velocity with different plasma parameters to study the behaviour of the waves i.e., frequency and growth rate. This chapter is organized as follows for the succeeding sections: the detailed analysis of electrostatic ion cyclotron wave for solving the expression of growth rate and frequency is delineated in Section 5.2. In Section 5.3, the outcomes of the theoretical modelling of the EIC wave have been compared with the results of the existing observations. The conclusion is outlined in Section 5.4.

5.2 INSTABILITY ANALYSIS

In this chapter, we studied the collisional multispecies magnetized dusty plasma that is enclosed in a uniform and static magnetic field B oriented along the z-direction. The proposed system is induced by an ion beam and consists of three species: electrons, ions and dust grain particles. Table 5.1 includes their notations.

An EIC wave exhibits a characteristic frequency ω and propagation wave vector k oriented in the y-z plane and its alignment is roughly perpendicular to the applied magnetic field. In addition, we provide a proposed system with a transverse dc electric field E in the direction of x. This introduction of an electric field induces $\vec{E}\times\vec{\mathrm{B}}$ drift and has a magnitude $v_E\left(=\frac{cE}{B}\right)$, oriented in the y-direction and c is the speed of light.

Table 5.1: Species and their notations considered in the model.

S. No.	Species	Equilibrium density	Drift Velocity	Velocity	Mass	Charge	Temperature	Collisional Frequency
1.	Electrons	n_e	$u_{ed} \parallel \hat{z}$	u_e	m_e	$-e$	T_e	υ_e
2.	Ions	n_{it}	0	u_t	m_i	e	T_i	υ_i
3.	Dust Particles	n_d	0	u_d	m_d	Q_d	T_d	υ_d
4.	Ion beam	n_{ib}	0	$u_b\ \hat{z}$	m_i	e	T_b	0

In equilibrium, the quasi-neutrality condition says

$$en_{it} + en_{ib} = en_e + Q_d n_d \,. \tag{5.1}$$

Applying the BGK collision model [39, 40], the following is the expression for the kinetic dispersion relation that governs the behaviour of electrostatic modes in a collisional dusty plasma and is expressed as follows

$$\varepsilon(\omega,k) = 1 + \sum_{\alpha} \chi_\alpha = 0 \,, \tag{5.2}$$

where χ_α are the susceptibilities of the electrons, ions, dust grains and ion beam, respectively.

The electron, ion, dust grains and ion beam susceptibilities are given as follows

$$\chi_e = \frac{2\omega_{ep}^2}{k^2 v_{et}^2}\left[1 + \frac{\omega_1 + i\upsilon_e}{k_z v_{et}} \sum_n \Gamma_n^e Z\left(\frac{\omega_1 + i\upsilon_e}{k_z v_{et}}\right)\right]\left[1 + \frac{i\upsilon_e}{k_z v_{et}} \sum_n \Gamma_n^e Z\left(\frac{\omega_1 + i\upsilon_e}{k_z v_{et}}\right)\right]^{-1} . \tag{5.3}$$

$$\chi_i = \frac{2\omega_{ip}^2}{k^2 v_{it}^2}\left[1 + \frac{\omega_2 + i\upsilon_i}{k_z v_{it}} \sum_n \Gamma_n^i Z\left(\frac{\omega_2 - n\omega_{ic} + i\upsilon_i}{k_z v_{it}}\right)\right]\left[1 + \frac{i\upsilon_i}{k_z v_{it}} \sum_n \Gamma_n^i Z\left(\frac{\omega_2 - n\omega_{ic} + i\upsilon_i}{k_z v_{it}}\right)\right]^{-1} . \tag{5.4}$$

$$\chi_d = \frac{2\omega_{dp}^2}{k^2 v_{dt}^2}\left[1 + \frac{\omega + i\upsilon_d}{k v_{dt}} Z\left(\frac{\omega + i\upsilon_d}{k v_{dt}}\right)\right]\left[1 + \frac{i\upsilon_d}{k v_{dt}} Z\left(\frac{\omega + i\upsilon_d}{k v_{dt}}\right)\right]^{-1} . \tag{5.5}$$

$$\chi_b = \frac{2\omega_{ip}^2}{k^2 v_{it}^2}\frac{n_{ib}}{n_{it}}\frac{T_i}{T_b}\left[1 + \frac{\omega - k_z u_b - n\omega_{ic}\left(1 - T_b/T_i\right)}{k_z v_{bt}} \sum_n \Gamma_n^i Z\left(\frac{\omega - k_z u_b - n\omega_{ic}}{k_z v_{bt}}\right)\right]. \tag{5.6}$$

where $\omega_1 = \omega - k_y v_E - k_z u_{ed}$ and $\omega_2 = \omega - k_y v_E + k_z u_t$; k_y and k_z are the wave vector oriented along y and z-direction; $\omega_{ic}\left(=\frac{eB}{m_i c}\right)$ represents the ion cyclotron frequency; $\Gamma_n^{\alpha} = I_n(\mu_\alpha)\exp(-\mu_\alpha)$, where $\mu_\alpha\left(=\frac{k_y^2\rho_\alpha^2}{2}\right), \rho_\alpha\left(=\sqrt{\frac{v_{\alpha t}^2}{\omega_{\alpha c}^2}}\right)$ denotes the gyroradius, I_n represents the modified n[th] order Bessel function; Z depicts the plasma dispersion function [41] and other parameters are tabulated in Table 5.2.

Table 5.2: Notations and their formulas

S. No.	Notations	Terms	Formula
1.	ω_{ep}	Electron plasma frequency	$\sqrt{\frac{4\pi n_e e^2}{m_e}}$
2.	ω_{ip}	Ion plasma frequency	$\sqrt{\frac{4\pi n_{it} e^2}{m_i}}$
3.	ω_{dp}	Dust plasma frequency	$\sqrt{\frac{4\pi n_d Q_d^2}{m_d}}$
4.	v_{et}	Electron thermal velocity	$\sqrt{\frac{2KT_e}{m_e}}$
5.	v_{it}	Ion thermal velocity	$\sqrt{\frac{2KT_i}{m_i}}$
6.	v_{dt}	Dust thermal velocity	$\sqrt{\frac{2KT_d}{m_d}}$
7.	v_{bt}	Beam thermal velocity	$\sqrt{\frac{2KT_b}{m_i}}$

Analytical solutions of Eq. (5.2) are possible in some regimes by introducing some simplifying conditions. We are only concerned with the phase-velocity regime for the EICWs (Drummond and Rosenbluth). [42]

$$\frac{\omega_1 + i\upsilon_e}{k_z v_{et}} << 1. \tag{5.7}$$

$$\frac{\omega_2 - n\omega_{ic} + i\upsilon_i}{k_z v_{it}} >> 1. \tag{5.8}$$

$$\frac{\omega + i\upsilon_d}{k v_{dt}} >> 1. \tag{5.9}$$

$$\frac{\omega - k_z u_b - n\omega_{ic}}{k_z v_{bt}} << 1\ . \tag{5.10}$$

Equation (5.3) can be simplified by assuming $\mu_e << 1$, and utilizing only $n = 0$ term because $\Gamma_0^e = 1$ and $\Gamma_n^e = 0$ when $n \neq 0$. This presumption allows us to conveniently expand the plasma dispersive function $Z(\xi)$ within the framework of kinetic theory [43] as follows:

$$Z(\xi_\alpha) = -2\xi_\alpha + \frac{2}{3}\xi_\alpha^3 + ... + i\sqrt{\pi}\, e^{-\xi_\alpha^2} \quad \text{if } \xi_\alpha << 1. \tag{5.11}$$

$$Z(\xi_\alpha) = -\frac{1}{\xi_\alpha} - \frac{1}{2\xi_\alpha^3} + ... + i\sqrt{\pi}\, e^{-\xi_\alpha^2} \quad \text{if } \xi_\alpha >> 1\ , \tag{5.12}$$

where $\xi_e = \frac{\omega_1 + i\upsilon_e}{k_z v_{et}}$, $\xi_i = \frac{\omega_2 - n\omega_{ic} + i\upsilon_i}{k_z v_{it}}$, $\xi_d = \frac{\omega + i\upsilon_d}{k v_{dt}}$ and $\xi_b = \frac{\omega - k_z u_b - n\omega_{ic}}{k_z v_{bt}}$.

So, Equation (5.3) can be rewritten after using the value of plasma dispersion function i.e., Eq. (5.11)

$$\chi_e = \frac{2\omega_{ep}^2}{k^2 v_{et}^2}\left[1 + i\sqrt{\pi}\,\frac{\omega_1}{k_z v_{et}}\left(1 + \frac{\sqrt{\pi}\upsilon_e}{k_z v_{et}}\right)\right]. \tag{5.13}$$

Here, in the above expression, using limit Eq. (5.7). So, Eq. (5.13) abridges to

$$\chi_e = \frac{2\omega_{ep}^2}{k^2 v_{et}^2}\left[1 + \frac{\sqrt{\pi}\upsilon_e}{k_z v_{et}}\right]. \tag{5.14}$$

For the ions, we can approximate the Eq. (5.4) by retaining only n=0 and n=1 terms in the χ_i summation; including ions-neutral collisions and further for resonant interaction of the wave, assuming $\omega \approx \omega_{ic}$, $\frac{\upsilon_i}{\omega} \ll 1$ and $\frac{\upsilon_i}{\omega - \omega_{ic}} \ll 1$, and utilizing the recursive correlation [44] $\sum_{n \neq 1} \Gamma_n^i \frac{1}{1-n} = \frac{1}{\mu_i}\left[1 - \Gamma_0^i\right]$, the Eq. (5.4) reduces to

$$\chi_i = \frac{2\omega_{ip}^2}{k^2 v_{it}^2}\left[1 - \frac{\Gamma_1^i \omega_2}{(\omega_2 - \omega_{ic})} - \frac{1 - \Gamma_0^i}{\mu_i} + i\sqrt{\pi}\,\frac{\omega_2}{k_z v_{ii}}\Gamma_1^i\, e^{-\xi_i^2} - \frac{i\upsilon_i \Gamma_1^i}{(\omega_2 - \omega_{ic})}\right]. \tag{5.15}$$

Equation (5.5) can be solved by substituting Eqs. (5.9) and (5.12), here we have neglected the dust collision frequency because the mass of dust is very large. Hence, $\omega_{ic} \gg \omega_{dc}$, where

$\omega_{dc}\left(=\frac{Q_d B}{m_d c}\right)$ is the dust cyclotron frequency. So, it is possible to consider the dust particles to be non-magnetized and this Eq. abridges to

$$\chi_d = -\frac{\omega_{dp}^2}{\omega^2}. \tag{5.16}$$

In this context, we can ignore this term $\frac{\omega_{dp}^2}{\omega^2} << 1$. Also, $\frac{\omega_{dp}^2}{\omega^2} << \chi_i$.

Equation (5.6) can be solved by substituting Eqs. (5.10) and (5.11) and retaining only the n=0 term. The expression is as follows

$$\chi_b = \frac{2\omega_{ip}^2}{k^2 v_{it}^2}\frac{n_{ib}}{n_{it}}\frac{T_i}{T_b}\left[1+i\sqrt{\pi}\left(\frac{\omega-k_z u_b}{k_z v_{bt}}\right)\right]. \tag{5.17}$$

Substituting Eqs. (5.14), (5.15), (5.16) and (5.17) in Eq. (5.2), we get

$$\varepsilon(\omega,k) = 1+\frac{2\omega_{ep}^2}{k^2 v_{et}^2}\left[1+\frac{\sqrt{\pi}\upsilon_e}{k_z v_{et}}\right]+\frac{2\omega_{ip}^2}{k^2 v_{it}^2}\left[1-\frac{\Gamma_1^i\omega_2}{(\omega_2-\omega_{ic})}-\frac{1-\Gamma_0^i}{\mu_i}+i\sqrt{\pi}\,\frac{\omega_2}{k_z v_{ii}}\Gamma_1^i\,\mathrm{e}^{-\xi_i^2}-\frac{i\upsilon_i\Gamma_1^i}{(\omega_2-\omega_{ic})}\right]$$
$$+\frac{2\omega_{ip}^2}{k^2 v_{it}^2}\frac{n_{ib}}{n_{it}}\frac{T_i}{T_b}\left[1+i\sqrt{\pi}\left(\frac{\omega-k_z u_b}{k_z v_{bt}}\right)\right]. \tag{5.18}$$

This results in the dispersion relation of resonant EIC instability for collisional dusty plasma.

$$\varepsilon_r(\omega,k)+i\varepsilon_i(\omega,k)=0, \tag{5.19}$$

where real and imaginary parts correspond to

$$\varepsilon_r(\omega,k) = 1+\frac{2\omega_{ep}^2}{k^2 v_{et}^2}\left[1+\frac{\sqrt{\pi}\upsilon_e}{k_z v_{et}}\right]+\frac{2\omega_{ip}^2}{k^2 v_{ti}^2}\left[1-\frac{\Gamma_1^i\omega_2}{(\omega_2-\omega_{ic})}-\frac{1-\Gamma_0^i}{\mu_i}\right]+\frac{2\omega_{ip}^2}{k^2 v_{it}^2}\frac{n_{ib}}{n_{it}}\frac{T_i}{T_b}. \tag{5.20}$$

$$\varepsilon_i(\omega,k) = \sqrt{\pi}\,\frac{2\omega_{ip}^2}{k^2 v_{it}^2}\left[\frac{\omega_2}{k_z v_{ii}}\Gamma_1^i\,\mathrm{e}^{-\xi_i^2}-\frac{\upsilon_i\Gamma_1^i}{(\omega_2-\omega_{ic})}+\frac{n_{ib}}{n_{it}}\frac{T_i}{T_b}\frac{\omega-k_z u_b}{k_z v_{bt}}\right]. \tag{5.21}$$

The wave is either growing or damped, the dispersion relation i.e., Eq. (5.18) is used to determine the solutions for the EIC waves. The real part of the frequency i.e., ω_r is represented by

$$\varepsilon_r(\omega,k)\big|_{\omega=\omega_r} = 0. \tag{5.22}$$

The frequency imaginary part is defined by [45]

$$\omega_i = \left.\frac{-\varepsilon_i(\omega,k)}{\frac{\partial \varepsilon_r(\omega,k)}{\partial \omega}}\right|_{\omega=\omega_r} . \tag{5.23}$$

Determining the real and imaginary parts of the Eqs. (5.22) and (5.23) and leading to

$$\omega_r = \omega_{ic}(1+\Delta) + k_y v_E - k_z u_t , \tag{5.24}$$

where

$$\Delta = \frac{\Gamma_1^i}{1-\Gamma_1^i - \frac{1-\Gamma_0^i}{\mu_i} + \frac{T_i}{T_e}\left(1+\frac{k^2 T_e}{4\pi n_e e^2}\left\{1+\frac{\sqrt{\pi}\upsilon_e}{k_z v_{et}}\right\}\right) + \frac{n_{ib}}{n_{it}}\frac{v_{it}^2}{u_b^2}} .$$

In terms of ion beam energy, the real frequency expression is as follows

$$\omega_r = \omega_{ic}(1+\Delta) + k_y v_E - k_z u_t , \tag{5.25}$$

where $$\Delta = \frac{\Gamma_1^i}{1-\Gamma_1^i - \frac{1-\Gamma_0^i}{\mu_i} + \frac{T_i}{T_e}\left(1+\frac{k^2 T_e}{4\pi n_e e^2}\left\{1+\frac{\sqrt{\pi}\upsilon_e}{k_z v_{et}}\right\}\right) + \frac{n_{ib}}{n_{it}}\frac{m_i v_{it}^2}{(2eE)}} ,$$

where (eE) is the energy of the ion beam

$$\omega_i = -\sqrt{\pi}\frac{\left(\omega_r - k_y v_E + k_z u_t - \omega_{ic}\right)^2}{\Gamma_1^i \omega_{ic}}\left[\begin{array}{l}\Gamma_1^i \dfrac{\left(\omega_r - k_y v_E + k_z u_t\right)}{k_z v_{it}} e^{-\xi_i^2} - \dfrac{\upsilon_i \Gamma_1^i}{\left(\omega_r - k_y v_E + k_z u_t - \omega_{ic}\right)} \\ + \dfrac{n_{ib}}{n_{it}}\dfrac{T_i}{T_b}\dfrac{\omega_r - k_z u_b}{k_z v_{bt}}\end{array}\right] . \tag{5.26}$$

The analytical expressions for the real frequency and growth rate are given in Eqs. (5.24) and (5.26) of the EICWs in collisional plasma under the transverse dc electric field. If $v_E \to 0$ and $\upsilon_i = \upsilon_e = 0$, these mathematical formulations are similar to the results of Chow and Rosenberg [24, 33] reported in their prior works in the absence of a beam. Moreover, we replicate the expressions of Anshu et al. [38] in the absence of collisions and a beam.

Taking into consideration the dust effect, the growth rate expression i.e., Eq. (5.26), alters to

$$\omega_i = -\sqrt{\pi}\left[\frac{\Gamma_1^i \dfrac{\left(\omega_r - k_y v_E + k_z u_t\right)}{k_z v_{it}} \mathrm{e}^{-\xi_i^2} - \dfrac{\upsilon_i \Gamma_1^i}{\left(\omega_r - k_y v_E + k_z u_t - \omega_{ic}\right)} + \dfrac{n_{ib}}{n_{it}} \dfrac{T_i}{T_b} \dfrac{\omega_r - k_z u_b}{k_z v_{bt}}}{\dfrac{2\omega_{ip}^2}{k^2 v_{it}^2} \Gamma_1^i \dfrac{\omega_{ic}}{\left(\omega_r - k_y v_E + k_z u_t - \omega_{ci}\right)^2} + \dfrac{2\omega_{dp}^2}{\omega_r^3}}\right] . \quad (5.27)$$

5.3 RESULTS AND DISCUSSION

In this chapter, the analytical model has been developed in a collisional magnetized plasma to study the resonant EIC instability induced by an ion beam with negatively charged dust grains while incorporating an electric field using the kinetic theory. The developed model aims to analyse the relationship between various plasma parameters with real frequency, growth rate, etc. The effect of the collisions, beam velocity, gyro-radius and relative density ratio on the wave is studied. The equations that hold accountable for the EIC wave in Sec. 5.2 are used to calculate the frequency and the rate of growth. The graphs have been plotted using the MATLAB program for the analytically solved equations i.e., for real frequency and the growth rate. The modified plasma parameters used in our calculation are obtained from various experimental and theoretical papers [8, 14, 17, 28] and are tabulated in Table 5.3.

Figures 5.1(a) and (b) depict the impact of variation of beam velocity on the real frequency and growth rate of the wave against normalized wave number k_z/k for the above-mentioned parameters. Figure 5.1 (a) portrays that as the wave number augments in plasma, the real frequency of instability increases which can be seen by the dispersion relation of the EIC wave. Moreover, the real frequency of the instability also increases with the increase in beam velocities. As shown in Figure 5.1 (b), there is no maximum growth rate for the beam modes with velocities $u_b = 1.2\times10^6$ cm/sec and $u_b = 1.8\times10^6$ cm/sec. The maximum growth rate falls from 2.5×10^5 rad/sec to 9×10^4 rad/sec as the velocity rises from $u_b = 2.2\times10^6$ cm/sec to $u_b = 3.2\times10^6$ cm/sec. These results are analogous to Prakash et al. [8] without collisions.

Table 5.3: Plasma parameters are specified in this model.

Terms	Values
e (Electronic charge)	$4.8\times10^{-10}\,statcoul$
Q_d (Dust charge)	$\left(10^3-10^4\right)e$
m_d (Dust mass)	$10^{12}\times1.67\times10^{-24}\,gm$
m_e (Electron mass)	$9.1\times10^{-28}\,gm$
m_i (Ion mass)	$39\times1.67\times10^{-24}\,gm$
T_e (Electron temperature)	$0.3\,eV$
T_i (Ion temperature)	$0.3\,eV$
n_{it} (Ion density)	$10^9\,cm^{-3}$
n_e (Electron density)	$\left(1\times10^9-0.2\times10^9\right)cm^{-3}$
n_d (Dust density)	$(1-5)\times10^4\,cm^{-3}$
n_{ib} (Beam density)	$2.5\times10^8\,cm^{-3}$
c (Speed of light)	$3\times10^{10}\,cm/\mathrm{s}$
B (Magnetic field)	$\left(0-6\right)kG$
K (Boltzmann constant)	$1.38\times10^{-16}\,erg/Kel$
k_z	$0.1\,cm^{-1}$
k_y	$1\,cm^{-1}$
υ_e (Electron collisional frequency)	$4\times10^5\,\mathrm{sec}^{-1}$
υ_i (Ion collisional frequency)	$1\times10^3\,\mathrm{sec}^{-1}$
u_{ed} (Critical electron drift velocity)	$6\times10^7\,cm/\mathrm{sec}$
n_{ib}/n_{it}	$0.1-5$
E (Electric field)	$0.35\,stat\ V\ cm^{-1}$
v_E	$3.3\times10^4\,cm/\mathrm{s}$
u_t (Ion velocity)	$1.7\times10^5\,cm/\mathrm{s}$
u_b (Ion beam velocity)	$4\times10^7\,cm/\mathrm{s}$

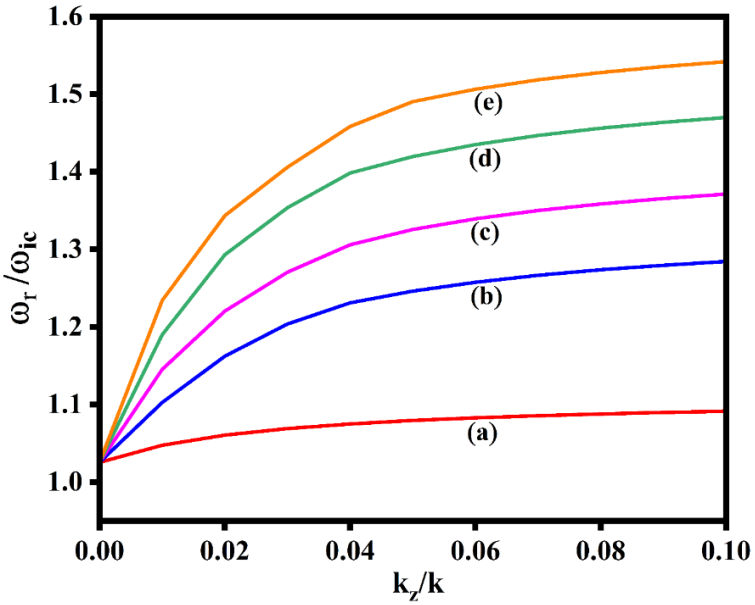

Figure 5.1 (a): The normalized frequency graph with respect to k_z/k for different beam velocities u_b i.e., (a) $u_b = 1.2\times10^6$ cm/sec, (b) $u_b = 1.8\times10^6$ cm/sec, (c) $u_b = 2.2\times10^6$ cm/sec, (d) $u_b = 2.8\times10^6$ cm/sec and (e) $u_b = 3.2\times10^6$ cm/sec.

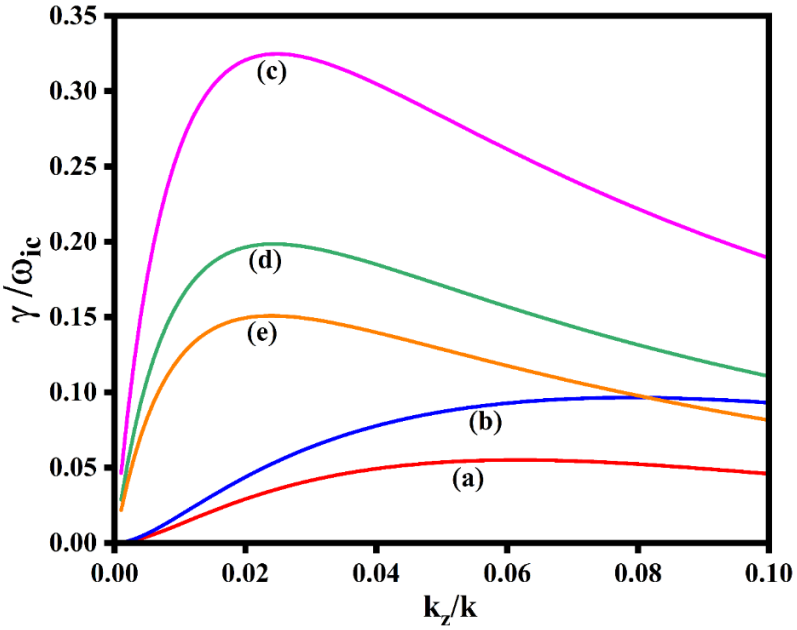

Figure 5.1 (b): The normalized growth rate graph with respect to k_z/k for different beam velocities u_b i.e. (a) $u_b = 1.2\times10^6$ cm/sec, (b) $u_b = 1.8\times10^6$ cm/sec, (c) $u_b = 2.2\times10^6$ cm/sec, (d) $u_b = 2.8\times10^6$ cm/sec and (e) $u_b = 3.2\times10^6$ cm/sec.

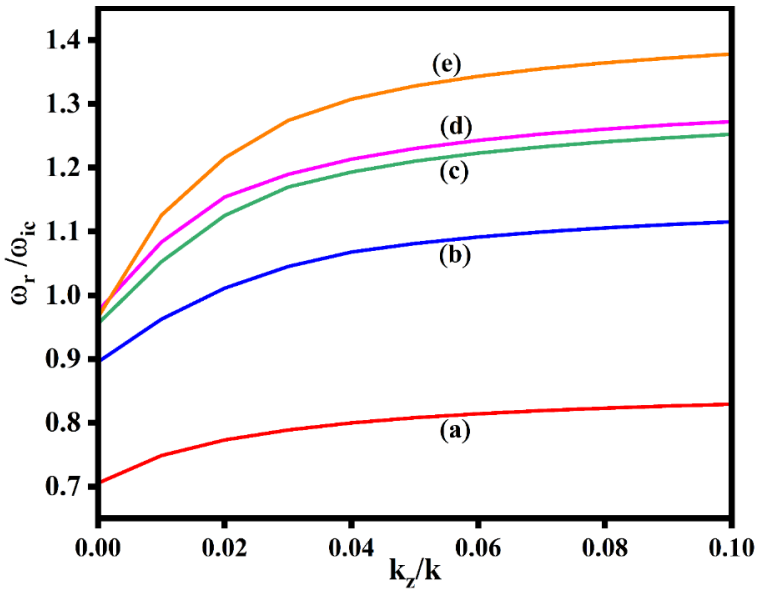

Figure 5.2: The normalized real frequency ω_r/ω_{ic} graph with respect to k_z/k for varying δ i.e., (a) $\delta=1$, (b) $\delta=2$, (c) $\delta=3$, (d) $\delta=4$ and $\delta=5$.

The normalized real frequency variation for different sets of relative density ratios i.e., (a) $\delta=1$, (b) $\delta=2$, (c) $\delta=3$, and (d) $\delta=4$ and $\delta=5$ has been plotted in Figure 5.2 against normalized wavenumber. As the wavenumber augment, the frequency of the instability augment. This result matches with the theoretical paper of Prakash et al. [8] in the absence of collisions. Furthermore, with an increase in relative density ratio, the frequency augments. This result matches with the Chow and Rosenberg [33] observations in the absence of collisions.

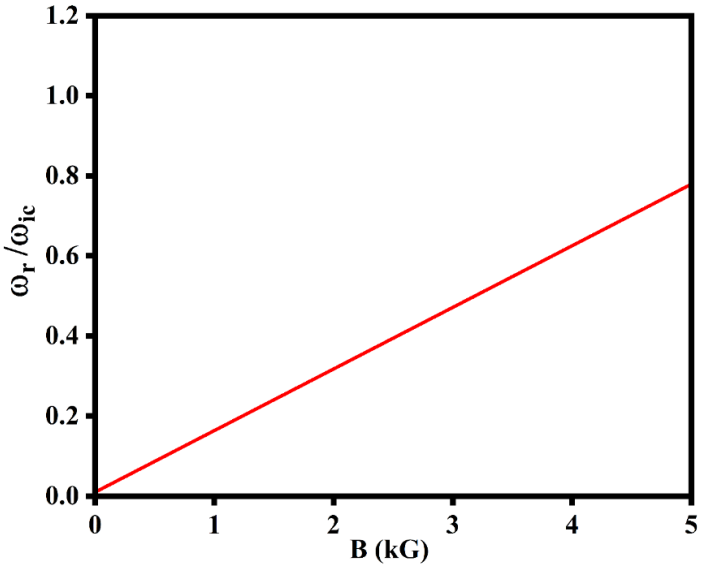

Figure 5.3 (a): The normalized real frequency ω_r/ω_{ic} versus magnetic field $B(\text{in kG})$.

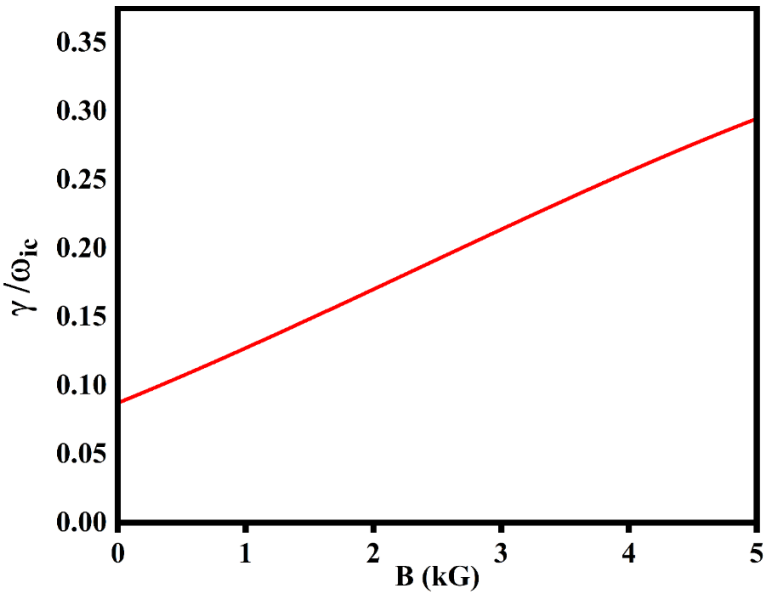

Figure 5.3 (b): The normalized growth rate γ/ω_{ic} with respect to the magnetic field $B(\text{in kG})$.

The relationship of normalized frequency and the growth rate is depicted in Figures 5.3 (a) and (b), respectively with the magnetic fields. The graphs demonstrate that the frequency and the growth rate of the EIC wave correlate linearly to the magnetic field for constant $u_b = 7\times10^5 cm/\sec$. As the magnetic field grows, so do the waves' frequency and growth rate. It can be concluded that with the addition of collisions, the frequency and growth rate decrease as compared to collisionless cases [38]. The outcomes of Koepke and Amatucci [16], Hendel et al. [28] and Motley and D' Angelo [11] are comparable to this outcome without collisions.

Figures 5.4 (a) and 5.4 (b) illustrate the impact of normalized growth rate on the relative density ratio of the wave for varying u_b and υ_i. As the relative density ratio augment in plasma, the growth rate of instability increases. It might be because as δ increases, the plasma density of electrons decreases relative to the plasma density of ions. For increasing the values of δ, an ion's effective mass $\mathrm{m_{ieff}}\left(=\frac{\mathrm{m_i}}{\delta}\right)$ is smaller than m_i, and because of its higher mobility, the growth rate of the instability gets enhanced. Figure 5.4 (a) demonstrates unequivocally that, in accordance with the growth rate expression i.e., Eq. (5.26), the normalized growth rate increases with an increase in u_b. When δ goes from 4 to 8, the maximum growth rate increases by a factor of 4.3 for $u_b = 1.8\times10^6$ cm/sec and by a factor of 3.9 for $u_b = 1.0\times10^6$ cm/sec. This graph in the absence of collisions is analogous to the result of Prakash et al. [8]. From Figure 5.4 (b), it can be seen that the growth rate also reduces for increasing values of υ_i, the ion collision

frequency. Further, for fixed υ_e, it is found that a rise in ion collision frequency results in the expected stabilizing effect. Our result is analogous to the findings of Bharuthram et al. [35] in the absence of a beam.

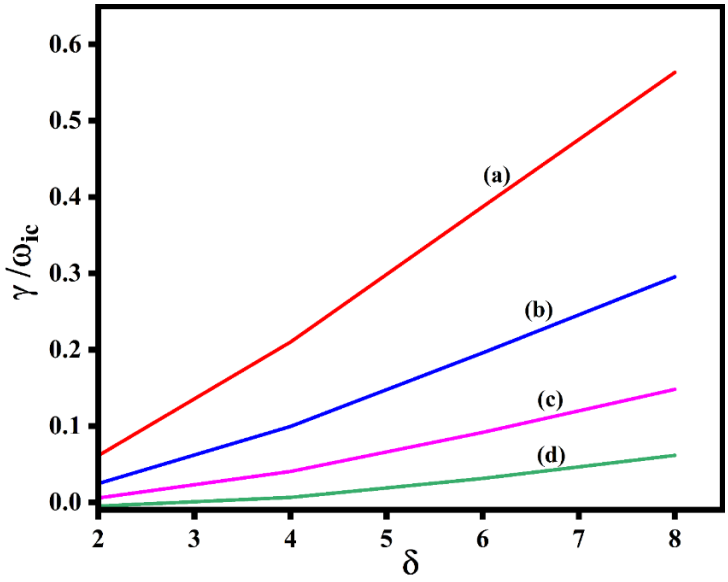

Figure 5.4 (a): Variation in the normalized γ/ω_{ic} with relative density ratio for varying beam velocities u_b i.e., (a) $u_b = 2.2\times10^6$ cm/sec, (b) $u_b = 1.8\times10^6$ cm/sec, (c) $u_b = 1.4\times10^6$ cm/sec and (d) $u_b = 1.0\times10^6$ cm/sec.

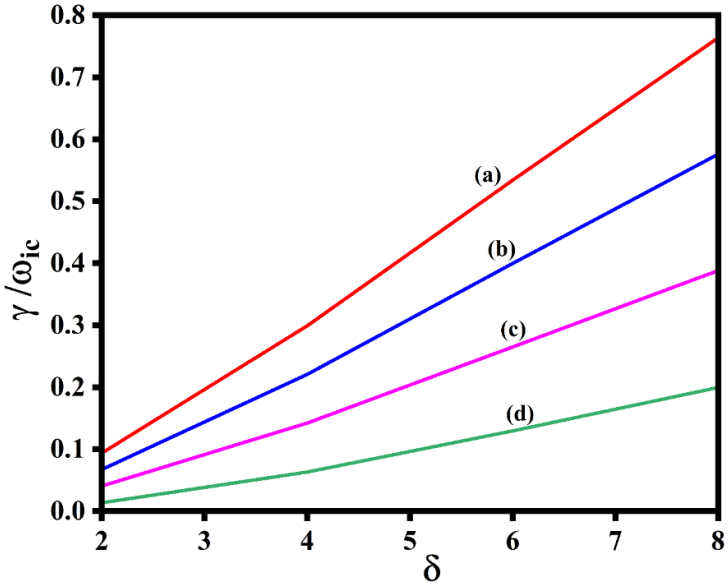

Figure 5.4 (b): Variation in the normalized growth rate γ/ω_{ic} with relative density ratio $\delta\left(=n_i^0/n_e^0\right)$ for different ion collisional frequencies υ_i i.e., (a) $\upsilon_i = 2\times10^3$ rad/sec, (b) $\upsilon_i = 4\times10^3$ rad/sec, (c) $\upsilon_i = 6\times10^3$ rad/sec and (d) $\upsilon_i = 8\times10^3$ rad/sec.

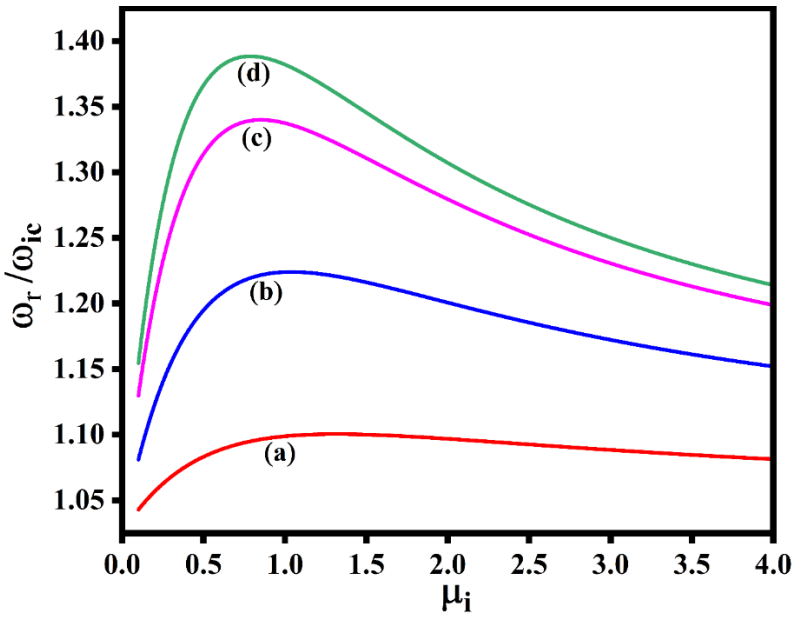

Figure 5.5 (a): Variation in normalized real frequency ω_r/ω_{ic} with the finite gyro-radius parameter μ_i of EIC wave with the electric field in the presence of collisions for varying δ i.e., (a) $\delta = 0.4$, (b) $\delta = 1.4$, (c) $\delta = 3$, and (d) $\delta = 4$.

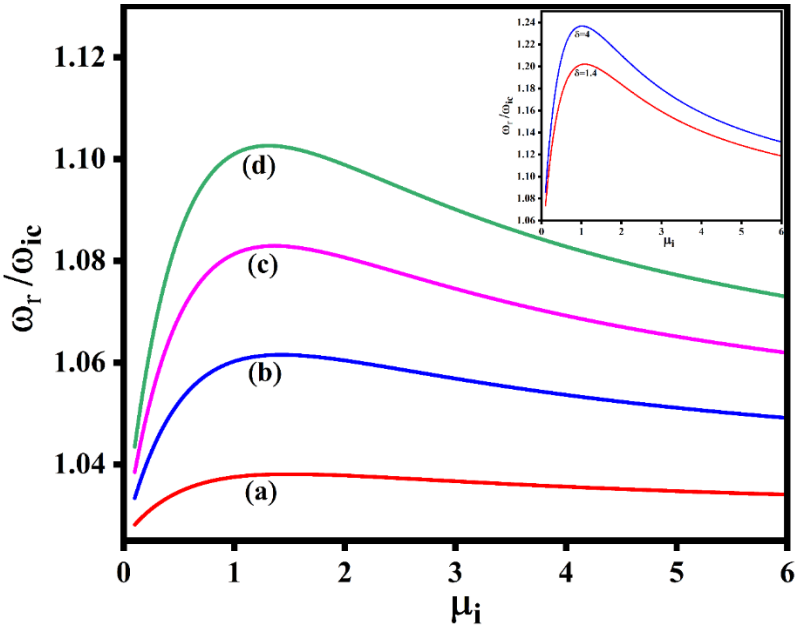

Figure 5.5 (b): Variation in normalized real frequency ω_r/ω_{ic} with the finite gyro-radius parameter μ_i without the electric field for varying δ i.e., (a) $\delta = 0.4$, (b) $\delta = 1.4$, (c) $\delta = 3$, and (d) $\delta = 4$ in the presence of collisions and inset of Figure 5.5 (b) portrays the collisionless case for the same.

The normalized real frequency variation corresponding to the gyro-radius parameter has been plotted in Figures 5.5 (a) and (b) for different sets of relative density ratios i.e., δ (a) $\delta = 0.4$, (b) $\delta = 1.4$, (c) $\delta = 3$, and (d) $\delta = 4$, both with and without an electric field, respectively. From plots, it can be noted that the frequency value rises with increasing gyro-radius parameters until they reach their peak value, after which there is a decline in magnitude for all values of the relative density ratio. In addition, with the rise in the relative density ratio, the real frequency augments. We can conclude that after the inclusion of the electric field, the real frequency follows a similar trend as in the case of the absence of the electric field despite the rise in their values. This is because of the reason that the Doppler effect is caused by $\vec{E} \times \vec{B}$ drift among particles, which is induced by the occurrence of an electric field. As a result, the waves' frequency grows when a dc transverse electric field is applied. The inset of Figure 5.5 (b) shows the result for $\upsilon_e = \upsilon_i \to 0$. We can say that the frequency, in collisionless case, is more as compared to collisional plasma because the charged particles can react more swiftly to an external perturbation than in collisional plasma. This result matches with the theoretical paper of Chow and Rosenberg [33] and Anshu et al. [38].

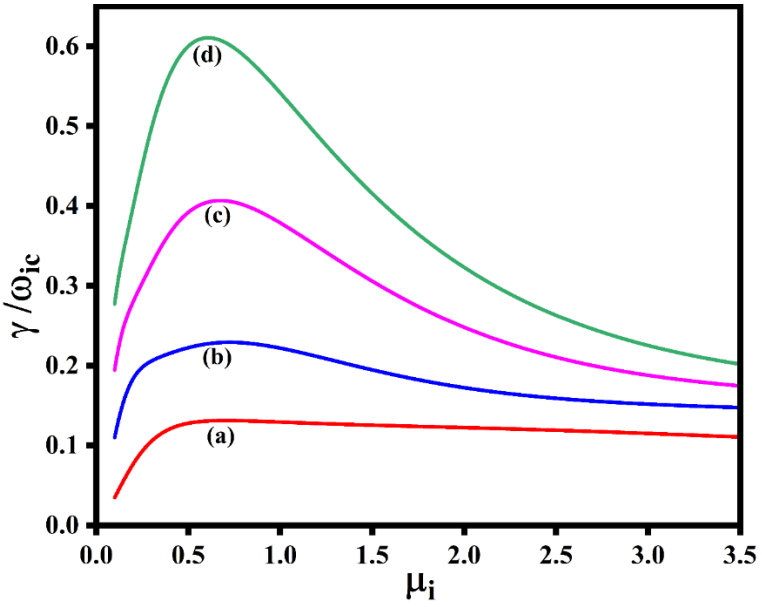

Figure 5.6 (a): Variation in normalized growth rate γ/ω_{ic} with the finite gyro-radius parameter μ_i of EIC wave for varying δ i.e., (a) $\delta = 0.4$, (b) $\delta = 1.4$, (c) $\delta = 3$, and (d) $\delta = 4$.

Figure 5.6 (a) portrays the plot of normalized growth rate as a function of the gyro-radius parameter for varying δ i.e., (a) $\delta = 0.4$, (b) $\delta = 1.4$, (c) $\delta = 3$, and (d) $\delta = 4$, respectively. From Figure 5.6 (a), it can be observed that with an increase in values of the gyro-radius

parameter, the rate of growth of the instability first augments and then attains a maximum value, i.e., $\gamma = 5.0\times10^{4}$ sec^{-1} for $\mu_i = 0.61$ at $\delta = 4$. After attaining maximum value, the instability's growth rate decreases. It can also be inferred that with the increase in the relative density ratio, the growth rate of the unstable wave augments. When $\upsilon_e = \upsilon_i \to 0$ and $\nu_E \to 0$ in Eq. (5.26), the growth rate increases in some values despite the same trend and its corresponding value $\gamma = 8.2\times10^{4}$ sec^{-1} for $\delta = 4$. This result is in good agreement with the observation of Chow and Rosenberg [33] and in the absence of collisions, this result matches with Anshu et al. [38].

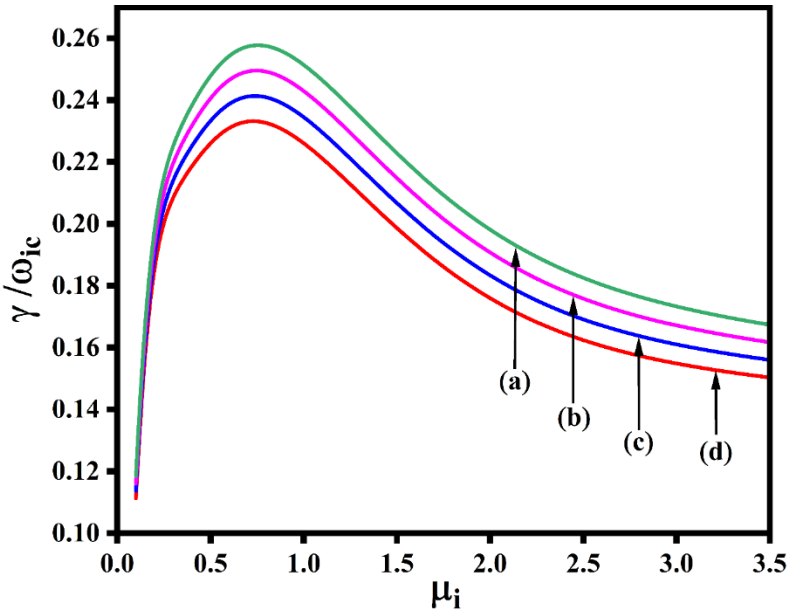

Figure 5.6 (b): The normalized growth rate γ/ω_{ic} variation corresponding to the finite gyro-radius parameter μ_i for different ion collisional frequencies υ_i i.e. (a) $\upsilon_i = 2\times10^{3}$ rad/sec, (b) $\upsilon_i = 4\times10^{3}$ rad/sec, (c) $\upsilon_i = 6\times10^{3}$ rad/sec, (d) $\upsilon_i = 8\times10^{3}$ rad/sec.

Figure 5.6 (b) depict the impact of variation in ion collision frequency on the growth rate with finite gyro-radius parameter, respectively. From the plot, it can be noted that the growth rate values rise with increasing gyro-radius parameters until they reach their peak value, after which there is a decline in magnitude. It can also be seen that the growth rate reduces for increasing values of υ_i, the ion collision frequency. Further, for fixed υ_e, it is found that a rise in ion collision frequency results in the expected stabilising effect. Our results are analogous to the findings of Bharuthram et al. [35].

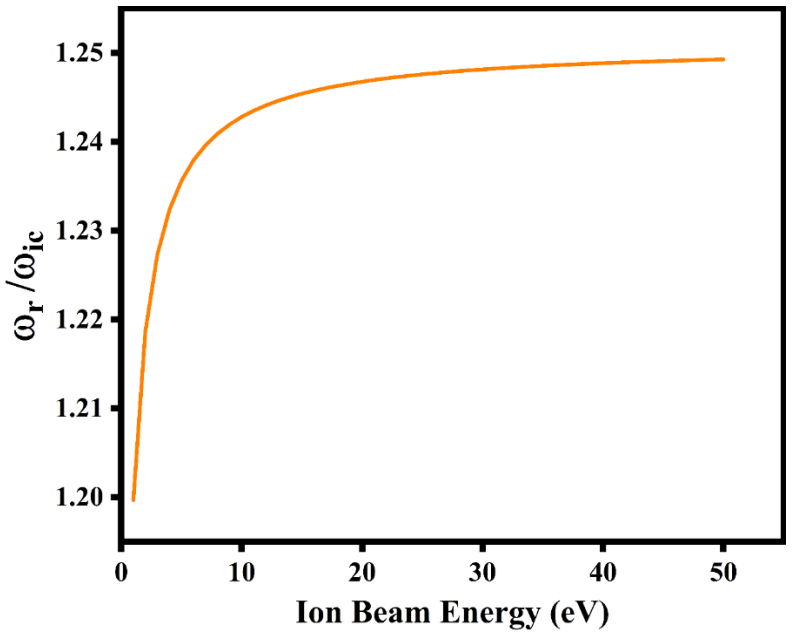

Figure 5.7 (a): The normalized real frequency ω_r/ω_{ic} versus ion beam energy of EIC wave.

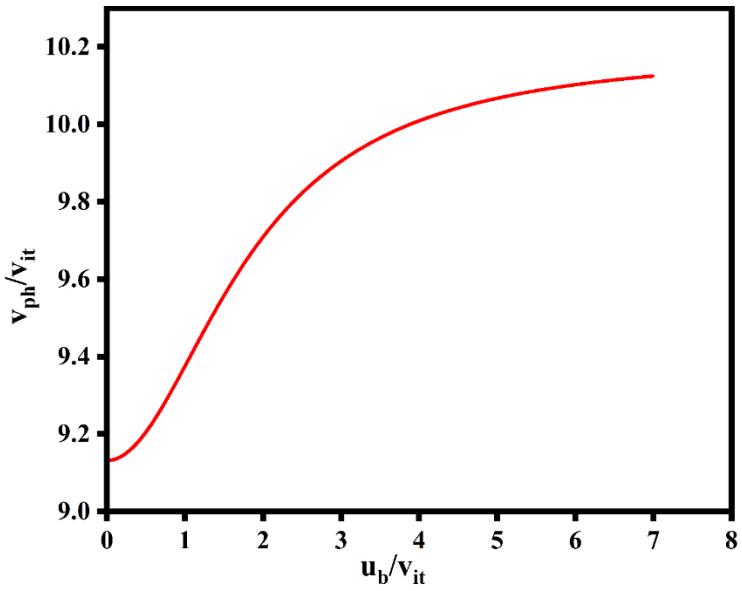

Figure 5.7 (b): The normalized phase velocity v_{ph}/v_{it} versus normalized velocity of the beam u_b/v_{it} of EIC wave.

The normalized real frequency and phase velocity plots as a function of ion beam energy and beam velocity are portrayed in Figures 5.7 (a) and 5.7 (b). Both the graphs demonstrate that with an increase in energy and velocity of the beam, the frequency and the phase velocity of the wave augments, respectively. This is because the resonance condition plays a vital role in this instability. As the beam velocity rises, the resonance condition for beam ions and the excited wave is more likely to be achieved which in turn increases the ion beam energy. This increase

in beam energy results in higher kinetic energy and thermal motion of the ion beams. As a result, the background plasma and the beam ions interact more effectively, leading to a more effective exchange of energy between the two. Because of this stronger interaction, the frequency of the wave rises, which in turn increases the phase velocity of the wave. These results are analogous to the results of Hendel et al. [28].

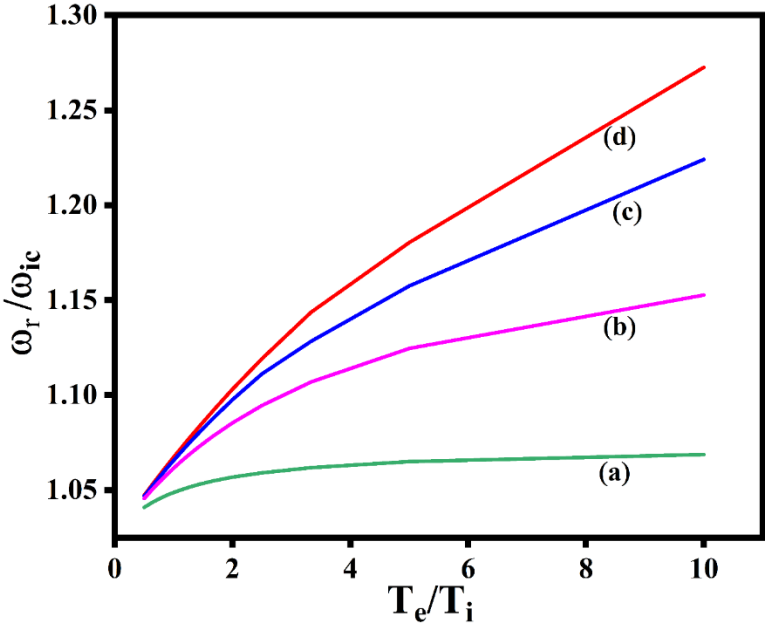

Figure 5.8: The normalized real frequency ω_r/ω_{ic} with varying beam velocity u_b i.e., (a) $u_b = 2\times10^6$ cm/sec, (b) $u_b = 4\times10^6$ cm/sec, (c) $u_b = 6\times10^6$ cm/sec and (d) $u_b = 8\times10^6$ cm/sec as a function of temperature ratio (T_e/T_i).

The effect of varying beam velocity u_b i.e., (a) $u_b = 2\times10^6$ cm/sec, (b) $u_b = 4\times10^6$ cm/sec, (c) $u_b = 6\times10^6$ cm/sec and (d) $u_b = 8\times10^6$ cm/sec has been shown on the normalized frequency with the T_e/T_i in Figure 5.8. The normalized frequency of the wave augments with the rise in T_e/T_i. Using Eq. (5.24), it is clear that when T_e/T_i rises, Δ value rises which in turn increases the frequency. This outcome is consistent with the findings of Kindel and Kennel in the absence of collisions [39]. Moreover, higher beam velocity typically results in an augmentation in EIC wave frequency.

The normalized growth rate graph versus dust number density $n_d^0\left(cm^{-3}\right)$ for varying values of ion collision frequency is illustrated in Figure 5.9 (a) respectively. According to the graphical analysis, the normalized growth rate and dust number density have an inverse relationship,

which is consistent with Eq. (5.27). Additionally, when the frequency of ion collisions augments, the growth rate of the wave reduces.

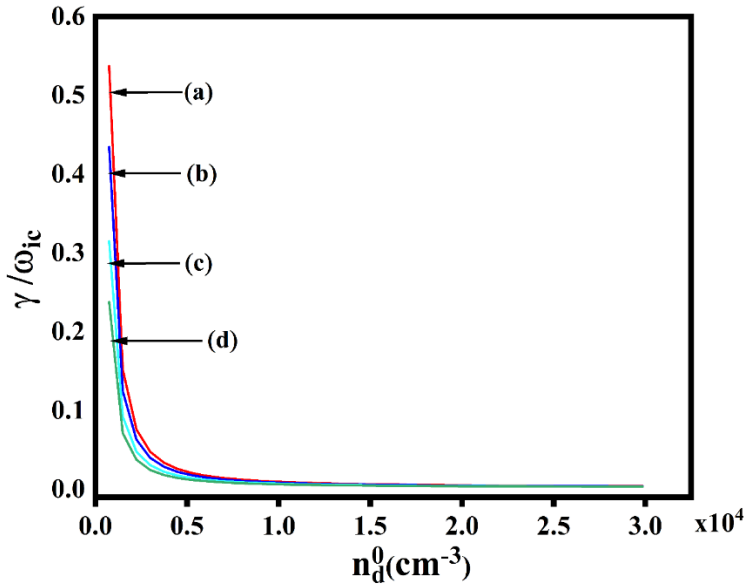

Figure 5.9 (a): The normalized growth rate γ/ω_{ic} of the wave with different ion collisional frequencies υ_i i.e., (a) $\upsilon_i = 2\times10^3$ rad/sec, (b) $\upsilon_i = 4\times10^3$ rad/sec, (c) $\upsilon_i = 6\times10^3$ rad/sec, and (d) $\upsilon_i = 8\times10^3$ rad/sec as a function of dust grain number density $n_d^0\left(cm^{-3}\right)$.

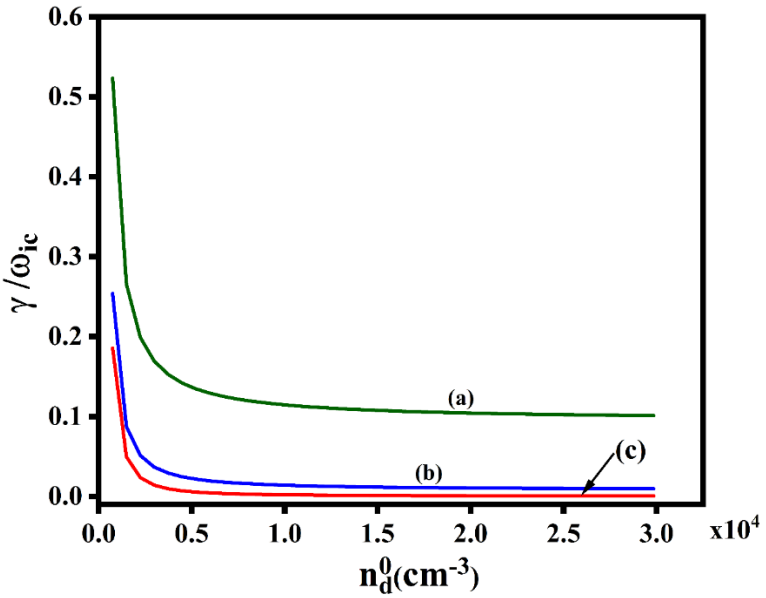

Figure 5.9 (b): The normalized growth rate γ/ω_{ic} for varying u_b i.e., (a) $u_b = 2.2\times10^6$ cm/sec, (b) $u_b = 1.8\times10^6$ cm/sec and (c) $u_b = 1.2\times10^6$ cm/sec as a function of dust grain number density $n_d^0\left(cm^{-3}\right)$ of the wave.

The normalized growth rate graph versus dust number density $n_d^0\left(cm^{-3}\right)$ for varying values of beam velocity is illustrated in Figure 5.9 (b), respectively. As the dust number density augments, the normalized growth rate decreases. This is because the rise in dust particles reduces the number of readily available electrons per dust grain. In turn, this leads to an increased need for electrons among the dust particles as a whole. This increased electron demand from the numerous dust particles leads to a fall in average dust grain charge Q_d^0, which, in turn, lowers the growth rate of the wave. Furthermore, with the rise in beam velocity, the growth rate of the wave increases.

5.4 CONCLUSION

The resonant ion cyclotron instability induced by an ion beam under the outcome of an electric field has been presented via kinetic theory in the collisional magnetized dusty plasma. The study of collisions and beam velocity has been examined for various plasma parameters like gyro-radius, growth rate and frequency etc. The wave's dispersive relationship has been deduced and plotted for various beam velocities and relative density ratio. It was found that with an increase in wave number and beam velocity, the frequency of the wave increases. The real frequency and growth rate augment with an augment in the relative density ratio. The impact of the gyro-radius parameter on the frequency and the growth rate of the wave for varying relative density ratio and ion collision frequencies was also examined. It was discovered that the frequency and the rate of growth first rise as the gyroradius parameter augments before starting to fall as the gyroradius parameter further augments. Furthermore, it has been found that the effect of an ion collision stabilizes the growth rate of instability. The outcome of an electric field on the frequency was also examined and it was observed that in the presence of an electric field, the amplitude of the wave augments. The growth rate and frequency of the waves rise along with the magnetic field strength, emphasizing the stronger connection between the plasma particles and the magnetic fields. The frequency and phase velocity of the wave augments with a rise in beam velocity and beam energy. The frequency increased as the electron to ion temperature ratio and beam velocity increased, according to the temperature study of the EIC wave at different beam velocities. Our findings are sensitive to the dust particles, which play a significant role in influencing the instability and it was examined that with the increasing values of dust density, the growth rate of the wave decreases. It was discovered that the growth rate amplitude was lower in collisional plasma than in the collisionless plasma because the collisions between neutrals and plasma particles reduce their collective oscillations, which over

time causes their amplitudes to gradually decrease. The acquired results were compared to the already existing observations and are in good agreement [8, 28, 33, 35, 38, 39].

In addition to being crucial for comprehending the stability, heating of plasma and plasma confinement the observed instability may be related to bounded dusty plasma system [46] and could be useful in space plasma physics [47, 48].

REFERENCES

[1] S. Seiler, M. Yamada, *Nuclear Fusion* **19**, 469 (1979).

[2] A. Kumar, R. Dhawan, R. Gupta, J. Sharma, *Materials Today: Proceedings* **62**, 3263 (2022).

[3] L. Xiang, D.J. Wu, L. Chen, *The Astrophysical Journal* **857**, 108 (2018).

[4] J. Sharma, S.C. Sharma, *Physics of Plasmas* **17**,123701 (2010).

[5] K. Rani, S.C. Sharma, *Progress in Electromagnetics Research B* **71**, 167 (2016).

[6] S. Seiler, M. Yamada, H. Ikezi, *Physical Review Letters* **37**, 700 (1976).

[7] S.M. Khorashadizadeh, A.R. Niknam, E. Rastbood, *IEEE Transactions on Plasma Science* **40**, 429 (2011).

[8] V. Prakash, S.C. Sharma, V. Vijayshri, R. Gupta, *Physics of Plasmas* **21**, 033701 (2014).

[9] N. D'Angelo, *Journal of Geophysical Research* **78**, 3987 (1973).

[10] N. D'Angelo, R.W. Motley, *The Physics of Fluids* **5**, (1962).

[11] R.W. Motley, N. D'Angelo, *The Physics of Fluids* **6**, 296 (1963).

[12] R. Bergmann, *Journal of Geophysical Research: Space Physics* **89**, 953 (1984).

[13] K.-y. Yi, Z.-a. Wei, J.X. Ma, Q. Liu, Z.-y. Li, *Physics of Plasmas* **27**, 043704 (2020).

[14] A. Barkan, N. D'Angelo, R.L. Merlino, *Planetary and Space Science* **43**, 905 (1995).

[15] D.M. Suszcynsky, S.L. Cartier, R.L. Merlino, N. D'Angelo, *Journal of Geophysical Research: Space Physics* **91**, 13729 (1986).

[16] M.E. Koepke, W.E. Amatucci, *IEEE transactions on Plasma Science* **20**, 631 (1992).

[17] S.C. Sharma, M. Sugawa, V.K. Jain, *Physics of Plasmas* **7**, 457 (2000).

[18] D.L. Correll, N. Rynn, H. Böhmer, *The Physics of Fluids* **18**, 1800 (1975).

[19] R.L. Merlino, A. Barkan, C. Thompson, N. D'angelo, *Physics of Plasmas* **5**, 1607 (1998).

[20] N. D'Angelo, *Planetary and Space Science* **38**, 1143 (1990).

[21] A.A. El-bendary, *Advanced Studies in Theoretical Physics* **6**, 863 (2012).

[22] P.K. Shukla, A.A. Mamun, *Journal of Plasma Physics* **65**, 97 (2001).

[23] S.C. Sharma, J. Sharma, *Physics of Plasmas* **17**, 043704 (2010).

[24] V.W. Chow, M. Rosenberg, *Planetary and Space Science* **43**, 613 (1995).

[25] A. Kumar, V.K. Tripathi, *Laser and Particle Beams* **30**, 9 (2012).

[26] S.C. Sharma, M.P. Srivastava, *Physics of Plasmas* **8**, 679 (2001).

[27] J.P. Hauck, H. Böhmer, N. Rynn, G. Benford, *Journal of Plasma Physics* **19**, 237 (1978).

[28] H.W. Hendel, M. Yamada, S.W. Seiler, H. Ikezi, *Physical Review Letters* **36**, 319 (1976).

[29] M. Sugawa, *Plasma Physics and Controlled Fusion* **30**, 235 (1988).

[30] P. Kumar, V.K. Tripathi, *Physics of Plasmas* **15**, 052107 (2008).

[31] V. Prakash, S.C. Sharma, V. Vijayshri, R. Gupta, *Progress in Electromagnetics Research M* **36**, 161 (2014).

[32] S.C. Sharma, K. Sharma, A. Gahlot, *Physics of Plasmas* **20**, 053704 (2013).

[33] V.W. Chow, M. Rosenberg, *Planetary and Space Science* **44**, 465 (1996).

[34] M. Yamada, S. Seiler, H.W. Hendel, H. Ikezi, *The Physics of Fluids* **20**, 450 (1977).

[35] R. Bharuthram, P. Singh, M. Rosenberg, V.W. Chow, *Physica Scripta* **1998**, 223 (1998).

[36] V. Prakash, V. Vijayshri, S.C. Sharma, R. Gupta, *Physics of Plasmas* **20**, 053701 (2013).

[37] V. Prakash, V. Vijayshri, S.C. Sharma, R. Gupta, *Physics of Plasmas* **20**, 063701 (2013).

[38] Anshu, J. Sharma, S.C. Sharma, *Contributions to Plasma Physics* **62**, e202200073 (2022).

[39] J.M. Kindel, C.F. Kennel, *Journal of Geophysical Research* **76**, 3055 (1971).

[40] S.L. Ossakow, K. Papadopoulos, J. Orens, T. Coffey, *Journal of Geophysical Research* **80**, 141 (1975).

[41] B.D. Fried, S.D. Conte, The plasma dispersion function: the Hilbert transform of the Gaussian, *Academic Press* (2015).

[42] W.E. Drummond, M.N. Rosenbluth, *The Physics of Fluids* **5**, 1507 (1962).

[43] A. Bers, M.N. Rosenbluth, R.Z. Sagdeev, *MN Rosenbluth and RZ Sagdeev eds* **1**, (1983).

[44] D.B. Melrose, Instabilities in Space and Laboratory plasmas (1986).

[45] N.A. Krall, A.W. Trivelpiece, R.A. Gross, *American Journal of Physics* **41**, 1380 (1973).

[46] M. Rosenberg, P.K. Shukla, *Physics of Plasmas* **5**, 3786 (1998).

[47] A. Le, L.-J. Chen, B. Wetherton, B. Keenan, A. Stanier, *Frontiers in Astronomy and Space Sciences* **9**, 1100472 (2023).

[48] C.A. Cattell, F.S. Mozer, I. Roth, R.R. Anderson, R.C. Elphic, W. Lennartsson, E. Ungstrup, *Journal of Geophysical Research: Space Physics* **96**, 11421 (1991).

6

Analytical Modelling of Inhomogeneous Energy Density Driven Instability (IEDDI) in a Magnetized Dusty Plasma Cylinder

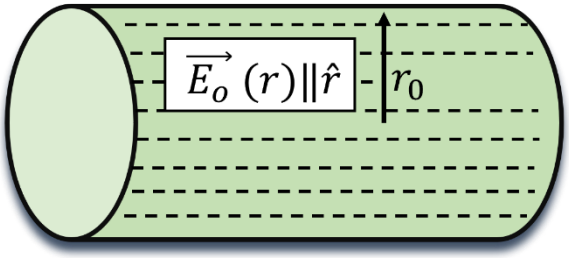

Plasma System

Electric field model for plasma system

Previously, all theoretical model was developed using the kinetic treatment approach but in Chapter 6, we have developed an analytical model of Inhomogeneous Energy Density Driven Instability (IEDDI) while incorporating the effect of dust particles in a collisional magnetized plasma cylinder using the fluid theory. The localization of the electric field gives rise to IEDDI. In this chapter, a comparative analysis of the instability has been done in the presence and absence of dust grains. The different plasma parameters impact has been studied on the behaviour of instability i.e., frequency and growth rate. The effect of an electric field on IEDDI was examined. Further, the response of dust grains number density and dust grain size on IEDDI was also evaluated.

PUBLICATION

Anshu, Jyotsna Sharma, and Suresh C. Sharma, "Analytical Modelling of Inhomogeneous Energy Density Driven (IEDD) Instability in a Magnetized Dusty Plasma Cylinder*", Brazilian Journal of Physics*, 54 (8), 2024.

6.1 INTRODUCTION

The study of plasma has become indispensable due to its pervasive nature. Therefore, it is not surprising that research into "plasmas"[1-6] is proposed in several waves [7-12], instabilities [13-16], and astrophysical phenomena [17-20]. The dust may have a significant impact on the plasma, and it was discovered in the solar wind, comet tails, industries [21-23] and laboratories [24-27]. The nature of plasma as a whole is reformed by the presence of these massive particles affecting the overall quasi-neutrality condition in waves [28-31] and instabilities [13]. Due to the potential applications of waves and instabilities [32] in plasma like Hall thrusters are forefront propulsion systems that effectively use plasma to move spacecraft, making them perfect for deep-space missions [33-35], this field of research is of great interest. Instabilities in plasma have been investigated by numerous researchers [15, 36-39] through diverse methods, including kinetic theory, kappa distribution and fluid theory. Additionally, it has been noted that relative drift or inhomogeneities caused by an electric field tend to drive these instabilities [40-43]. Among these instabilities, the two major instabilities are inhomogeneous energy density driven instability and the density gradient driven instability. The major difference is that the IEDDI develops when the energy density inside a fluid or plasma is distributed unevenly. Rather than only fluctuations in density, it is also driven by variations in the electric field of the system. This instability can arise as a result of disturbances (localisation in electric field) from one region to another region, leading to instability. On the other side, density gradient driven instability is caused when the density of the plasma varies throughout different regions of the plasma. This instability is driven by the buoyant forces which are related with the density gradients [44-47].

An IEDDI [11, 15, 39, 48] has drawn significant interest in a plethora of space, planetary, and geophysical systems. This instability can occur because of the free energy provided by the inhomogeneous electric field. Inhomogeneities in the background of the plasma may result in an area with negative energy density, and a nonlocal wave packet may couple the areas of both the energies, i.e., positive and negative, which may result in waves to grow [37, 38, 49]. This is the physical mechanism underlying the IEDDI. IEDD waves have a wide frequency range that is close to the ion cyclotron frequency and typically propagate in the $\vec{E}\times\vec{\mathrm{B}}$ direction [15, 50-52]. The key parameter to use in observing the change from one type of wave to another is the parameter R, i.e. $R = k_\theta v_E(r)/k_z v_{ed}$, the ratio of the azimuthal and axial doppler shifts in cylindrical coordinates [15, 53]. The EICWs are driven by the current, which is known as EIC

instability [7] for $R<<1$,i.e., small ν_E and large ν_{ed} cases. For $R>>1$, i.e. the situation of large ν_E and small ν_{ed}, the EICWs are driven by an inhomogeneous electric field which is known as IEDDI [38, 54]. The IEDDI is amalgamation of two regime i.e., reactive and dissipative [4, 55]. The field-aligned current is primarily responsible for the IEDDI in the dissipative regime. A nearby region of positive and negative wave-energy density drives the IEDDI in the reactive domain, and in most cases no field-aligned current is needed [49, 54]. The IEDD theory was primarily suggested by Ganguli et al. [49, 50, 54] and is relied on the nonlocal approximation. Koepke et al. [15] experimentally verified the IEDDI in Q-machine at West Virginia University, and they have shown that the variation in the electric field affects the IEDD mode amplitude. Koepke et al. [36] experimentally identified the IEDDI in the laboratory. They reported that azimuthal and axial doppler shift ratio has an impact on inhomogeneous energy density driven mode, i.e., frequency of the instability increases with the ratio. Ganguli [37] has reported the IEDDI using both fluid and kinetic formalism, and a comparative study is shown between them. He depicted that as the wavevector and magnitude of the drift increase, the growth rate of the instability increases. Amatucci et al. [56] observed the reactively produced plasma waves in the ion-cyclotron frequency range in the laboratory, followed by a transverse dc electric field. Koepke et al. [38] investigated the various nonlocal eigenmodes of inhomogeneity-driven plasma instability for the very first time in sodium plasma. They observed that with the gyro-radius parameter increment, the growth rate of the instability augments initially, attains peak value and then decreases.

To the best of the authors' knowledge, no theoretical model has been proposed to study the IEDDI in the transverse dc electric field presence in a dusty magnetized collisional plasma cylinder via fluid theory. Drawing inspiration from the work described above that only focus on the experimental studies [15, 38] of the IEDDI in the absence of dust particles, we proposed a theoretical model in this present chapter to understand the role of plasma parameters, i.e., dust density, relative density ratio and gyroradius parameter etc. on the IEDDI in a collisional magnetized plasma cylinder having negatively charged dust particles in the existence of a transverse dc electric field. Moreover, this current model shows a comparative study for both cases, i.e., in the presence and absence of dust particles and the impact of different plasma parameters on the frequency and the growth rate of instability is studied.

This chapter is organized as follows for the succeeding sections: the detailed analysis of IEDDI using the motion and continuity equation for solving the expression of growth rate and frequency is delineated in Section 6.2. In Section 6.3, the outcomes of the theoretical modelling of instability have been compared with the results of the existing experiments. The conclusion is outlined in Section 6.4.

6.2 INSTABILITY ANALYSIS

In this chapter, we studied the collisional multispecies magnetized dusty plasma cylinder of radius $r_{0,}$ as shown in Figure 1.

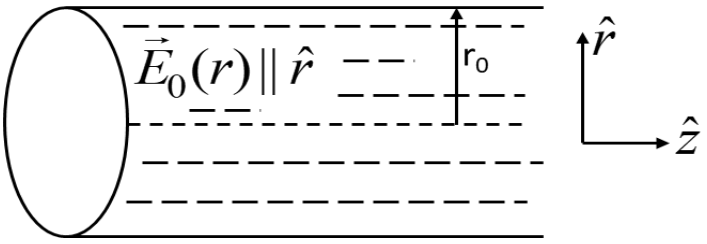

Figure 6.1: Schematic of electric field model with negatively charged dust grains.

The proposed system consists of three species: electrons, ions and dust particles, and their notations can be tabulated in Table 6.1.

Table 6.1: Species and their notations considered in the model.

S. No.	Species	Equilibrium density	Drift Velocity	Mass	Charge	Temperature	Collisional Frequency
1.	Electrons	n_e^0	$v_{ed} \| \hat{z}$	m_e	$-e$	T_e	υ_e
2.	Ions	n_i^0	0	m_i	e	T_i	0
3.	Dust Particles	n_d^0	0	m_d	Q_d^0	T_d	0

We take into account a uniform static magnetic field B in the z-direction and a localized dc electric field $E_0(r)$ in the radial direction, such as

$$\begin{aligned} \vec{E}_0(r) &= E_0(\mathrm{r}) \qquad \text{for } \mathrm{r} \le \mathrm{r}_0 \\ &= 0 \qquad\quad \text{for } \mathrm{r} > \mathrm{r}_0 \end{aligned} . \tag{6.1}$$

Due to an electric field, the $\vec{E}\times\vec{B}$ drift induces, having a magnitude $\vec{v}_E(r)=\frac{c\vec{E}_0(r)\text{ x }\vec{B}}{\vec{B}^2}$, where c is the speed of light. The localization of electric field gives rise to IEDDI. In equilibrium, the quasi-neutrality condition says

$$-en_i^0+en_e^0+Q_d^0n_d^0\approx 0. \tag{6.2}$$

An electrostatic perturbation is given by

$$\phi_1=\phi_0(r)\exp[-i(\omega t-\vec{k}.\vec{r})]. \tag{6.3}$$

The equation of motion

$$m\frac{d\vec{v}}{dt}=-e\vec{E}-\frac{e}{c}\vec{v}\times\vec{B}-\frac{\nabla(nT)}{n}-m\vec{v}\upsilon\,. \tag{6.4}$$

is used to explain the behaviour of electrons in the plasma. On linearization and solving Eq. (6.4), we get the perpendicular and parallel components of perturbed velocities,

$$\vec{v}_{1\perp}=\frac{e}{m_e}\frac{[i(\omega_1+i\upsilon_e)\nabla_\perp\phi_1+\nabla_\perp\phi_1\times\omega_{ec}]}{[(\omega_1+i\upsilon_e)^2-\omega_{ec}^2]}-\frac{T_e}{m_en_e^0}\frac{[i(\omega_1+i\upsilon_e)\nabla_\perp n_e^1+\nabla_\perp n_e^1\times\omega_{ec}]}{[(\omega_1+i\upsilon_e)^2-\omega_{ec}^2]}. \tag{6.5}$$

$$v_{1z}=\frac{-ek_z\phi_1}{m_e(\omega+i\upsilon_e)}+\frac{T_e}{m_e}\frac{k_zn_e^1}{(\omega+i\upsilon_e)n_e^0}, \tag{6.6}$$

where $\omega_1=\omega-k_\theta v_E-k_zv_{ed}$, $\omega_{ec}\left(=\frac{eB}{m_ec}\right)$ is the electron cyclotron frequency; k_z and k_θ are the propagation vector in z and θ - directions, respectively.

Using perturbed velocities, i.e., Eqs. (6.5) and (6.6) in the continuity equation

$$\frac{\partial n}{\partial t}+\nabla.(n\vec{v})=0\,. \tag{6.7}$$

The perturbed electron density can be evaluated and written as

$$n_e^1=\frac{\frac{n_e^0e}{m_e\omega_1}\left(\frac{(\omega_1+i\upsilon_e)\nabla_\perp^2\phi_1}{(\omega_1+i\upsilon_e)^2-\omega_{ec}^2}-\frac{k_z^2\phi_1}{(\omega_1+i\upsilon_e)}\right)}{1-\frac{v_{et}^2k_z^2}{\omega_1(\omega_1+i\upsilon_e)}+\frac{(\omega_1+i\upsilon_e)\nabla_\perp^2v_{et}^2}{\omega_1[(\omega_1+i\upsilon_e)^2-\omega_{ec}^2]}}, \tag{6.8}$$

where $v_{et}\left(=\frac{T_e}{m_e}\right)^{1/2}$ is the thermal velocity of the electron.

In the short wavelength limit, i.e., $\omega_1 << k_\perp v_{et}$ and using $\omega_1 << \omega_{ec}$, $\omega_1 << i\upsilon_e$, Eq. (6.8) becomes

$$n_e^1 = \frac{n_e^0 e\phi_1}{T_e\left(1-\frac{i\upsilon_e\omega_1}{k_z^2\frac{T_e}{m_e}}\right)}. \tag{6.9}$$

Similarly, the perturbed ion density is obtained in the limit $\omega_2 \sim \omega_{ic}$ and $\frac{k_\perp v_{it}}{\omega_2-\omega_{ic}} << 1$.

$$n_i^1 = -\frac{en_i^0}{m_i}\left(\frac{\nabla_\perp^2\phi_1}{\omega_2^2-\omega_{ic}^2}-\frac{k_z^2\phi_1}{\omega_2^2}\right), \tag{6.10}$$

where $v_{it}\left(=\frac{T_i}{m_i}\right)^{1/2}$ denotes ion thermal velocity, and $\omega_2 = \omega - k_9 v_E$ and $\omega_{ic}\left(=\frac{eB}{m_i c}\right)$ is the ion cyclotron frequency.

CASE I: IN THE ABSENCE OF DUST GRAINS

Substituting Eqs. (6.9) and (6.10) in Poisson's Equation

$$\nabla^2\phi_1 = 4\pi e\left(n_e^1 - n_i^1\right), \tag{6.11}$$

we get a second-order differential equation in ϕ_1 and solve it for an axially symmetric case, we obtain

$$\frac{\partial^2\phi_1}{\partial r^2}+\frac{1}{r}\frac{\partial\phi_1}{\partial r}+p_1^2\phi_1 = 0. \tag{6.12}$$

or

$$\nabla_\perp^2\phi_1 + p_1^2\phi_1 = 0. \tag{6.13}$$

Here

$$p_1^2 = \frac{-\frac{\omega_{ep}^2}{v_{et}^2}\left(1-\frac{i\upsilon_e\omega_1}{k_z^2 v_{et}^2}\right)-k_z^2+\frac{\omega_{ip}^2 k_z^2}{\omega_2^2}}{\left(1-\frac{\omega_{ip}^2}{\omega_2^2-\omega_{ic}^2}\right)}, \tag{6.14}$$

where $\omega_{ep}\left(=\frac{4\pi n_e^0 e^2}{m_e}\right)^{1/2}$ and $\omega_{ip}\left(=\frac{4\pi n_i^0 e^2}{m_i}\right)^{1/2}$ are the electron and ion plasma frequency, respectively.

The Bessel equation's solution is given by

$$\phi_1 = A_1 J_0\left(p_{1n} r\right),\ p_1 \sim p_{1n}, \tag{6.15}$$

where $J_0\left(p_{1n} r\right)$ denotes the zero-order Bessel functions of argument $\left(p_{1n} r\right)$ and A_1 is a constant. At $r = r_0$, $\phi_1 = 0$. Hence, $\phi_1 = A_1 J_0\left(p_{1n} r_0\right) = 0$ i.e., $p_{1n} = \frac{x_n}{r_0}$ (n=1, 2, ….) where x_n represents the Bessel function's zeroes. If $J_0(x) = 0$, $x = 2.404$ and therefore $p_{1n} = \frac{2.404}{r_0}$.

From Eq. (6.14) and simplifying it, we obtain

$$1 - \frac{\omega_{ip}^2}{\omega_2^2 - \omega_{ic}^2}\frac{p_{1n}^2}{p_{1n}^2 + k_z^2} + \frac{\omega_{ep}^2\left(1 + \frac{i\upsilon_e\omega_1}{k_z^2 v_{et}^2}\right)}{v_{et}^2\left(1 + \frac{\upsilon_e^2\omega_1^2}{k_z^4 v_{et}^4}\right)\left(p_{1n}^2 + k_z^2\right)} - \frac{\omega_{ip}^2}{\omega_2^2}\frac{k_z^2}{p_{1n}^2 + k_z^2} = 0. \tag{6.16}$$

Solving Eq. (6.16) and using $\frac{\upsilon_e^2\omega_1^2}{k_z^4 v_{et}^4} << 1$, we obtain

$$\varepsilon_r\left(\omega, k\right) + i\varepsilon_i\left(\omega, k\right) = 0, \tag{6.17}$$

where

$$\varepsilon_r = 1 - \frac{\omega_{ip}^2}{\omega_2^2 - \omega_{ic}^2}\frac{p_{1n}^2}{p_{1n}^2 + k_z^2} + \frac{\omega_{ep}^2}{v_{et}^2\left(p_{1n}^2 + k_z^2\right)} - \frac{\omega_{ip}^2}{\omega_2^2}\frac{k_z^2}{p_{1n}^2 + k_z^2}, \tag{6.18}$$

$$\varepsilon_i = \frac{\omega_{ep}^2\upsilon_e\omega_1}{k_z^2 v_{et}^4\left(p_{1n}^2 + k_z^2\right)}. \tag{6.19}$$

Let $\omega = \omega_r + i\gamma$ is the solution of Eq. (6.17), assuming the wave is either growing or damped.

Real part is obtained as follows

$$\varepsilon_r(\omega,k)\big|_{\omega=\omega_r}=0. \tag{6.20}$$

The imaginary part is given by [57]

$$\gamma=\left.\frac{-\varepsilon_i(\omega,k)}{\dfrac{\partial\varepsilon_r(\omega,k)}{\partial\omega}}\right|_{\omega=\omega_r}. \tag{6.21}$$

The real frequency can be obtained by solving Eqs. (6.18) and (6.20), we obtain

$$1-\frac{\omega_{ip}^2}{(\omega_r-k_\theta v_E)^2}\frac{k_z^2}{p_{1n}^2}\frac{1}{\alpha}-\frac{\omega_{ip}^2}{\{(\omega_r-k_\theta v_E)^2-\omega_{ic}^2\}}\frac{1}{\alpha}=0, \tag{6.22}$$

where $\alpha\approx\dfrac{\omega_{ip}^2}{c_s^2}\dfrac{1}{p_{1n}^2}$; $c_s\left(=\frac{T_e}{m_i}\right)^{1/2}$.

Multiply Eq. (6.22) by $\{(\omega_r-k_\theta v_E)^2\}\{(\omega_r-k_\theta v_E)^2-\omega_{ic}^2\}$, we get

$$\omega_{2r}^4-\omega_{2r}^2\left(\omega_{ic}^2+\frac{\omega_{ip}^2}{\alpha}+\frac{\omega_{ip}^2k_z^2}{p_{1n}^2\alpha}\right)+\omega_{ic}^2\frac{\omega_{ip}^2k_z^2}{p_{1n}^2\alpha}=0. \tag{6.23}$$

Equation (6.23) is biquadratic in ω_{2r} , where we consider $\omega_{2r}=\omega_r-k_\theta v_E$, and root is

$$\omega_r=k_\theta v_E+\sqrt{\omega_{ic}^2+c_s^2\left(p_{1n}^2+k_z^2\right)}. \tag{6.24}$$

Equation (6.24) corresponds to the real frequency of IEDDI with the presence of a transverse dc electric field and absence of dust particles.

Solving Eqs. (6.19) and (6.21), the imaginary part is as follows

$$\gamma=\frac{-1}{2}\frac{\left(\dfrac{\upsilon_e\left\{1-k_zv_{ed}\left(1+R\right)\right\}}{k_z^2v_{et}^4}\dfrac{m_i}{m_e}\dfrac{1}{\delta}\right)\left[\left(\omega_r-k_\theta v_E\right)^2-\omega_{ic}^2\right]^2}{\left(\omega_r-k_\theta v_E\right)\left(p_{1n}^2\right)}. \tag{6.25}$$

where $R\left(=\dfrac{k_\theta v_E}{k_zv_{ed}}\right);\delta\left(=\dfrac{n_i^0}{n_e^0}\right)$.

Equation (6.25) corresponds to the growth rate of the IEDDI in the presence of a transverse dc electric field without dust grains.

CASE II: IN THE EXISTENCE OF DUST GRAINS

Perturbed density behaviour for dust is written as

$$n_d^1 = \frac{n_d^0 Q_d^0 \nabla_\perp^2 \phi_1}{m_d \omega_2^2}. \tag{6.26}$$

Here, it is assumed that dust is unmagnetized as $m_d = 10^{12} m_p$. Therefore, the dust gyro frequency $\omega_{dc}\left(=\frac{Q_d^0 B}{m_d c}\right)$ becomes very small; hence, we can neglect it. Also, $\omega_2 >> \omega_{dc}$. For the dust particle, on the application of probe theory, the acquired charge on the dust particle Q_d is set to get balanced with the plasma currents on the surface and defined by [58-60]

$$\frac{-dQ_d}{dt} = I_e + I_i. \tag{6.27}$$

Current due to electrons and ions on the surface of the particle can be understood as

$$I_e = -\pi a^2 e\left(\frac{8T_e}{\pi m_e}\right)^{1/2} n_e^0 \exp\left(\frac{e\left(\phi_g - V\right)}{T_e}\right). \tag{6.28}$$

$$I_i = \pi a^2 e\left(\frac{8T_i}{\pi m_i}\right)^{1/2} n_i^0 \exp\left(\frac{1-e\left(\phi_g - V\right)}{T_i}\right), \tag{6.29}$$

where $(\phi_g - V)$ denotes the dust particle surface and plasma potential difference; "a" denotes the radius of the dust grain sphere. In equilibrium, $|I_e^0| = |I_i^0|$.

The fluctuations due to the charge on dust particles can be depicted as

$$\frac{dQ_d^1}{dt} + \eta Q_d^1 = -|I_e^0|\left(\frac{n_i^1}{n_i^0} - \frac{n_e^1}{n_e^0}\right), \tag{6.30}$$

where $\eta = \frac{|I_e^0|e}{C_d}\left(\frac{1}{T_e} + \frac{1}{T_i - e\phi_g^0}\right)$ represents the charging rate of dust; $Q_d^1 = Q_d - Q_d^0$ represents

the perturbed charge on dust; $C_d = \left(a\left(1+\frac{a}{\lambda_{ed}} \right) \right)$ denotes the capacitance of dust particle [61]; λ_{ed} represents the electron Debye length.

$$Q_d^1 = \frac{e\,|\,I_e^0\,|}{i(\omega+i\eta)}\left(\frac{-1}{m_i}\left(\frac{\nabla_\perp^2\phi_1}{\omega_2^2-\omega_{ic}^2} - \frac{k_z^2\phi_1}{\omega_2^2} \right) - \frac{\phi_1}{T_e\left(1-\frac{i\upsilon_e\omega_1}{k_z^2\frac{T_e}{m_e}} \right)} \right). \tag{6.31}$$

Substituting Eqs. (6.9), (6.10), (6.26) and (6.31) in Poisson's equation

$$\nabla^2\phi_1 = 4\pi\left(n_e^1 e - n_i^1 e + n_d^0 Q_d^1 + Q_d^0 n_d^1 \right). \tag{6.32}$$

Simplifying it and using Eq. $\nabla_\perp^2\phi_1 + p_2^2\phi_1 = 0$, we get

$$p_2^2 = \frac{-\frac{\omega_{ep}^2}{v_{et}^2}\left(1-\frac{i\upsilon_e\omega_1}{k_z^2 v_{et}^2} \right) - k_z^2 + \frac{\omega_{ip}^2 k_z^2}{\omega_2^2} + \frac{i\beta\omega_{ip}^2}{\omega+i\eta}\frac{n_e^0}{n_i^0}\frac{k_z^2}{\omega_2^2} - \frac{i\beta\omega_{ep}^2}{\omega+i\eta}\frac{1}{v_{et}^2\left(1-\frac{i\upsilon_e\omega_1}{k_z^2 v_{et}^2} \right)}}{1-\frac{\omega_{ip}^2}{\omega_2^2-\omega_{ic}^2} - \frac{i\beta\omega_{ip}^2}{\omega+i\eta}\frac{n_e^0}{n_i^0}\frac{1}{\omega_2^2-\omega_{ic}^2}}, \tag{6.33}$$

where $\beta = 0.397\omega_{ip}^2\left(1-\frac{1}{\delta}\right)\left(\frac{a}{v_{et}}\right)\left(\frac{m_i}{m_e}\right)$ is the coupling parameter and if $\beta \to 0$ in Eq. (6.33), we can recover the expression in the absence of dust grains i.e., Eq. (6.14).

Using the same procedure as was done earlier, we solve Eq. (6.33) to get

$$\varepsilon_r = 1 - \frac{\omega_{ip}^2}{\omega_2^2-\omega_{ic}^2}\frac{p_{2n}^2}{p_{2n}^2+k_z^2} + \frac{\omega_{ep}^2}{v_{et}^2\left(p_{2n}^2+k_z^2 \right)} - \frac{\omega_{ip}^2}{\omega_2^2}\frac{k_z^2}{p_{2n}^2+k_z^2} + \beta G, \tag{6.34}$$

where

$$G = \frac{\eta\omega_{ip}^2}{\omega_2^2-\omega_{ic}^2}\frac{p_{2n}^2}{p_{2n}^2+k_z^2}\frac{1}{\omega^2+\eta^2}\frac{1}{\delta} - \frac{\eta\omega_{ip}^2}{\omega_2^2}\frac{k_z^2}{p_{2n}^2+k_z^2}\frac{1}{\omega^2+\eta^2}\frac{1}{\delta} - \frac{\omega\upsilon_e\omega_1\omega_{ep}^2}{k_z^2 v_{et}^4}\frac{1}{p_{2n}^2+k_z^2}\frac{1}{\omega^2+\eta^2}$$
$$- \frac{\eta\omega_{ep}^2}{v_{et}^2}\frac{1}{p_{2n}^2+k_z^2}\frac{1}{\omega^2+\eta^2}.$$

$$\varepsilon_i = \frac{\omega_{ep}^2 \upsilon_e \omega_1}{k_z^2 v_{et}^4 \left(p_{2n}^2 + k_z^2\right)}\left(1 - \frac{\beta\eta}{\omega^2+\eta^2}\right) + \frac{\beta\omega}{\omega^2+\eta^2}\frac{1}{\delta\left(p_{2n}^2+k_z^2\right)}\left(\frac{\omega_{ip}^2 p_{2n}^2}{\omega_2^2 - \omega_{ic}^2} - \frac{\omega_{ip}^2 k_z^2}{\omega_2^2}\right) + \frac{\beta\omega\omega_{ep}^2}{\omega^2+\eta^2}\frac{1}{v_{et}^2\left(p_{2n}^2+k_z^2\right)}. \tag{6.35}$$

Following the same method as was done in Case I, the real frequency expression is given as

$$\omega_r = k_\theta v_E + \sqrt{\omega_{ic}^2 + c_s^2\left(p_{2n}^2 + k_z^2\right) + \frac{\beta Z_d (p_{2n}^2 + k_z^2) c_s^2}{n_e^0 \pi a^2 \nu_{et}}}, \tag{6.36}$$

where Z_d is the dust charge state.

Equation (6.36) represents the real frequency of the instability in the presence of a transverse dc electric field with dust. If $\beta \to 0$ in Eq. (6.36) we retrieve the expression of real frequency without dust, i.e., Eq. (6.24).

The expression for growth rate can be obtained by solving Eqs. (6.21) and (6.35),

$$\gamma = \frac{-1}{2}\frac{\left(\frac{\upsilon_e\left\{1 - k_z v_{ed}\left(1+R\right)\right\}}{k_z^2 v_{et}^4}\frac{m_i}{m_e}\frac{1}{\delta} - \beta N\right)\left[\left(\omega_r - k_\theta v_E\right)^2 - \omega_{ic}^2\right]^2}{\left(\omega_r - k_\theta v_E\right)\left(p_{2n}^2 - \frac{\beta}{\eta}M\right)}, \tag{6.37}$$

where $N = N_1 - N_2$;

$$N_1 = \frac{\eta\upsilon_e\left\{1 - k_z v_{ed}\left(1+R\right)\right\}}{k_z^2 v_{et}^4}\frac{m_i}{m_e}\frac{1}{\delta(\omega_r^2+\eta^2)} + \frac{\omega_r p_{2n}^2}{(\{\omega_r - k_\theta v_E\}^2 - \omega_{ic}^2)}\frac{1}{\delta(\omega_r^2+\eta^2)}.$$

$$N_2 = \frac{\omega_r k_z^2}{(\omega_r - k_\theta v_E)^2}\frac{1}{\delta(\omega_r^2+\eta^2)} + \frac{\omega_r}{\delta(\omega_r^2+\eta^2)v_{et}^2}\frac{m_i}{m_e}.$$

$$M = \frac{[(\omega_r - k_\theta v_E)^2 - \omega_{ic}^2]^2}{(\omega_r^2+\eta^2)\delta}(M_1 + M_2 + M_3),$$

here, $M_1 = \eta^2 p_{2n}^2[(\omega_r - k_\theta v_E)^2 - \omega_{ic}^2]^2 + \frac{\omega_r \eta^2 p_{2n}^2}{(\omega_r^2+\eta^2)(\omega_r - k_\theta v_E)} + \frac{\eta^2 k_z^2}{(\omega_r - k_\theta v_E)^4}$.

$$M_2 = \frac{\omega_r \eta^2 k_z^2}{(\omega_r^2+\eta^2)(\omega_r - k_\theta v_E)^3} + \frac{k_z^2 \eta \delta(\omega_r^2+\eta^2)}{\beta(\omega_r - k_\theta v_E)^4} + \frac{\omega_r \eta^2 m_i}{(\omega_r^2+\eta^2)(\omega_r - k_\theta v_E) m_e v_{et}^2}.$$

$$M_3 = \frac{\upsilon_e \eta m_i (2\omega_r - k_\theta v_E - k_z v_{ed})}{2k_z^2 v_{et}^4 m_e (\omega_r - k_\theta v_E)} + \frac{\omega_r^2 \upsilon_e \eta m_i (\omega_r - k_\theta v_E - k_z v_{ed})}{k_z^2 v_{et}^4 m_e (\omega_r^2+\eta^2)(\omega_r - k_\theta v_E)}.$$

Equation (6.37) represents the growth rate of IEDDI with the inclusion of dust in the presence of a transverse dc electric field. If $\beta \to 0$ in Eq. (6.37) we retrieve the expression of growth rate without dust, i.e., Eq. (6.25).

6.3 RESULTS AND DISCUSSION

In this chapter, the analytical model has been developed in a collisional magnetized plasma cylinder to study the IEDDI with negatively charged dust grains while incorporating an electric field using the fluid theory in the presence and absence of dust particles. The developed model aims to analyse the relationship between various plasma parameters, i.e., real frequency, growth rate etc. The effect of the electric field, magnetic field and relative density ratio on the instability is studied in both the cases. The equations that hold accountable for IEDDI in Sec. 6.2 are used to calculate the frequency and the rate of growth for the same. The graphs have been plotted using the MATLAB programme for the analytically solved equations i.e., for real frequency and the growth rate. The modified plasma parameters used in our calculation are obtained from Koepke et al. [15, 38] experimental papers are tabulated in Table 6.2.

Figures 6.2 (a) and (b) portray the plot of normalized real frequency and growth rate in the absence of dust grains as a function of the gyro-radius parameter. From Figure 6.2 (a), it can be inferred that with the increase in the gyro-radius parameter, the frequency of the instability increases. From Figure 6.2 (b), it can be observed from the graph that with an increase in values of the gyro-radius parameter, the rate of growth of the instability first augments and then attains a maximum value, i.e., $\gamma = 3.2\times10^5$ sec^{-1} for $b_i = 0.08$. After attaining maximum value, the instability's growth rate decreases. Moreover, it can also be observed that the normalized growth rate of instability decreases by a factor of ~3.8 when gyroradius changes from 0.2 to 0.6 whereas in the experimental observation of Koepke et al. [38], it upsurges by a factor of ~3. This result is in good agreement with this experimental observation.

Table 6.2: Plasma parameters are specified in this model.

Terms	Values
e (Electronic charge)	$4.8\times10^{-10}\,statcoul$
Q_d^0 (Dust charge)	$\left(10^3-10^4\right)e$
m_d (Dust mass)	$10^{12}\times1.67\times10^{-24}\,gm$
m_e (Electron mass)	$9.1\times10^{-28}\,gm$
m_i (Ion mass)	$22\times1.67\times10^{-24}\,gm$
T_e (Electron temperature)	$0.2\ eV$
T_i (Ion temperature)	$0.2\ eV$
n_i^0 (Initial ion density)	$10^9\,cm^{-3}$
n_e^0 (Initial electron density)	$\left(1\times10^9-0.2\times10^9\right)cm^{-3}$
n_d^0 (Dust density)	$(1-5)\times10^4\,cm^{-3}$
c (Speed of light)	$3\times10^{10}\,cm/\mathrm{s}$
B (Magnetic field)	$\left(0.1-4.5\right)kG$
$\delta\left(=n_i/n_e\right)$ (Relative density ratio)	$1-10$
$b_i(=k_\theta\rho_i)^2$ (Gyro-radius parameter)	$0-0.9$
K (Boltzmann constant)	$1.38\times10^{-16}\,erg/Kel$
k_z	$0.65\ cm^{-1}$
k_θ	$2.8\ cm^{-1}$
υ_e (Electron collisional frequency)	$3.22\times10^8\,\mathrm{sec}^{-1}$
v_{ed} (Electron drift velocity)	$1.76\times10^4\,cm/\mathrm{sec}$
v_E (Electric field)	$3.3\times10^8/B(Gauss)$
r_0 (Plasma radius)	$3\ cm$
a (Dust grain size)	$(1-5)\times10^{-4}\,cm$

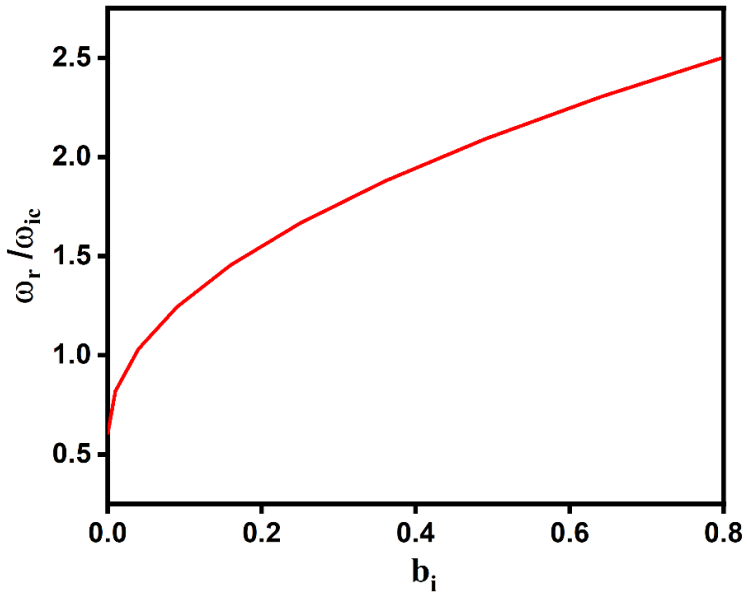

Figure 6.2 (a): Variation in normalized real frequency ω_r/ω_{ic} with the finite gyro-radius parameter $b_i(=k_\theta\rho_i)^2$ of IEDDI in the absence of dust grains.

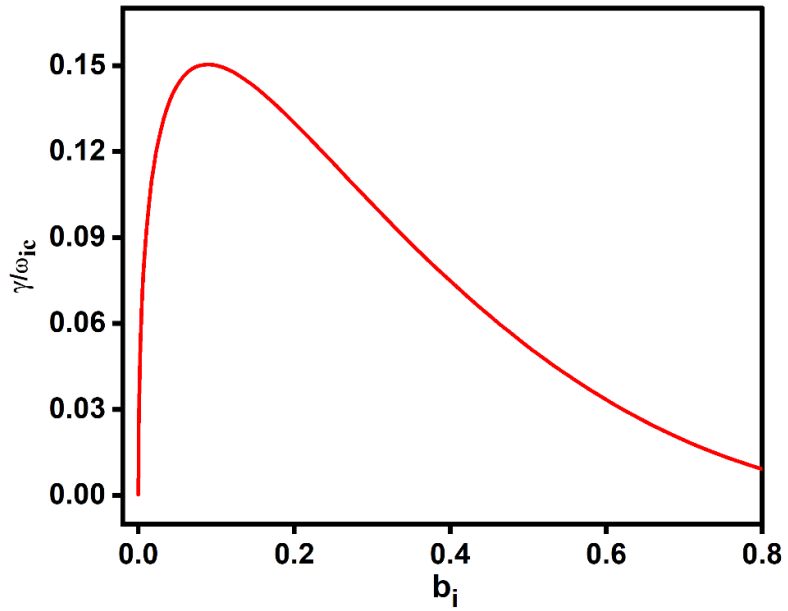

Figure 6.2 (b): Variation in normalized growth rate γ/ω_{ic} with the finite gyro-radius parameter $b_i(=k_\theta\rho_i)^2$ of IEDDI in the absence of dust grains.

Figures 6.2 (a) and (b) portray the plot of normalized real frequency and growth rate in the absence of dust grains as a function of the gyro-radius parameter. From Figure 6.2 (a), it can be inferred that with the increase in the gyro-radius parameter, the frequency of the instability

increases. From Figure 6.2 (b), it can be observed from the graph that with an increase in values of the gyro-radius parameter, the rate of growth of the instability first augments and then attains a maximum value, i.e., $\gamma = 3.2\times10^{5}$ sec^{-1} for $b_i = 0.08$. After attaining maximum value, the instability's growth rate decreases. Moreover, it can also be observed that the normalized growth rate of instability decreases by a factor of ~3.8 when gyroradius changes from 0.2 to 0.6 whereas in the experimental observation of Koepke et al. [38], it upsurges by a factor of ~3. This result is in good agreement with this experimental observation.

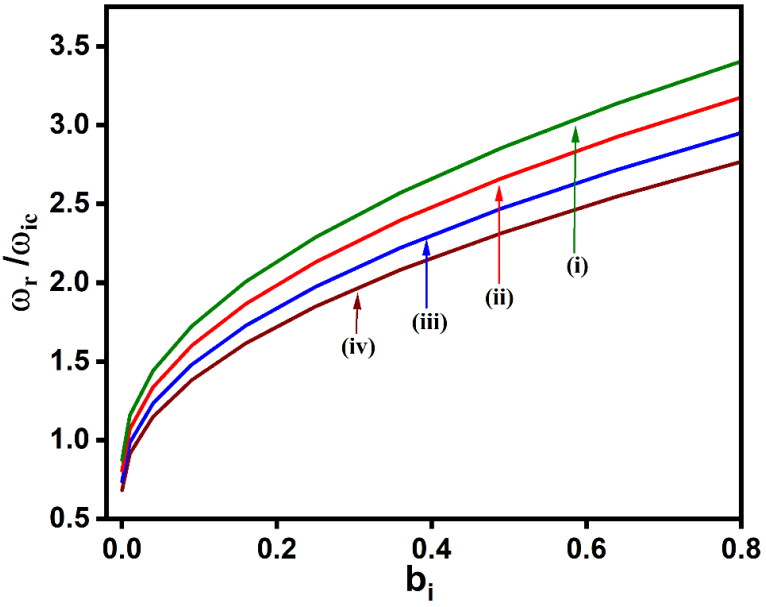

Figure 6.3 (a): The normalized real frequency ω_r/ω_{ic} variation for different values of $\delta\left(=n_i^0/n_e^0\right)$, i.e., (i) $\delta=8$, (ii) $\delta=6$, (iii) $\delta=4$, and (iv) $\delta=2$ corresponding to the finite gyro-radius parameter $b_i(=k_\theta\rho_i)^2$ in the presence of dust.

In the presence of dust grains, the normalized real frequency variation corresponding to the gyro-radius parameter has been plotted in Figure 6.3 (a) for different sets of relative density ratios, respectively. Figure 6.3 (a) represents the normalized real frequency plot versus gyro-radius parameter for various relative density ratio i.e., (i) $\delta=8$, (ii) $\delta=6$, (iii) $\delta=4$, and (iv) $\delta=2$.With the increase in the gyro-radius parameter, the instability frequency augments. Moreover, with the rise in relative density ratio, the frequency also augments.

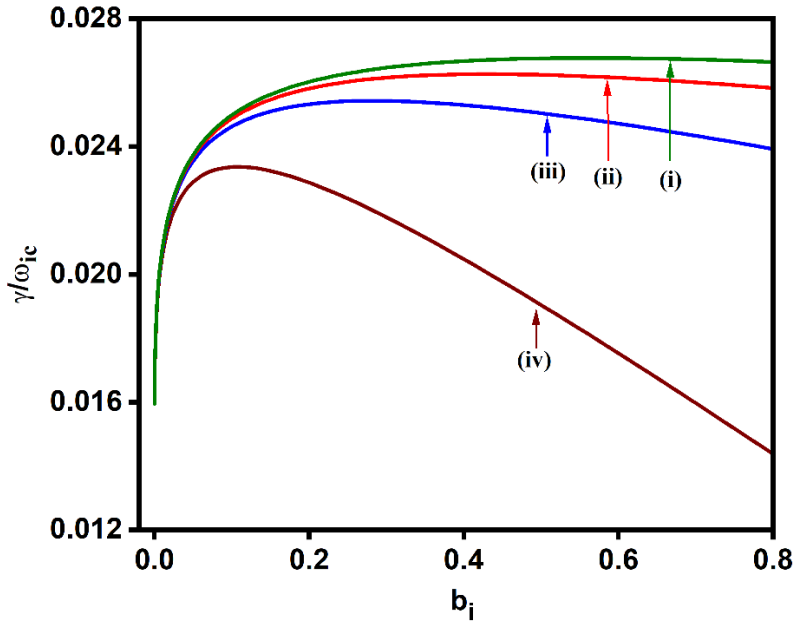

Figure 6.3 (b): The normalized growth rate γ/ω_{ic} variation for different values of $\delta\left(=n_i^0/n_e^0\right)$, i.e., (i) $\delta=8$, (ii) $\delta=6$, (iii) $\delta=4$, and (iv) $\delta=2$ in the existence of dust corresponding to the finite gyro-radius parameter $b_i(=k_\theta\rho_i)^2$.

In the presence of dust grains, the normalized growth rate variation corresponding to the gyro-radius parameter has been plotted in Figure 6.3 (b) for different sets of relative density ratios, respectively. Figure 6.3 (b) represents the normalized growth rate plot versus the gyro-radius parameter for various relative density ratio, i.e., (i) $\delta=8$, (ii) $\delta=6$, (iii) $\delta=4$, and (iv) $\delta=2$. From the plot, it can be noted that the growth rate value rises with increasing gyro-radius parameter until they reach their peak value, after which there is a decline in magnitude for all values of the relative density ratio. Hence, we can say that there is a significant decrease in the growth rate by a factor of ~ 6.5 as dust grains included for $\delta = 4.0$ as compared with the growth rate without the dust grains in the above-mentioned graph. In addition, with the rise in the relative density ratio, the instability growth rate augments and the decline in magnitude becomes less sharp. We can conclude that after the inclusion of dust particles, both real frequency and growth rate follows the similar trend as in the case of absence of the dust in spite of slight modifications in their values.

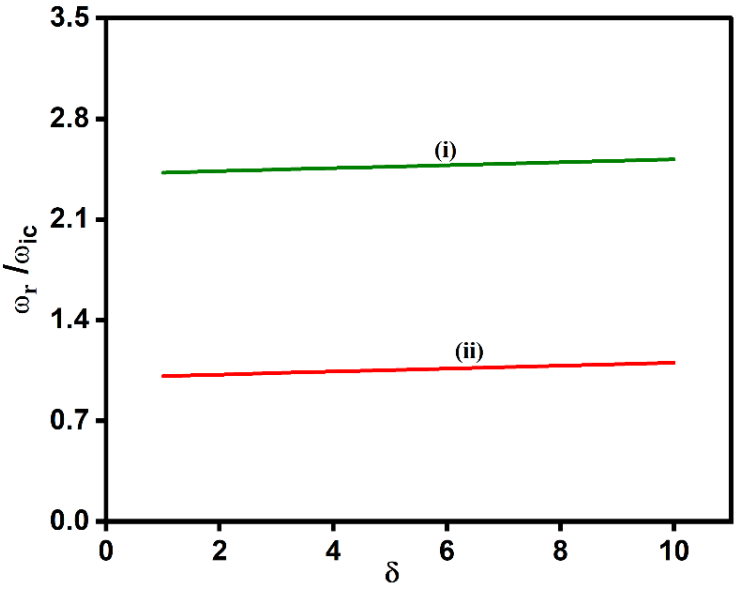

Figure 6.4 (a): The normalized real frequency of IEDDI as a function of relative density ratio $\delta\left(=n_i^0/n_e^0\right)$ (i) in the electric field presence and (ii) in the electric field absence.

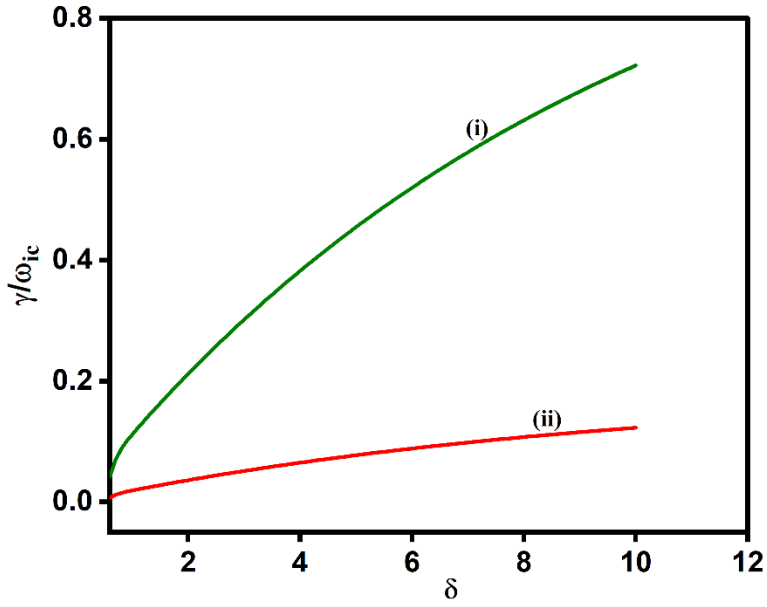

Figure 6.4 (b): Variation in the normalized growth rate γ/ω_{ic} with relative density ratio $\delta\left(=n_i^0/n_e^0\right)$ in the (i) presence and (ii) absence of an electric field.

In the existence and non-existence of a dc electric field, Figures 6. 4 (a) and (b) illustrate the impact of normalized real frequency and growth rate on the relative density ratio of the instability. In the existence of dust charge variations, we observed that the normalized real

frequency and growth rate of IEDDI is in a linear relationship with respect to the $\delta\left(=n_i^0/n_e^0\right)$, and it can be verified from Eqs. (6.36) and (6.37). As the negatively charged dust grains augment in plasma, the real frequency and the growth rate of instability increase. It might be because as δ increases, the plasma density of electrons decreases relative to the plasma density of ions. For increasing values of δ, an ion's effective mass $m_{ieff}=\frac{m_i}{\delta}$ is smaller than m_i, and because of its higher mobility, the frequency and growth rate of the instability gets enhanced. It can also be compared from the graphs that the addition of an electric field enhanced the instability's real frequency and growth rate. The real frequency maximum value is measured at $\omega_r=1.64\times10^6\,rad/\sec$ when there is an electric field involved, and it drops to $\omega_r=7.2\times10^5\,rad/\sec$ as $v_E\to0$ in Eq. (6.36). The growth rate maximum value is estimated at $\gamma=3.5\times10^5\,\sec^{-1}$ when there is an electric field involved, and it drops to $\gamma=6.0\times10^4\,\sec^{-1}$ as $v_E\to0$ in Eq. (6.37). Therefore, we can infer that the frequency and rate of growth have slightly changed as an outcome of the addition of the electric field. This is due to the fact that the addition of an electric field generates $\vec{E}\times\vec{B}$ drift, which results in the doppler effect, and as a result, instability's real frequency augments.

Figure 6.5 (a) represents the growth rate variation with the k_z/k_θ for different values of v_E/v_{it} in the absence of dust. On increasing the values of k_z/k_θ, the growth rate increases significantly initially; after that, there is a bitsy change in the growth rate of IEDDI. Furthermore, with the increasing values of v_E/v_{it}, the growth rate augments. The trend of growth rate with k_z/k_θ follows the same trend as observed in experimental results of Ganguli [37] (cf. Figure 5). Figure 6.5 (b) shows the growth rate variation with the k_z/k_θ for different values of v_E/v_{it} in the presence of dust using Eq. (6.37). With increasing k_z/k_θ values, the growth rate of IEDDI follows the same increasing trend similar to the case of without dust. But the value of growth rate degrades after the introduction of dust grains when compared to the value of growth rate without dust grains. Furthermore, there is also rise in the value of growth rate with the increasing values of v_E/v_{it}.

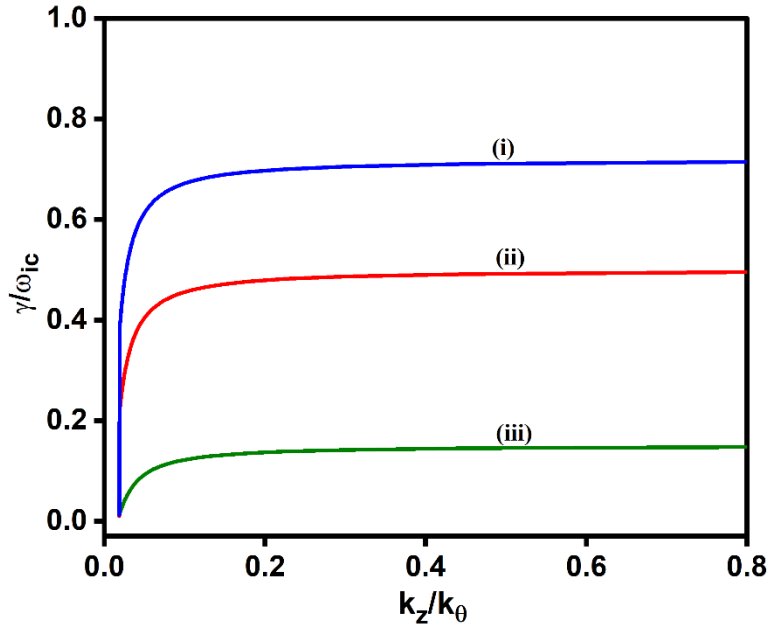

Figure 6.5 (a): The normalized growth rate γ/ω_{ic} versus normalized wave vector k_z / k_θ of IEDDI for varying values of the electric field v_E / v_{it}, i.e., (i) v_E / v_{it}=5.5 (ii) v_E / v_{it}=3.5 and (iii) v_E / v_{it}=2 in the absence of dust.

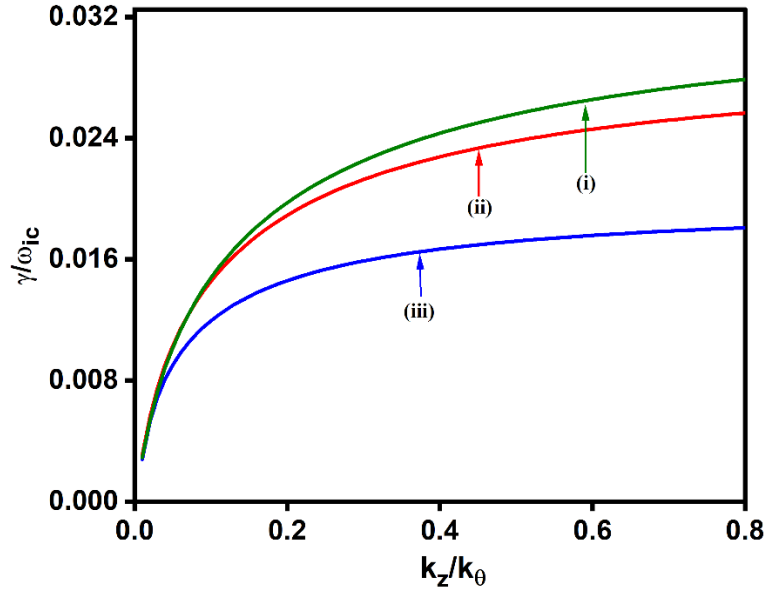

Figure 6. 5 (b): The normalized growth rate as a function of the normalized wave vector k_z / k_θ of IEDDI for different values of the electric field v_E / v_{it}, i.e., (i) v_E / v_{it}=5.5 (ii) v_E / v_{it}=3.5 and (iii) v_E / v_{it}=2 in the presence of dust.

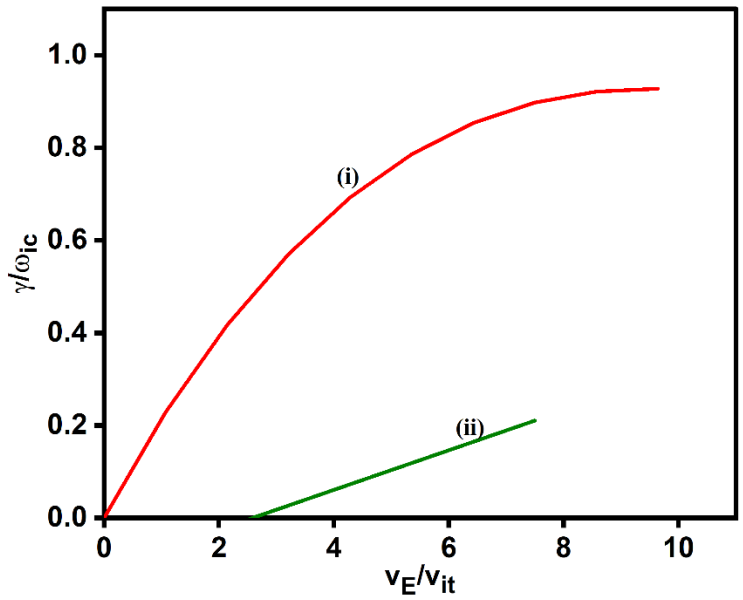

Figure 6.6: The normalized growth rate γ/ω_{ic} with respect to transverse dc electric field v_E / v_{it} of IEDDI for (i) existence of dust grains, and (ii) non-existence of dust grains.

We have also portrayed the growth rate graph in Figure 6.6. as a function of v_E / v_{it} in the occurrence and non-occurence of dust particles. As we increase v_E / v_{it}, the growth rate of the instability increases in both the cases. In the presence of dust charge variations, the rate of increment of instability's growth rate is small while the rate of increment of growth rate is more in the absence of dust. It can be concluded from this graph that the absence of dust charge fluctuations enhances the growth rate of IEDDI. The growth rate graph displays a trajectory that is consistent with the observed trend described in the experimental investigation done by Ganguli et al. [37] (cf. Figure 3) in the absence of dust grains.

Figure 6.7 portrays the variation of normalized frequency with respect to v_E / v_{it} in the absence of dust grain particles. It can be noticed that with the increasing magnitude of radial electric field strength, the IEDDI growth rate increases. This is ascribed to the fact that if $\vec{E} \times \vec{B}$ drift is there, then the effects of doppler shift may result in IEDDI to grow. Our theoretical result is in good agreement with the experimental observation of Ganguli [37] (cf. Figure 6).

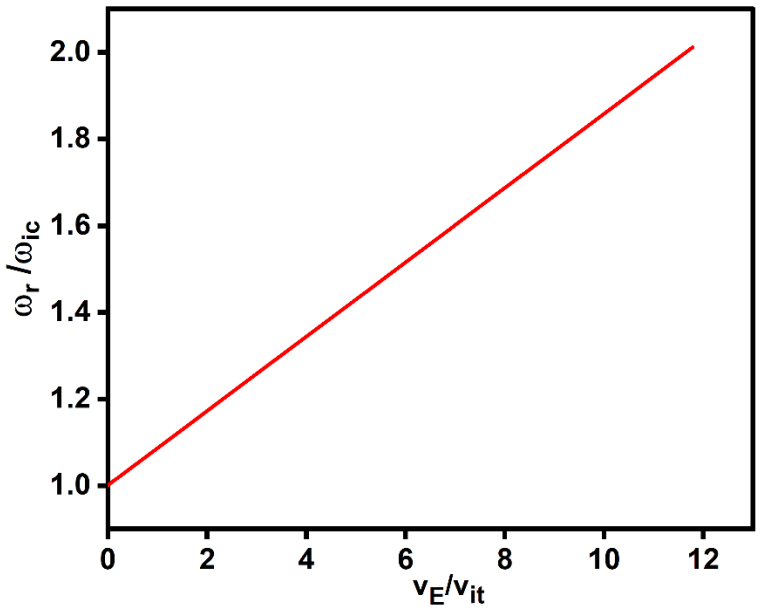

Figure 6.7: The normalized real frequency ω_r/ω_{ic} versus v_E/v_{it} of IEDDI in the absence of dust.

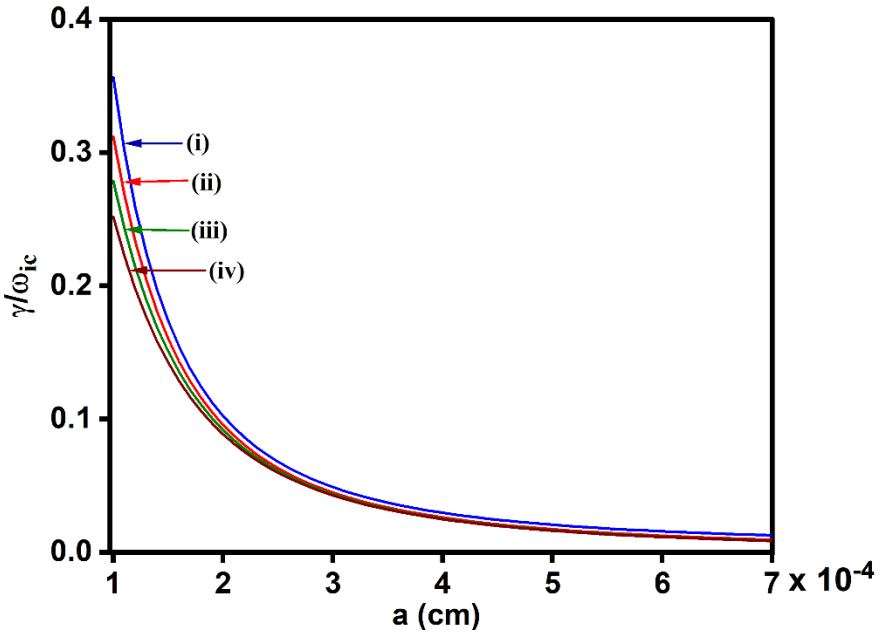

Figure 6.8: The normalized growth rate γ/ω_{ic} variation for different values of $\delta\left(=n_i^0/n_e^0\right)$, i.e., (i) $\delta=8$, (ii) $\delta=6$, (iii) $\delta=4$, and (iv) $\delta=2$ corresponding to the dust grain size $a(cm)$ of IEDDI.

Figure 6.8 shows the dust grain size variation with respect to the normalized growth rate for varying values of relative density ratio. The graph shows that, as predicted by Eq. (6.37), the size of the dust grains has an inverse relationship with the normalized growth rate. This is because the intergrain distance decreases with the increment in dust grain size, which in turn increases the screening of one dust particle charge over another, further lowering the dust grain potential. Because of this, the average dust grain charge Q_d^0 starts to fall, resulting in the instability's growth rate decline. It is also possible to deduce from Eqs. (6.37) to (6.26) how the dust particles affect the growth rate of the instability. Two parameters are involved in these equations: η, the dust charging rate and other one is β, the coupling parameter, or the interaction between the plasma and dust particles. Furthermore, with increasing values of δ, the instability rate of growth augments.

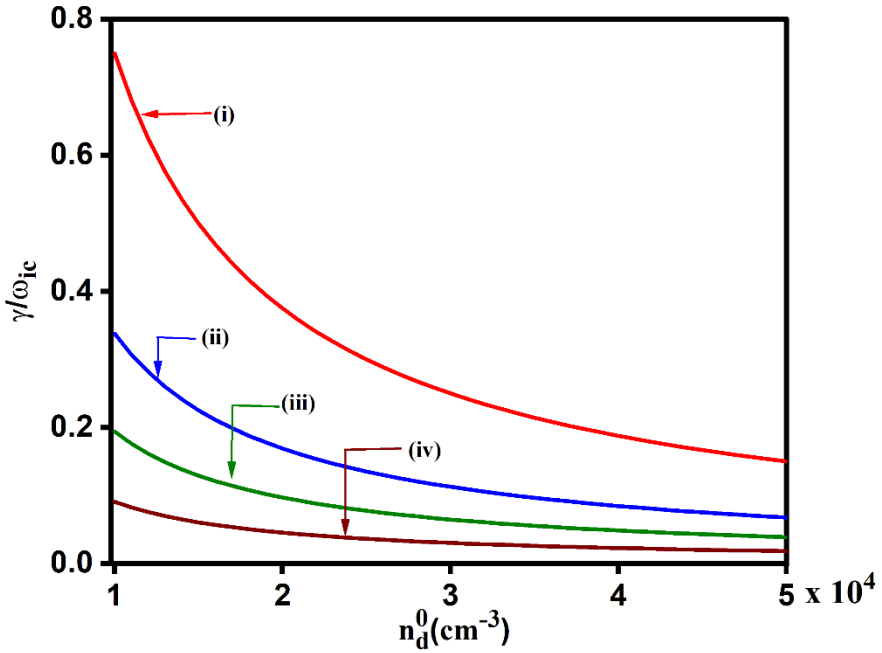

Figure 6.9: The normalized growth rate γ/ω_{ic} variation for different values of dust grain size $a(cm)$, i.e., (i) $a=2\times10^{-4}cm$, (ii) $a=3\times10^{-4}cm$, (iii) $a=4\times10^{-4}cm$, and (iv) $a=6\times10^{-4}cm$ with respect to the dust grains $n_d^0\left(cm^{-3}\right)$ number density.

The normalized growth rate graph versus the dust number density for varying values of dust size is illustrated in Figure 6.9. It is found that as the dust particle number density rises, the rate of growth of the instability decreases. This is because the number of available electrons per dust

grain reduces as the quantity of dust particles rises, revealing that the total demand for electrons among the dust particles is enormous. Reduced average dust grain charge Q_d^0 causes a drop-in growth rate of the instability. In addition to this, from Figure 6.9, we can see that with the increasing values of the size of the dust grains, the growth rate reduces, as explained by Figure 6.8. For dust density greater than $3\times10^4 cm^{-3}$, the growth rate is not majorly influenced by the number density of the dust grains.

There are currently no theoretical findings in the literature that takes into account how dust particles affect IEDDI. As a result, our theoretical findings are crucial for comprehending and illuminating the significance of the number density and dust grain size of the dust particles in the IEDDI.

6.4 CONCLUSION

The IEDDI in the collisional magnetized plasma cylinder under the outcome of electric field has been observed. Study of absence and presence of dust grains has been studied for various plasma parameters like gyro-radius, relative density ratio etc. It was concluded that the inclusion of dust particles has altered the behaviour of IEDDI i.e., with the increasing values of dust grain size and dust density, the growth rate of instability decreases. The gyro-radius augments with an increase in relative density ratio. Moreover, the instability's real frequency and growth rate also augment with an augment in the relative density ratio and wave vector. The impact of the gyro-radius parameter on the frequency and the growth rate of instability was also examined. It was discovered that the frequency grows as the gyro-radius parameter augments, but the rate of growth first rises as the gyroradius parameter augments before starting to fall as the gyroradius parameter further augments. The outcome of an electric field on the frequency and rate of growth are also considered, and it was found that with the addition of an electric field, frequency and rate of growth both rises. The acquired results were compared to the already available experimental observations [15, 37] and a good agreement was found.

The outcomes of our analytical model can be used to explain a wide range of experiments including AMICIST [62], SCIFER [63], and ALEXIS [64] in Earth's ionosphere, and might be beneficial for other space applications [18]. For ionospheric issues connected to broadband electrostatic wave measurements, the use of the IEDDI mechanism is of special relevance [51].

REFERENCES

[1] N.J.P. D'Angelo, *Space Science*, **38**, 1143 (1990).

[2] P.K. Shukla, *Physics of Plasmas* **8**, 1791 (2001).

[3] P.K. Shukla, A.A. Mamun, Introduction to Dusty Plasma Physics, *CRC Press* (2015).

[4] V. Gavrishchaka, M.E. Koepke, G. Ganguli, *Physics of Plasmas* **3**, 3091 (1996).

[5] F. Schmidt, F. Muecksch, Y. Weisblum, J. Da Silva, E. Bednarski, A. Cho, Z. Wang, C. Gaebler, M. Caskey, M.C. Nussenzweig, *New England Journal of Medicine* **386**, 599 (2022).

[6] M.E. Koepke, *Physics of Plasmas* **9**, 2420 (2002).

[7] M.E. Koepke, W.E. Amatucci, *IEEE Transactions on Plasma Science* **20**, 631 (1992).

[8] S.C. Sharma, M. Sugawa, V.K. Jain, *Physics of Plasmas* **7**, 457 (2000).

[9] J. Sharma, S.C. Sharma, V.K. Jain, A. Gahlot, *Physics of Plasmas* **20**, 033706 (2013).

[10] M.E. Koepke, J.J. Carroll Iii, M.W. Zintl, *Physics of Plasmas* **5**, 1671 (1998).

[11] W.E. Amatucci, D.N. Walker, G. Ganguli, D. Duncan, J.A. Antoniades, J.H. Bowles, V. Gavrishchaka, M.E. Koepke, *Journal of Geophysical Research: Space Physics* **103**, 11711 (1998).

[12] J. Sharma, S.C. Sharma, *Physics of Plasmas* **17**, 123701 (2010).

[13] K.R. Segwal, S.C. Sharma, *IEEE Transactions on Plasma Science* **46**, 775 (2018).

[14] S. Seiler, M. Yamada, H. Ikezi, *Physical Review Letters* **37**, 700 (1976).

[15] M.E. Koepke, W.E. Amatucci, J.J. Carroll Iii, T.E. Sheridan, *Physical Review Letters* **72**, 3355 (1994).

[16] A.M. DuBois, E. Thomas Jr, W.E. Amatucci, G. Ganguli, *Physical Review Letters* **111**, 145002 (2013).

[17] M.E. Koepke, J.J. Carroll Iii, M.W. Zintl, *Journal of Geophysical Research: Space Physics* **104**, 14397 (1999).

[18] A.A. Chernyshov, A. Spicher, A.A. Ilyasov, W.J. Miloch, L.B.N. Clausen, Y. Saito, Y. Jin, J.I. Moen, *Physics of Plasmas* **25**, 042902 (2018).

[19] D.A. Mendis, M. Rosenberg, *Annual Review of Astronomy and Astrophysics* **32**, 419 (1994).

[20] J. Glanz, *Science* **264**, 28 (1994).

[21] R.L. Merlino, J.A. Goree, *Physics Today* **57**, 32 (2004).

[22] R.L. Merlino, *Plasma Physics Applied* **81**, 73 (2006).

[23] J. Winter, *Physics of Plasmas* **7**, 3862 (2000).

[24] S.H. Kim, J.R. Heinrich, R.L. Merlino, *Planetary and Space Science* **56**, 1552 (2008).

[25] A. Barkan, N. D'Angelo, R.L. Merlino, *Planetary and Space Science* **43**, 905 (1995).

[26] R.L. Merlino, A. Barkan, C. Thompson, N. D'Angelo, *Physics of Plasmas* **5**, 1607 (1998).

[27] R.L. Merlino, A. Barkan, C. Thompson, N. D'Angelo, *Plasma Physics and Controlled Fusion* **39**, A421 (1997).

[28] J. Sharma, S.C. Sharma, *Contributions to Plasma Physics* **62**, e202200073 (2022).

[29] K.R. Segwal, S.C. Sharma, *IEEE Transactions on Plasma Science* **46**, 797 (2018).

[30] S.C. Sharma, M. Sugawa, *Physics of Plasmas* **6**, 444 (1999).

[31] J. Sharma, S. Singh, A. Kumar, M.A. Hossain, S.H. Ahammad, A.N.Z. Rashed, *Brazilian Journal of Physics* **53**, 128 (2023).

[32] L. Chen, Waves and Instabilities in Plasmas, *World Scientific* (1987).

[33] J. Tyagi, S. Singh, H.K. Malik, *Journal of Theoretical and Applied Physics* **12**, 39 (2018).

[34] H.K. Malik, J. Tyagi, D. Sharma, *AIP Advances* **9**, (2019).

[35] J. Tyagi, D. Sharma, H.K. Malik, *Journal of Theoretical and Applied Physics* **12**, 227 (2018).

[36] M.E. Koepke, W.E. Amatucci, J.J. Carroll Iii, V. Gavrishchaka, G. Ganguli, *Physics of Plasmas* **2**, 2523 (1995).

[37] G. Ganguli, *Physics of Plasmas* **4**, 1544 (1997).

[38] M.E. Koepke, J.J. Carroll Iii, M.W. Zintl, C.A. Selcher, V. Gavrishchaka, *Physical Review Letters* **80**, 1441 (1998).

[39] J.J. Carroll Iii, Experimental Investigation of the IEDD Instability, West Virginia University (1997).

[40] S.C. Sharma, K. Sharma, A. Gahlot, *Physics of Plasmas* **20**, 053704 (2013).

[41] B.P. Pandey, S.V. Vladimirov, A. Samarian, *Physics of Plasmas* **16**, 113708 (2009).

[42] A.A. Galeev, M.N. Rosenbluth, R.Z. Sagdeev, R.N. Sudan, Handbook of Plasma Physics (1983).

[43] A.A. Ilyasov, A.A. Chernyshov, M.M. Mogilevsky, I.V. Golovchanskaya, B.V. Kozelov, *Physics of Plasmas* **22**, 032906 (2015).

[44] Y. Liu, J. Lei, M. Li, Y. Ling, J. Yuan, *Physics of Plasmas* **25**, 102901 (2018).

[45] Munish, R. Dhawan, R. Kumar, H.K. Malik, *Journal of Taibah University for Science* **16**, 725 (2022).

[46] M. Rosenberg, P.K. Shukla, *Planetary and Space Science* **51**, 1 (2003).

[47] R. Dhawan, D. Sharma, H.K. Malik, *Journal of Theoretical and Applied Physics* **16**, 1 (2022).

[48] W.E. Amatucci, M.E. Koepke, J.J. Carroll Iii, T.E. Sheridan, *Geophysical Research Letters* **21**, 1595 (1994).

[49] G. Ganguli, Y.C. Lee, P.J. Palmadesso, *The Physics of Fluids* **31**, 823 (1988).

[50] G. Ganguli, P. Palmadesso, Y.C. Lee, *Geophysical Research Letters* **12**, 643 (1985).

[51] G. Ganguli, M.J. Keskinen, H. Romero, R. Heelis, T. Moore, C. Pollock, *Journal of Geophysical Research: Space Physics* **99**, 8873 (1994).

[52] K.I. Nishikawa, G. Ganguli, Y.C. Lee, P.J. Palmadesso, *Journal of Geophysical Research: Space Physics* **95**, 1029 (1990).

[53] T. Chang, G.B. Crew, J.R. Jasperse, Physics of Space Plasmas (1987): Proceedings of the 1987 Cambridge Workshop in Geoplasma Physics, Ionosphere-Magnetosphere-Solar Wind Coupling Processes, *Scientific Publishers* (1988).

[54] G. Ganguli, Y.C. Lee, P. Palmadesso, *The Physics of Fluids* **28**, 761 (1985).

[55] V.V. Gavrishchaka, M.E. Koepke, G.I. Ganguli, *Journal of Geophysical Research: Space Physics* **102**, 11653 (1997).

[56] W.E. Amatucci, D.N. Walker, G. Ganguli, J.A. Antoniades, D. Duncan, J.H. Bowles, V. Gavrishchaka, M.E. Koepke, *Physical Review Letters* **77**, 1978 (1996).

[57] N.A. Krall, A.W. Trivelpiece, *American Journal of Physics* **41**, 1380 (1973).

[58] E.C. Whipple, T.G. Northrop, D.A. Mendis, *Journal of Geophysical Research: Space Physics* **90**, 7405 (1985).

[59] M.R. Jana, A. Sen, P.K. Kaw, *Physical Review E* **48**, 3930 (1993).

[60] R.K. Varma, P.K. Shukla, V. Krishan, *Physical Review E* **47**, 3612 (1993).

[61] M.S. Barnes, J.H. Keller, J.C. Forster, J.A. O'Neill, D.K. Coultas, *Physical Review Letters* **68**, 313 (1992).

[62] J. Bonnell, P. Kintner, J.E. Wahlund, K. Lynch, R. Arnoldy, *Geophysical Research Letters* **23**, 3297 (1996).

[63] P.M. Kintner, J. Bonnell, R. Arnoldy, K. Lynch, C. Pollock, T. Moore, *Geophysical Research Letters* **23**, 1873 (1996).

[64] A.M. DuBois, E. Thomas Jr, W.E. Amatucci, G. Ganguli, *Journal of Geophysical Research: Space Physics* **119**, 5624 (2014).

7

CONCLUSION AND FUTURE PROSPECTIVE

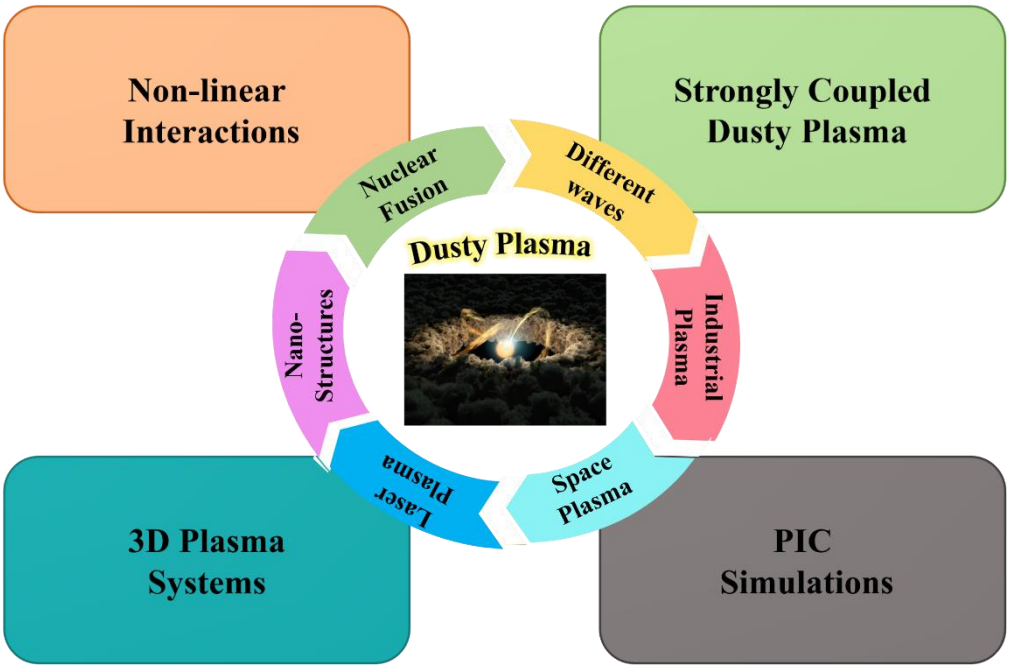

The main aim of this chapter is to summarize the key observations, revelations, and conclusions that have emerged during the research. This chapter also includes chapter-specific summaries. We will explore the future prospects and directions that have been disclosed as a result of the research in the following sections of this chapter, which will be a vital platform for us.

7.1 Conclusion

In the framework of this thesis, the theoretical modelling of electrostatic waves in a magnetized dusty plasma has been elucidated. The research conducted for the current thesis intends to advance knowledge of the phenomena of wave propagation in dusty plasma and the consequent effect on the growth of the wave and instabilities. By virtue of the findings in the aforementioned chapters, it can be concluded that dust in ambient plasma not only creates a fresh collective phenomenon but also modifies an already-existing phenomenon. The introduction of dust changes the dispersion characteristics of the waves. Besides this, the effect of the transverse direct current electric field has also been studied. The main objective of this thesis is to obtain the analytical expressions governing the dynamics of the waves and instabilities and their effect on different plasma parameters like the gyroradius parameter, temperature, relative density ratio etc. For this motive, various theoretical model has been proposed in the magnetized dusty plasma. Moreover, some of these models have been studied in the collisionless and collisional plasma and the effect of collisions has also been investigated with different plasma parameters. A free energy source or an external ion/electron beam tends to excite different waves and instabilities in the dusty plasma. The findings obtained from the analytical models show strong agreement with both theoretical predictions and the experimental data put forth by several researchers. Our findings set forth in this thesis may be expected to have a strong impact on the applications of space and fusion plasmas. The findings obtained from this thesis have been concluded as follows:

- Firstly, the LHWs excitation has been examined by electron beam using the kinetic treatment in a magnetized dusty plasma. The electrostatic LHWs via Cerenkov interaction are driven to instability and the dispersion relation has been inferred. It has been investigated the impact of dust grain size on the excitation of LHWs. The growth rate and the frequency of LHWs augments with the relative density ratio. The growth rate and frequency of the LHWs decrease as the size of the dust grain increases. The critical drift velocity for mode excitation decreases as the relative density ratio of dust grains increases, resulting in an increase in the phase velocity. Furthermore, it was shown that the growth rate of the unstable mode is proportional to the one-half power of the density of the beam and increases with beam density. LHWs can be studied in tokamak plasmas, lunar dusty plasma and have recently received significant attention for affecting the current drive at a very high density.

- Then we developed the model for current-driven EICWs in a magnetized dusty plasma in the existence of a transverse dc electric field, and the frequency, growth rate, and other parameters of the EIC waves have been investigated. From the study of the growth rate and frequency of the waves, it was found that growth rate and frequency first increase with the increase in finite gyroradius parameter and then start decreasing with the gyroradius parameter in the presence and absence of an electric field. With the increase in relative density of negatively charged dust grains, both the growth rate and frequency of the EIC mode increase. The critical drift plays a vital role in the excitation of the mode, and it was found that with an augment in relative density ratio, the critical drift reduces. It was also observed that the magnetic field is directly proportional to both the growth rate and frequency of the waves. The frequency and critical drift are found to increase with an augment in electron to ion temperature ratio while the growth rate decreases with an augment in temperature ratio. It was observed that in spite of the small effect of dust grains on EIC waves, it modifies the properties of EIC waves. The growth rate of the wave decreases as the dust grains number density increases. The presence of an electric field enhances the amplitude of frequency and the growth rate. The present work has various applications in space and planetary systems, e.g., in the study of the magnetosphere of Uranus.
- The same model as before has been extended further in this thesis, but in the collisional magnetized dusty plasma. The presence of collisions as a whole change the dispersion relation (frequency and the growth rate) and the dynamics of the wave. The effect of collisions on the various plasma parameters has been studied. The impact of the gyro-radius parameter on the frequency and the growth rate of a wave for varying electron and ion collision frequencies was also examined and it has been found that the effect of an electron collision destabilizes the mode whereas the effect of an ion collision stabilizes the mode and the growth rate. The real frequency and growth rate augment with an augment in the relative density ratio. It was also discovered that as the relative density ratio rises, the critical drift reduces, which is essential for the mode's excitation. As the electron to ion temperature ratio rises, both the critical electron drift velocity and frequency rise and the growth rate reduces. It was also examined that with the increasing values of dust density, the growth rate of the wave decreases. The present work can be applied in various fields including fusion energy research, tokamak and plasma heating.

- After showing the effect of collisions on EICWs in a magnetized dusty plasma in the previous chapter, an analytical model has been proposed in the collisional plasma driven by an ion beam in the presence of a dc electric field using the kinetic treatment. The effect of an ion beam has been examined for various plasma parameters on the instability. It was found that with an increase in wave number and beam velocity, the frequency of the wave increases. The frequency and phase velocity of the wave augments with a rise in beam velocity and beam energy. The real frequency and growth rate augment with an augment in the relative density ratio. The impact of the gyro-radius parameter on the frequency and the growth rate of the wave for varying relative density ratio and ion collision frequencies was also examined. It has been found that the effect of an ion collision stabilizes the growth rate of instability. The frequency and velocity of the beam increase as the electron to ion temperature ratio increases. Our findings are sensitive to the dust particles and it was examined that with increasing values of dust density, the growth rate of the wave decreases. It was discovered that the growth rate amplitude was lower in collisional plasma than in the collisionless plasma because the collisions between neutrals and plasma particles reduce their collective oscillations, which over time causes their amplitudes to gradually decrease. The observed instability may be related to a bounded dusty plasma system and could be useful in space plasma physics.
- Finally, the IEDD instability in the collisional magnetized plasma cylinder under the outcome of an electric field has been observed. A comparative analysis of the instability has been done in the presence and absence of dust grains. It was concluded that the inclusion of dust particles has altered the behaviour of IEDD instability i.e., with the increasing values of dust grain size and dust density, the growth rate of instability decreases. The gyro-radius augments with an increase in relative density ratio. Moreover, the instability's real frequency and growth rate also augment with an augment in the relative density ratio and wave vector. The impact of the gyro-radius parameter was also examined and it was discovered that the frequency grows as the gyro-radius parameter augments, but the rate of growth first rises as the gyroradius parameter augments before starting to fall as the gyroradius parameter further augments. The addition of an electric field increases the frequency and growth rate. The outcomes of our analytical model can be used to explain a wide range of experiments in Earth's ionosphere, and might be beneficial for other space applications.

7.2 Future Prospective of the Present Work

The following are the potential ideas for discussion in the future regarding this present work:

- The present work is based on linear interactions between waves and the charged particles and this work can further be extended to nonlinear interactions and their impact on various waves and instabilities can be studied to analyse the plasma system.
- The model we have developed in the current work is based on analytical studies, but these models fell short of providing a thorough grasp of the large-scale complicated physical systems. Since such systems have a high degree of freedom, theoretical techniques are essentially impractical. As a result, computer simulations emerged as a potent tool for comprehending the behaviour of complex physical processes such as Particle-in-cell (PIC) Simulations. One can gain a more comprehensive knowledge of the behaviour of waves in a complicated system by including these simulations in our analytical model.
- The theoretical investigations can further be extended to strongly coupled dusty plasma. Due to their wide range of applications in space and astrophysics, such as plasma crystals, interiors of large planets, plasma created by laser compression of matter and laboratory plasmas, coupled plasma has enormous research potential.
- The theoretical findings can also be expanded to the astrophysical plasma parameters and the phenomenon of the waves can be studied in the future. This is the potential area of research which further expands our horizon of the universe.
- The "nano-dynamic" behaviour of systems at the kinetic level, such as the phase transitions, physics of liquids etc., can be studied using dusty plasma systems.
- The investigations can further be expanded to include 3D plasma systems, which provide a more precise and accurate representation of their behaviour.

Bio-Data

Ms. Anshu is a research scholar at the Department of Applied Physics, Delhi Technological University, Delhi, India since July 2018. Prior to this, she received her master's degree in Physics from the Department of Physics and Astrophysics, University of Delhi, Delhi in the year 2016 and her bachelor's degree (B.Sc. (H)) in Physics from Miranda House, University of Delhi, Delhi in the year 2013. She has been awarded the INSPIRE-SHE Fellowship during her graduation days from the Department of Science and Technology (DST), Govt. of India. She has also qualified the GATE in the year 2017. She has been awarded the Commendable Research Award for excellence in Research by DTU in the year 2023. She has received best oral and poster presentation award in PTS-2023, in virtual mode by Department of Physics, University of Lucknow, India, 20^{th} – 22^{nd} June, 2022 and in ICAMNOP-2023, Department of Applied Physics, DTU 2023, India, 20^{th} - 22^{nd} December, 2023. Her present research interests include the modelling and simulation of different waves and instabilities using different analytical methods in a magnetized dusty plasma.